

CLASSIFICATION OF FUNCTIONAL NEAR INFRARED SPECTROSCOPY SIGNALS TOWARDS BRAIN COMPUTER INTERFACE IMPLEMENTATION

A Thesis

Submitted by

YANAMALA VIJAY RAJ

For the award of the degree of

MASTER OF TECHNOLOGY, CLINICAL ENGINEERING

Jointly offered by

IIT Madras & CMC Vellore & SCTIMST Trivandrum



Jointly offered by

INDIAN INSTITUTE OF TECHNOLOGY MADRAS

CHRISTIAN MEDICAL COLLEGE VELLORE

**SREE CHITRA TIRUNAL INSTITUTE FOR MEDICAL SCIENCES AND
TECHNOLOGY TRIVANDRUM**

DECEMBER 2016

THESIS CERTIFICATE

This is to certify that the thesis titled “**Classification of Functional Near Infrared Spectroscopy Signals Towards Brain Computer Interface Implementation**” being submitted by **Yanamala Vijay Raj** to SCTIMST Trivandrum, for the award of the degree of **Master of Technology in Clinical Engineering** jointly offered by IIT Madras, CMC Vellore and SCTIMST Trivandrum, is a bonafide record of the research work done by him under our supervision. The contents of this thesis, in full or in parts, have not been submitted to any other Institute or University for the award of any degree or diploma.

The research work had been carried out at Sree Chitra Tirunal Institute of Medical Sciences and Technology Trivandrum, with joint collaboration of IIT Madras.

Dr Chandrasekharan Kesavadas
Guide,
Professor,
Department of Imaging sciences and
Interventional Radiology,
SCTIMST Trivandrum.

Dr. M. Manivannan
Co Guide,
Professor,
Dept. of Applied Mechanics,
IIT Madras.

Date:

ACKNOWLEDGEMENTS

I would like to express my deep gratitude to my master thesis guide Dr. Chandrasekharan Kesavadas of Department of Imaging sciences and Interventional Radiology at SCTIMST Trivandrum. He had consistently allowed me to work and constantly steered me in the right the direction whenever he thought I needed it.

Special thanks to my co-guide Dr. Manivannan M of Department of Applied Mechanics at IIT Madras. He had energetically contributed towards execution of Virtual Reality Android application in fNIRS BCI studies. He had actively helped in formulating ideas into implementation. The work put forwarded by his lab member Mr B. Chandra Sekhar is also appreciable.

I express my sincere gratitude to Dr. Mukesh Doble, Dr. Suresh Devasahayam, and Dr. Roy Joseph for coordinating the course and making this research a possibility.

I would like to thank my lab mate Mr Arun KM (PhD student, Medical Image Processing Lab, SCTIMST) who was very supportive during my project. I offer my sincere regards to my parents and friends who supported me in all respects during the course of the project.

ABSTRACT

KEYWORDS: Functional near Infrared Spectroscopy (fNIRS), Brain Computer Interface (BCI), Virtual Reality (VR), Random Forest (RF), and Linear Discriminant Analysis (LDA)

Stroke rehabilitation is a combined and coordinated use of medical, social, educational, and vocational measures to retrain a person who has suffered a stroke to his/her maximal physical, psychological, social, and vocational potential, consistent with physiologic and environmental limitations. Evidence from clinical trials supports the premise that early initiation of therapy favorably influences recovery from stroke. One of the latest reliable, exiting and proven ways of rehabilitation is by BCI based on fNIRS.

For targeting all range of Stroke impairments, we had developed three paradigms. First paradigm was designed for classifying brain state in motor execution active and rest states (Experiment 1). Second paradigm was designed for classifying brain state into motor execution and motor imagery (Experiment 2.1). The same paradigm was also used for classifying brain state into motor execution, motor imagery and rest states (Experiment 2.2). Third paradigm was designed for classifying brain state in VR motor imagery and rest states (Experiment 3). Motor imagery stimuli can also be better given with help of virtual reality. Replacing 2D paradigm (NIRstim) stimuli with VR stimuli, the functional response of stimuli can be increased and experiments can be conducted at ease, due to easy implementation of both motor execution and motor imagery task with VR.

Physiological noises from acquired signal was removed by novel wavelet transformation. Effect of differentiating signal, post noise reduction was studied. It effect on each experiment was reported. A new strategy for detecting optimal features for classification purpose, from features Mean, Variance, Skewness, Kurtosis, Peak, Sum of peaks and Number of peaks was designed and evaluated for designated four experiments and results are evaluated. RF was used both for feature selection and classification. LDA score and LDA_optimal model were used for classification. Robustness of three models were compared with respect to F1 score and best model for each experiment was evaluated. The run time of models was also studied. Finally the optimal features for each experiment was established.

CONTENT

ACKNOWLEDGEMENTS	iii
ABSTRACT	iv
LIST OF FIGURES	viii-xi
LIST OF TABLES	xii-xiii
ABBREVIATIONS	xiv
CHAPTER 1: INTRODUCTION AND STATEMENT OF PROBLEM	
FUNCTIONAL NEURO IMAGING	1
HEMO DYNAMIC RESPONSE	1-3
FUNCTIONAL NEAR INFRARED SPECTROMETRY (fNIRS)	3
fNIRS TYPES	4
fNIRS ADVANTAGES	5
PHYSIOLOGICAL PRINCIPLES OF fNIRS	6-7
BRAIN COMPUTER INTERFACE	7-9
STAGES IN BCI	10-12
VIRTUAL REALITY	13
VR ANDRIOD APP FOR MOTOR IMAGERY	14-15
VR REQUIREMENTS	15-16
PURPOSE OF STUDY	17-19
GOALS OF STUDY	20-21

CHAPTER 2: REVIEW OF LITERATURE

BCI FOR STROKE REHABILITATION	22-26
MOTOR IMAGERY	26-27
MOTOR IMAGERY FOR REHABILITATION	27-29
VR FOR REHABILITATION	29-31
PHYSICS OF FNIRS	32-34
NOISE REMOVAL	34
FOURIER TRANSFORMATION	35
WAVELET TRANSFORMATION	36-39
CLASSIFICATION TECHNIQUES	39-41
FEATURE EXTRACTION AND SELECTION	41-44
RANDOM FOREST	44-45
RF FEATURE RANKING	45-47

CHAPTER 3: METHODOLOGIES

fNIRS DATA ACQUISIZATION	47-54
PARADIGMS DESIGN	54-55
PARADIGM 1	55
PARADIGM 2	56-57
PARADIGM 3	58
VIRTUAL REALITY BASED MOTOR IMAGERY ANDRIOD APP...	58-60
WAVELET TRANSFORM FOR NOISE REMOVAL	61-63
DIFFERENTIATION OF SIGNAL	64-65
FEATURE EXTRACTION	66
FEATURE SELECTION	67

CLASSIFICATION	67-68
 CHAPTER 4: RESULTS	
EXPERIMENT1	69-77
EXPERIMENT 2.1 & 2.2	77-83
EXPERIMENT 3	84-89
FEATURES WITH BEST DISCRIMINATIVE POWER	89
 CHAPTER 5: DISCUSSION AND CONCLUSIONS	
MAJOR FINDING USING WAVELET TRANSFORMATION	90
DIFFERENTIATION OF SIGNAL	91
MAJOR FINDINGS	92-93
STRATEGY FOR CLASSIFICATION	93-94
FEATURE SELECTION	94
MAJOR FINDINGS	94-95
COMPARISION OF CLASSIFIERS	95-96
MAJOR FINDINGS	97
VR VIRTUAL REALITY FOR FNIRS BCI (VR fNIRS BCI)	98
RECOMMENDATIONS OF STUDY	99
RECOMMENDATIONS OF FURTHER STUDY	99-100
LIMITATIONS OF STUDY	101
 REFERENCES	 102-111
APPENDIX	112-116

LIST OF FIGURES

Figure 1	HDR expressed as percent in signal change	2
Figure 2	Blood flow relationship to cellular activity	2
Figure 3	Absorption spectrum of the blood	4
Figure 4	Absorption spectrum of Oxy hemoglobin, Deoxy hemoglobin and water	6
Figure 5	Hemodynamic response	7
Figure 6	Brain computer interface	8
Figure 7	ECoG electrodes	9
Figure 8	Stages in BCI	10
Figure 9	BCI to detect PP	24
Figure 10	BCI to detect MI	24
Figure 11	BCI to detect MI and provide concomitant of MI and P	25
Figure 12	Laterality Index in Pre and Post therapy	26
Figure 13	Reflections in turbid media	32
Figure 14	Pie chart of classifiers used in BCI	39
Figure 15	Motor montage	47
Figure 16	Signal quality	48
Figure 17	NIRStar Screenshot	48
Figure 18	NIRX fNIRS system	50
Figure 19	Source optodes (eight) and Detector optodes (eight)	50
Figure 20	Optodes fitted to cap, over motor cortex	51
Figure 21	Subject doing finger tapping task	51
Figure 22	VR headset	52
Figure 23	Subject with VR and fNIRs (Front view and top view)	52

Figure 24	Subject doing motor execution	52
Figure 25	Android phone with VR app mounted on VR headset	53
Figure 26	Block design	53
Figure 27	Extension and flexion images	56
Figure 28	Block design of Paradigm 2.1& 2.2	56
Figure 29	Block design of Paradigm 3	59
Figure 30	Screenshot of homepage of custom made VR motor imagery android app	59
Figure 31	Count down timer	59
Figure 32	Extension and flexion as seen in VR	60
Figure 33	Single channel loaded in wavelet toolbox (Signal with noise)	61
Figure 34	Db7 wavelet with level of 8 selected for multiresolution analysis	61
Figure 35	Multiresolution analysis of single channel data	61
Figure 36	Coefficient details	62
Figure 37	Matlab code for wavelet transformation (20 channels)	63
Figure 38	Raw signal (20 channels)	63
Figure 39	De-noised signal (left- 1 channel, right- 20 channels)	63
Figure 40	Noise in signal	63
Figure 41	Non-diff signal scatter plot (subject 16)	64
Figure 42	Diff signal scatter plot (subject 16)	64
Figure 43	Diff signal (left- 1channel, right- 20 channels)	65
Figure 44	Experiment 1: Area plot of non-diff signal	66
Figure 45	Experiment 1: Area plot of diff signal	66
Figure 46	Experiment 1: Active blocks	69
Figure 47	Experiment 1: Rest blocks	69
Figure 48	Experiment 1: Active block (left- non diff signal, right- diff signal)	70

Figure 49	Experiment 1: Rest block (left- non diff signal, right- diff signal)	70
Figure 50	Experiment 1: Feature matrix	70
Figure 51	Experiment 1: Second ranked features	72
Figure 52	Experiment 1: Second ranked features	73
Figure 53	Experiment 1: Third ranked features	73
Figure 54	Experiment 1: Frequencies of features	73
Figure 55	Experiment 1: Classification results	75
Figure 56	Experiment 1: F1 scores of LDA	75
Figure 57	Experiment 1: F1 scores of LDA_optimal	76
Figure 58	Experiment 1: F1 scores of LDA and LDA_optimal	76
Figure 59	Experiment 1: F1 scores of RF, LDA and LDA_optimal	77
Figure 60	Experiment 2: Raw signal	77
Figure 61	Experiment 2: Area plot of non diff signals	78
Figure 62	Experiment 2: Area plot of diff signals	78
Figure 63	Experiment 2: Scatter plot of diff signal	79
Figure 64	Experiment 2: Scatter plot of non diff signal	79
Figure 65	Experiment 2: Motor blocks (diff signals)	80
Figure 66	Experiment 2: Area plot of non-diff signal	80
Figure 67	Experiment 2: Motor imagery blocks (non-diff signals)	80
Figure 68	Experiment 2: Motor imagery blocks (non-diff signals)	81
Figure 69	Experiment 2: Rest blocks	81
Figure 70	Experiment 2: Block average of Motor, Motor Imagery and Rest (non-diff signals)	81
Figure 71	Experiment 2.1 : Frequency of features	82
Figure 72	Experiment 2.2: Frequency of features	83

Figure 73	Experiment 3: Scatter plot (non-diff signal)	84
Figure 74	Experiment 3: Scatter plot (diff signal)	84
Figure 75	Experiment 3: VR Motor Imagery blocks	85
Figure 76	Experiment 3: Rest blocks	85
Figure 77	Experiment 3: Block average of Active and Rest	85
Figure 78	Experiment 3: Frequency of features	87
Figure 79	Experiment 3: LDA and LDA_opt F1 scores	87
Figure 80	Experiment 3: LDA, LDA_optimal and RF F1 scores	88
Figure 81	Experiment 3: LDA and LDA_optimal run time	88
Figure 82	Wavelet transformation, Top picture: Raw signal, Middle picture: Signal denoised, Bottom picture: Noise in signal	90
Figure 83	Differentiation of signal increasing correlation in 2D feature space	91
Figure 84	Experiment 1- Left images are of active state (motor execution) and Right images are of rest state; Top images are of non diff signals and down images are of diff signal	92
Figure 85	Experiment 2.1-Top image is of diff signals of motor task and down image is of diff signals of motor imagery	93
Figure 86	Foot tapping in VR	111
Figure 87	Finger tapping in VR	111
Figure 88	Code for loading csv file having features and converting it into dataframe	112
Figure 89	Code for LDA classifier	113
Figure 90	Code for Random Forest classifier	114
Figure 91	RF Classification scores and Gridsearch CV results	114
Figure 92	MDI scores of RF	115
Figure 93	Code for optimal LDA classifier	115
Figure 94	Code for scatter plot	116

LIST OF TABLES

Table 1	Functional Imaging	3
Table 2	List of publications with motor execution task in fNIRS BCI	11
Table 3	List of publications with motor imagery task in fNIRS BCI	11
Table 4	LDA classifier used for classification purpose in fNIRS BCI	39
Table 5	SVM classifier used for classification purpose in fNIRS BCI	40
Table 6	ANN classifier used for classification purpose in fNIRS BCI	41
Table 7	HMM classifier used for classification purpose in fNIRS BCI	41
Table 8	List of features used for classification purpose	43
Table 9	Number of subjects recruited per experiment	49
Table 10	List of experiments and details about task, classification and paradigm	49
Table 11	Paradigm 1 details	55
Table 12	Paradigm 2 details	57
Table 13	Paradigm 3 details	60
Table 14	Parameter tuning for estimator	67
Table 15	Optimal parameters estimated for estimators	71
Table 16	Experiment 1: F1 scores and top three ranked feature	71
Table 17	Experiment 1: First ranked, second ranked and Third ranked features	72
Table 18	Experiment 1: Frequency of features	72
Table 19	Experiment 1: Frequency of First ranked features	74
Table 20	Experiment 1: Frequency of Second ranked features	74
Table 21	Experiment 1: Frequency of Third ranked features	74
Table 22	Experiment 2.1: RF F1 scores and Top three ranked features	82
Table 23	Experiment 2.1: First ranked, Second ranked and Third ranked	82

Table 24	Experiment 2.1: LDA, LDA_time, LDA_opt and LDA_opt_time	82
Table 25	Experiment 2.1: RF F1 scores and Top three ranked features	82
Table 26	Experiment 2.2: First ranked, Second ranked and Third ranked	83
Table 27	Experiment 2.2: LDA, LDA_time, LDA_opt and LDA_opt_time	83
Table 28	Experiment 3: Optimal parameters estimated for estimators	86
Table 29	Experiment 3: RF F1 scores and Top three ranked features	86
Table 30	Experiment 3: First ranked, Second ranked and Third ranked feature	86
Table 31	Experiment 3: LDA, LDA_time, LDA_opt and LDA_opt_time	86
Table 32	Experiment 3: Frequency of features in all experiments	89
Table 33	Experiment 1: Average F1 scores	95
Table 34	Experiment 1: Average run time	95
Table 35	Experiment 2.1: Average F1 scores	95
Table 36	Experiment 2.1: Average run time	95
Table 37	Experiment 2.2: Average F1 scores	95
Table 38	RF F1 scores and Top three ranked features	96
Table 39	Experiment 3: Average F1 scores	96
Table 40	Experiment 3: Average run time	96
Table 41	Average RF F1 scores	96
Table 42	Average LDA, LDA_optimal F1 scores	96
Table 43	Average LDA, LDA_optimal run time	97

ABBREVIATIONS

ANN	Artificial Neural Networking
AUC	Area under curve
BCI	Brain Computer Interface
BOLD	Blood oxygenation level dependent signal
CBF	Cerebral blood flow
DWT	Discrete Wavelet Transformation
EEG	Electro-encephalography
FES	Functional electric stimulator
FT	Fourier transform
F-NIRS	Functional near infrared spectrometry
F-MRI	Functional Magnetic resonance imaging
HbO	Oxy Hemoglobin
HbR	Deoxy Hemoglobin
HbT	Total Hemoglobin
HDR	Hemo Dynamic Response
HMM	Hidden Markov Model
ICA	Independent component analysis
LED	Light Emitting Diode
LI	Laterality Index
LDA	Linear Discriminant Analysis
MDI	Mean Decrease Impurity Importance
MEG	Magneto-encephalography
MI	Motor imagery
MRA	Multi resolution analysis
OT	Occupation Therapy
PP	Physical Practice
PCA	Principal Component Analysis
PET	Positron emission tomography
ROC	Receiver Operating Characteristic
SVM	Support Vector Machine
STFT	Short Time Fourier Transform
VR	Virtual Reality
VRT	Virtual Reality Therapy

CHAPTER 1: INTRODUCTION & STATEMENT OF PROBLEM

FUNCTIONAL NEURO IMAGING

Functional neuro-imaging has been widely used for brain mapping and understanding brain areas with respect to specific tasks given as stimuli. It has found wide uses in cognitive neuroscience, physiology, and neuropsychology. Further functional neuro-imaging is an important tool for rehabilitation research.

Several modalities have been used for brain signal acquisition. Common methods of functional neuro-imaging include

- Positron emission tomography (PET),
- Functional magnetic resonance imaging (fMRI),
- Electroencephalography (EEG),
- Magneto-encephalography (MEG),
- Single-photon emission computed tomography (SPECT)
- Functional near infrared spectroscopy(fNIRS)

Functional imaging attempts to measure the neuronal activity, via Hemodynamic response. EEG measures neuronal activity as electric activity, while MEG measures neuronal activity as magnetic activity. PET measures neuronal activity with respect to regional metabolic changes using positron emitting isotope of oxygen. fMRI measures changes in blood oxygenation that is direct correspondence with hemodynamic response. fNIRS measures changes in blood oxygenation in infrared absorption spectrum.

These techniques have been used for determining effects of brain injury and the rehabilitation changes in brain system. Mapping of neuroplasticity changes during rehabilitation can also be done by Neuro Imaging techniques.

HEMO DYNAMIC RESPONSE

Neuronal activity generates Hemodynamic response (HDR) that allows rapid flow of blood to active areas in brain. Smooth muscles, neurons, astrocytes, endothelial cells, pericytes form important role in maintaining blood brain barrier and delivering necessary nutrients to tissues and

also adjusting blood flow in intra-cranial space for maintaining homeostasis. Hemodynamic response is directly linked with brain activation and proved to be efficient way to map brain functions. When neuronal activity increases, cerebral blood flow rate also increases which is otherwise called HDR, and this increased cerebral blood flow increases ratio of oxygenated hemoglobin relative to deoxygenated hemoglobin in that activated area. This signal is called BOLD (Blood Oxygenation Level Dependent signal) and this BOLD signal forms import aspect in functional neuro-imaging modalities like fMRI.

HDR was used to generate brain images of both active and rest areas, which is basics for neuro-imaging techniques.

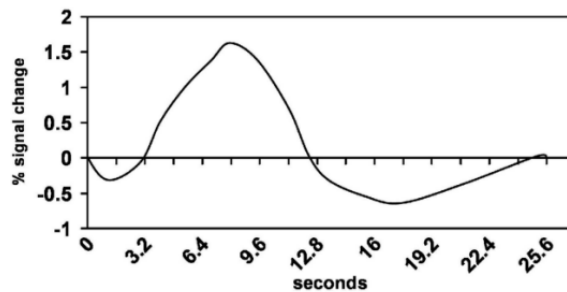


Figure 1: HDR expressed as percent in signal change (Crosson et al., 2010)

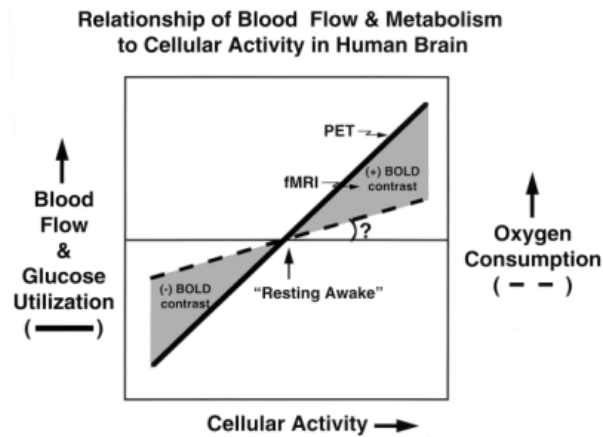


Figure 2: Blood flow relationship to cellular activity (Marcus E Raichle et al., 1998)

	Fnirs	Fmri	PET
Parameters	$\Delta[\text{HbO}_2]$, $\Delta[\text{HbR}]$, $\Delta[\text{HbT}]$	BOLD	Glucose metabolism
Temporal resolution	Best (<1 sec)	Intermediate (1 sec)	Worst (> 1 min)
Spatial resolution	Worst (1 sec)	Best (1 mm)	Intermediate (5 mm)
Motion sensitive	Moderate	High	High
Setup	General	Shielded room	Shielded room
Safety issues	None	Yes	Yes

Table 1: Functional imaging

FUNCTIONAL NEAR INFRARED SPECTROMETRY (fNIRS)

fNIRS is a noninvasive brain imaging technique, that works on the principle of near infrared spectrometry. The pioneers in fNIRS date back to 1977 (Jobsis et al., 1977). Initially it was used for measuring cerebral oxygenation for adults and new born (Alaraj & Slavin et al., 2009). Slowly fNIRS had found its need in assessing neurological and psychiatric disorders.

To tackle the ever increasing registered cases of brain disorders, portable and affordable neuro-imaging modality is required. The relatively new modality can fulfill the technical requirements of being portable, affordable, is fNIRS (functional near infrared spectrometry). It records the changes in the blood hemodynamic response and volumetric changes based on the attenuation of light by brain tissue.

NIRS is a technique of performing tissue oximetry using infrared light which is harmless electromagnetic radiation, to shine the tissue by means of a continuous beam of infrared light and to collect the re-emitted or transmitted light. The concentration of chromophores in blood (ie) oxy-hemoglobin and deoxy-hemoglobin can be measured or calculated based on attenuation of near infrared light. When the same NIRS technique is applied for measuring hemodynamic response it is called functional near infrared spectrometry.

The oxygenated and deoxygenated hemoglobin (two important chromophores in blood) states have considerably different absorption in infrared window. To be acquainted with the concentrations of oxy and deoxy hemoglobin, brain is radiated at two different wavelengths, possibly chosen where the spectra have the greatest differences. The general fNIRS technique uses constant light intensity

and is known as Continuous Wave near Infrared Spectroscopy (CW-NIRS). The most diffused wavelengths for CW-NIRS are 690 nm and 820 nm.

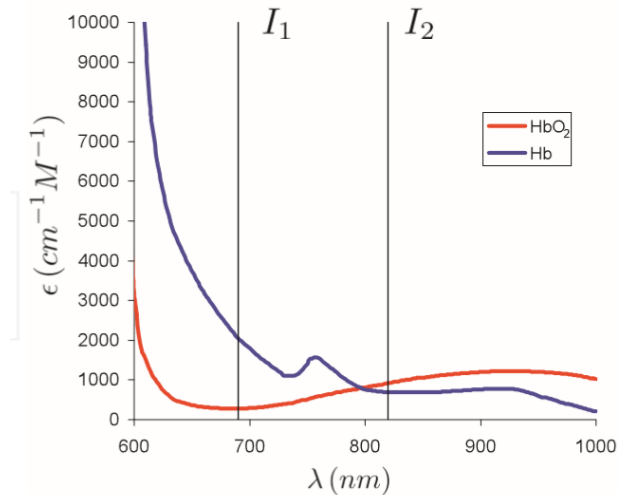


Figure3: The absorption spectrum that is the molar extinction coefficient vs. the wavelength, of the oxygenated (red) and deoxygenated (blue) states of the hemoglobin. I1 and I2 are the chosen wavelengths for Near Infrared Spectroscopy measurements (Matteo Caffini et al., 2012).

fNIRS is characterized by relatively high temporal resolution (sampling rate of 100Hz for Continuous wave type). fNIRS signals are not constant in resting phase, thereby implying that it can be used for studying of various physiological and cognitive phenomena in resting state.

fNIRS TYPES

Three different fNIRS techniques utilized are

- Continuous wave
- Frequency domain
- Time domain

Continuous wave instrument measures attenuation of constant light intensity in tissue. It is of low cost, ease of implementation, fast sampling, good signal to noise ratio. But this instrument can't be used for measuring the optical properties of tissues, absolute concentration of chromophores and the path length of light in tissue.

Time domain technique instrument working principle is based on sending picosecond long of light pulses to probed volume and measures its time of flight distribution. This technique can separate signals based on depth of penetration. Absolute concentration of chromophores and the path length of light travelled in tissue can also be measured.

Frequency domain instruments modulate light intensity at frequency and measure amplitude, phase and average intensity of light propagated in probed area. They can be used for separating superficial and cerebral components of signal. Absolute concentrations of chromophores can also be measured.

The fNIRS device used in this thesis is continuous wave type. Its operation is described in Physics of fNIRS section.

fNIRS ADVANTAGES

fNIRS is proved to advantageous in many functional studies, and the various advantages include

- i) Portable
- ii) High temporal resolution (better than fMRI, PET)
- iii) Quick and accurate measurement
- iv) Non motion sensitive
- v) No safety issues
- vi) Natural setting
- vii) Clinical friendly
- viii) Easy to setup and use
- ix) Cost efficient
- x) Can be used on all age range
- xi) Recorded for a longer time
- xii) Repeatable and reproducible
- xiii) Measure concentrations of Oxy and Deoxy Hemoglobin
- xiv) Compatible with other neuro imaging modalities
- xv) Best for Brain computer interface

PHYSIOLOGICAL PRINCIPLES OF fNIRS

fNIRS measurement is based on five physiological principles:

- i. Cerebral blood flow (CBF) increases in active brain areas,
- ii. Tissue is relatively transparent to NIR light,
- iii. NIR light is scattered strongly in all directions in tissue
- iv. Hemoglobin molecules of red blood cells absorb NIR light,
- v. Optical properties of hemoglobin depend on its oxygenation level,

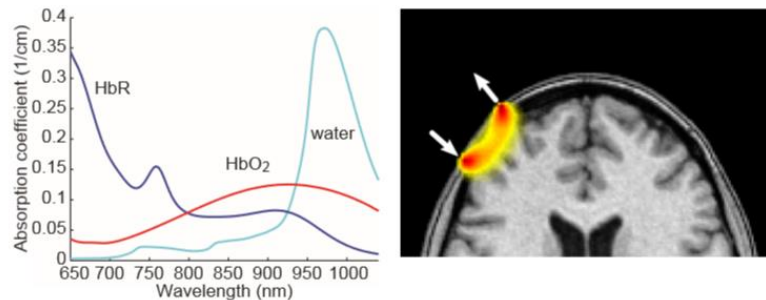


Figure 4: Absorption spectrum of Oxy hemoglobin, Deoxy hemoglobin and water (T Nasi et al., 2013)

When neuronal activity happens, a surge in hemodynamic response is seen, and due to increased concentrations of oxy-hemoglobin in area of interest, attenuation of light increases. Deoxy-hemoglobin in blood absorbs more red light than oxy-hemoglobin.

Based on attenuation of NIR light, concentrations of oxy hemoglobin and deoxy hemoglobin can be calculated. It was deciphered by various experiments that wavelength of range 650-950 nm, provided good optical window for detection of blood oxygen concentration levels. In other words, at this particular spectrum, the absorption of light by brain tissue is considerably low, allowing light to penetrate deep into brain tissues.

The NIR light scattered diffusively in all directions that makes it easy to measure attenuation of light at a few centimeters apart. The sensitivity volume of the light is shaped like a banana; the longer the distance between the source fiber and the detection point, the deeper the banana shape reaches in the tissue (H. Dehghani et al., 2009)

The fNIRS measurement is made through the scalp. Therefore, changes in scalp blood circulation, e.g., due to task-related stress, contribute to the signals.

Baseline of the fNIRS signal oscillates spontaneously along with the systemic circulation, including components related to pulsation of the blood vessels, respiration, vaso-motion, and autonomic regulation of the circulation (Y. Tong et al., 2010, H.Obrig et al., 2000).

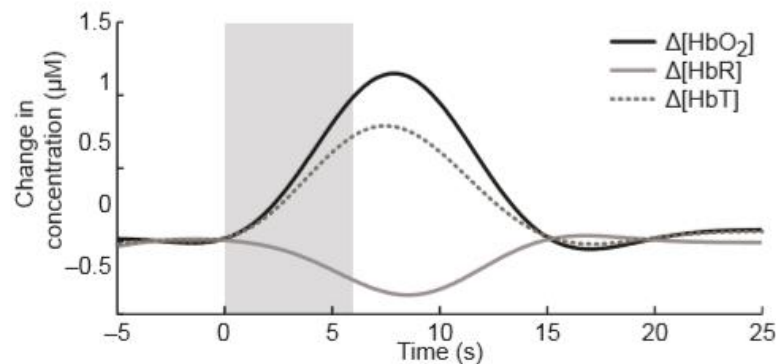


Figure5: Hemodynamic response (T.Näsi et al., 2010)

The hemodynamic response results from local vaso-dilation that increases the local CBF and raises the blood oxygenation level and volume. Consequently, the increased blood volume and oxygenation corresponds as increased $[\text{HbO}_2]$ and $[\text{HbT}]$, as well as a decreased $[\text{HbR}]$ with a smaller magnitude. The signals peak around 5 s after the stimulation onset (M. E. Raichle et al., 2006), and return back to the baseline with a time lag of about 5–10 s after the end of stimulation. Paradigms in our project were designed, keeping the hemodynamic response time in view. Active block was designed with time interval of 10 seconds, and rest block with time interval of 10 seconds.

BRAIN COMPUTER INTERFACE

Brain computer interface is a method of communicating based on neural activity of brain. BCI enables a direct communications pathway between the brain and the object to be controlled. The object to be controlled included FES, robotic arm, prosthetics and orthotics or any other communicating devices. The neural activity required in BCI can be recorded either invasively or non-invasively. The major objective of BCI is to provide new channel of output from brain (Wolpaw et al., 2000). BCI systems was developed mainly to rehab individuals, whose normal

output channels of peripheral nerves and muscles aren't functioning or damaged. BCI systems are the widely researched systems for rehabilitation purpose, and had been proved to be advantageous for severely disabled, locked in individuals with no reliable muscle control to interact with surroundings. Initial BCI were based on EEG and EMG signals. But later BCI systems based on fMRI, fNIRS have been developed. Current BCI tools can aid user in communication, interacting with environment and movement and muscle exercise.

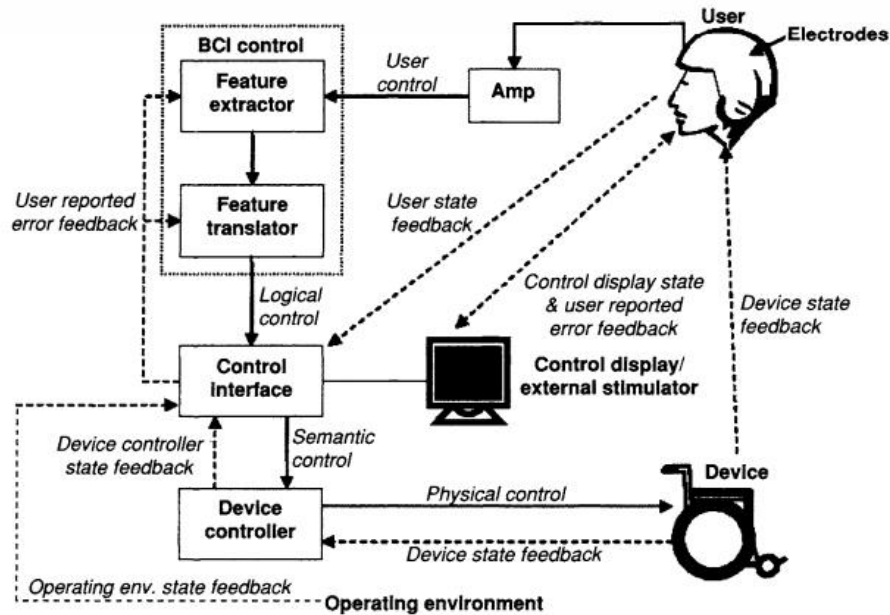


Figure 6: Brain computer interface (Mason and Birch 2003)

BCI systems can be briefly divided as invasive BCI, partial invasive BCI and noninvasive BCI. Chip implant based BCI systems, where chips are implanted in gray matter, had been developed for complete paralysis patients. Partial invasive BCI systems based on electrocorticography had been developed in last decade, where mesh shaped electrodes are implanted below the skull; thereby no implantation is made in gray matter. Partial invasive BCI has several advantages like better signal to noise ratio, higher spatial resolution, wide frequency range and long term stability. Noninvasive BCI are EEG, fMRI, MEG and fNIRS based systems.

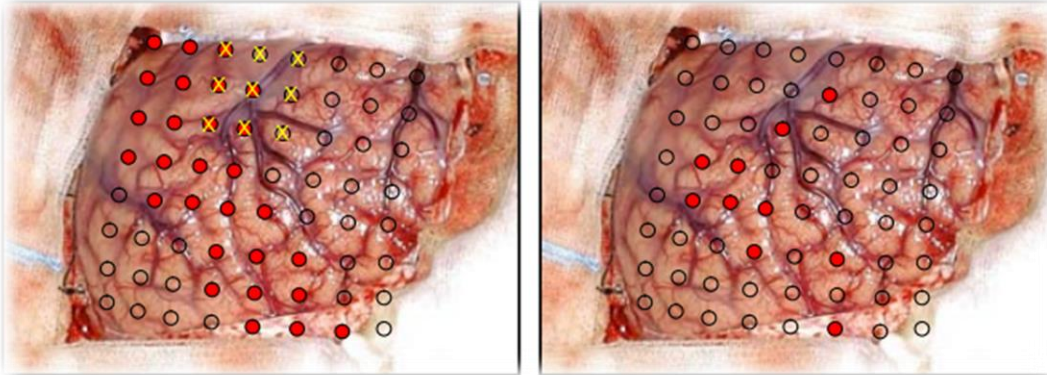


Figure 7: ECoG electrodes implanted over motor cortex (TN Lal et al., 2005)

BCI in addition to being a new interfacing output from the brain have also another important application as agents of inducing brain plasticity by neuro-feedback training. Through feedback of functional measures, the BCI is hoped to allow regions in the brain to actively learn using the BCI and attempt to restore normal functioning (SujeshSreedharan et al., 2013).

Functional electric stimulators attached to BCIs can allow motor recovery for paralyzed patients. They help in neuro-rehabilitation by activation of motor centers in the brain by feedback training of learning to use one's own paralyzed limbs by an alternate pathway. Thereby after a period of time with practice of FES-BCI, it would be possible for a patient to perform motor activity without need of FES, thanks to neuro-plasticity generated in brain with help of FES BCI systems (Birbaumer N et al., 2007; Daly JJ et al., 2008).

In this project we are more focused at developing BCI systems for stroke rehabilitation.

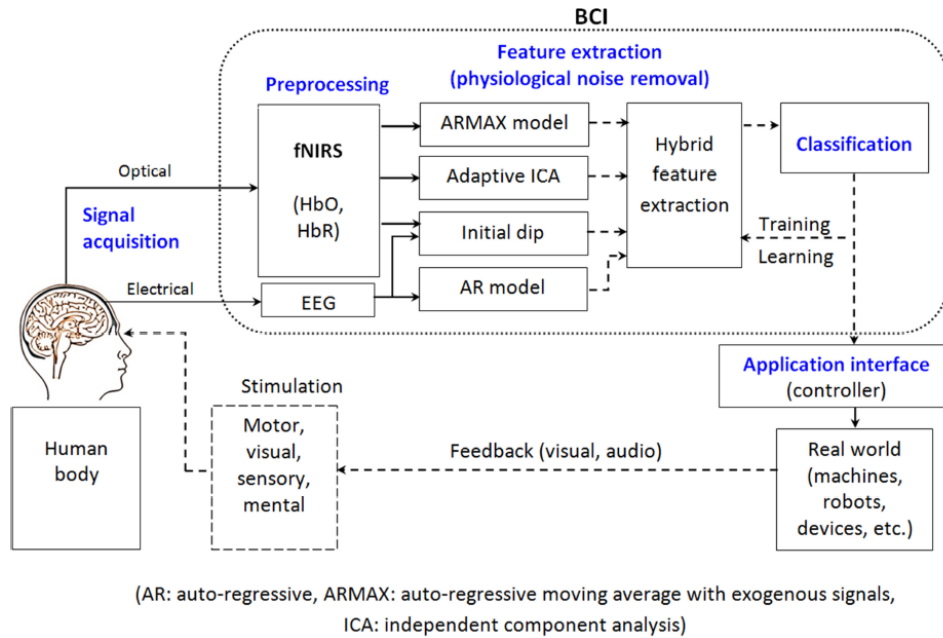


Figure 8: Stages in BCI (NomanNaseer et al., 2015)

STAGES IN BCI

BCI system consist of the following stages

- First stage: Suitable signals are acquired from appropriate brain imaging modality
- Second stage: Pre-processing of the signal obtained to remove noises and artifact
- Third stage: Features extracted
- Fourth stage: Features classified using a suitable classifier
- Fifth stage: Classified signals are transmitted to a computer or external device

Brain signal acquisition

The preliminary stage in BCI consists of acquisition of brain signals. The most common areas for acquisition are primary motor cortex and prefrontal cortex. Signals corresponding to mental counting, mental arithmetic, landscape imagery, music imagery are acquired from prefrontal, whereas signals corresponding to motor activity and motor imagery are acquired from motor cortex.

Suitable number of emitter/detector pair should be used, for adequate acquisition of neuronal signal. For prefrontal cortex, three emitter and 8 detectors was proved to be sufficient (Power et al., 2010), whereas for motor cortex, six emitter and six detector was proved to be sufficient (Sitaram et al., 2007). For our project, eight emitter and eight detectors system was used.

Activities from motor cortex like motor execution and motor imagery offer perfect choice for neuro-rehabilitation purpose. Motor execution stands for moving body by muscular activates involving muscular tensions. Various motor execution tasks like finger tapping, hand tapping, arm lifting, and hand grasping had been reported previously. Motor imagery stands for covert cognitive process of kinesthetic imagery of one’s own body movement. Motor imagery is one of the most used tasks for BCI, because it the easiest task that can be done by motor disabled patients. Motor imagery tasks like imagination of squeezing soft ball, imagination of complex sequence of finger tapping, imagination of extension and flexion of elbow, imagination of wrist flexion and imagination of unfolding of fingers.

Motor execution	Reference
finger tapping	Seo et al., 2012
arm lifting	Shin and Jeong 2014
hand grasping	Nagaoka et al., 2010
hand tapping	Khan et al., 2014
Knee extension	Shin and Jeong 2014

Table 2: List of publications with motor execution task in fNIRS BCI

Motor Imagery	Reference
Squeezing soft ball	Stangl et al., 2013
Complex finger sequence	Sitaram et al., 2013
Unfolding fingers	Mihara et al., 2013
Wrist flexion	Naseer and Hong 2013
Extension and flexion of elbow	Mihara et al., 2013
Feet tapping	Kaiser et al., 2014

Table 3: List of publications with motor imagery task in fNIRS BCI

Prefrontal cortex is other important area that can be considered for BCI. Tasks like mental arithmetic, music imagery, landscape imagery, mental writing, and object rotation, emotion inducing tasks, deception and visual stimuli.

Preprocessing of Signal

Acquired brain signals consist of lot of noise, like instrumental, experimental error and physiological noise.

Instrumental Noise: Noises arising from either device or external environment. These noises usually are of high frequency and can be easily removed by low pass filter. Further by minimizing external light interferences, instrumental noise can be drastically reduced.

Experimental error: Experimental errors include motion artifacts caused by dislocation or movement of optodes during experiment. Motion artifact corrections can be done by Wiener filtering method, PCA based filtering, wavelet analysis method and SavitzkyGolay type filters.

Physiological Noises: Heartbeat, respiration, Mayer waves and blood pressure fluctuations are mainly reported physiological noises in fNIRS signal. These can be removed by band filtering, PCA, ICA and wavelet transformation.

Feature extraction and selection

Post preprocessing of data, features are extracted and selected. The features are extracted from hemodynamic signals (HbO, HbR and HbT). Optimal features should be selected, that gives maximum discrimination and increases classification accuracy. The most commonly extracted features are signal mean, signal slope, signal variance, signal skewness, signal kurtosis, signal amplitude and signal peak.

Classification techniques

Classification techniques are used to identify patterns in signal acquired and discriminate signals into different states of brain based on optimal features selected (ie), motor execution or motor imagery, motor imagery or rest, motor execution or rest. Some of most commonly used classifiers are LDA, SVM, HMM and ANN.

VIRTUAL REALITY

Virtual reality is a computer generated environment of a three-dimensional image or environment that can be interacted with in a seemingly real or physical way by a person using special electronic equipment, such as a helmet with a screen inside or gloves fitted with sensors. It stimulates users senses in such a way that computer generated world is experienced as real. It also lets users navigate and interact with three dimensional virtual environments in real time and various feedbacks like auditory, sensory, vision, vibrotactile, haptic, proprioceptive, knowledge of performance and results can be given via VR to player or subject. By giving feedback about performance, increasing autonomy of player over VR task, and also lets user explore VR safely and independently.

The main benefits of virtual reality in medicine include:

- Safety
- Time
- Money
- Ability to re-use on a regular basis/skills refresh
- Can be used remotely
- Efficiency
- Realistic

Virtual reality based therapies (VRT) had been utilized to overcome inherent difficulties in traditional therapies. Therapies based on VRT can simulate, various environments that can be used for stimulating senses of patients suffering with phobias. Since VRT is flexible to use and operate, it can be performed in any place and at required amount of time. VRT can generate stimuli of greater magnitude compared to standard techniques. It also offers potential to develop human testing and training methods that allows researchers to modulate feedback senses accurately, thereby assessing and rehabilitating human cognitive and functional performances. This particular advantage had led to deployment of VR, as rehabilitation tool for neurological disorders patients.

VR had been used in health care for different purposes and found tremendously advantageous when compared to traditional methods. VR applications in medicine include surgical simulation, training, three dimensional anatomy and three dimensional physiological imaging. In psychology,

VR had been used for treatment of phobias such as fear of heights, fear of flying, fear of driving, fear of public speaking and claustrophobia. Neuro psychological evaluation and testing can be easily done in virtual environment with VR.

Virtual reality and motor imagery based training, induces cognitive and motor activities simultaneously. MI engages in planning, attention, information integration and processing; whereas VR provides stimuli.

VR had been used for rehabilitation of chronic stroke, alzheimer disease (AD), cerebral palsy, autism, cognitive impairments condition, dementia, attention deficit hyperactive disorder and various neurological disorders. It is also used as training tool for patients with learning disabilities, thereby by which complex tasks can be taught to them with VR, by breaking down of complex task into simple task and training them with simple task initially and later increase complexity of task. VR based training accompanied with gait analysis proved advantageous for rehabilitation for certain patients with motor functional disabilities.

VR ANDRIOD APP FOR MOTOR IMAGERY

VR is also effective tool in BCI studies, stimulating environments as required. Paradigms based on VR feedback have found recent interest in functional studies of brain. Simple task like finger tapping, motor execution, auditory and vision stimuli can be given easily via traditional paradigms. But when working with complex task like complex finger movement, proprioception, cognition, equilibrium of body motion and various other tasks, it is not possible to give multiple feedbacks to subject in normal paradigm. Motor imagery stimuli can also be better given with virtual reality. Replacing 2D paradigm (NIRstim) stimuli with virtual stimuli in form of VR feedback, the functional response of stimuli can be increased and experiments can be conducted at ease, due to easy implementation of both motor execution and motor imagery task with VR. Further details about VR app and its design was designed in discussion section.

VR headset, the device used for providing virtual reality for viewers/ subjects, had been deployed for a long time for computer games and other applications. VR headset has stereoscopic head mounted display which provides separate images for eye. High end VR headset also come with head tracking sensors like gyroscopes, accelerometers, structures light systems, eye tracking

sensors and gaming controls. The lenses can be adjusted for fine focus and distance of focus for comfortable viewing avoiding eye strain.

Since our study is experimental study of implementation of VR based stimuli for BCI, we had purchased “Domo nHance VR7” which can be used for smartphones upto 6 inches. It has aspherical optical lens, of diameter 33.5mm, and interpupillary distance between 73mm to 56mm. Virtual reality app was developed for motor imagery task. This VR app is basically a game that has repetitive active phase (stimuli) and rest phase (non stimuli). Once app is started, active phase runs starts and runs for a period of 10-15 seconds, followed by a rest phase for a period of time (10-15 seconds). Total run time of app usually have five active phase and five rest phase. This app can be manually synchronized with NIRstim paradigm.

VR REQUIREMENTS

Untiy game engine

Unity is a cross-platform game engine developed by Unity Technologies and used to develop video games for PC, consoles, mobile devices and websites. Unity allows specification of texture compression and resolution settings for each platform the game engine supports, and provides support for bump mapping, reflection mapping, parallax mapping, screen space ambient occlusion (SSAO), dynamic shadows using shadow maps, render-to-texture and full-screen post-processing effects. Unity's graphics engine's platform diversity can provide a shader with multiple variants and a declarative fallback specification, allowing Unity to detect the best variant for the current video hardware; and if none are compatible, fall back to an alternative shader that may sacrifice features for performance.

Monodevelop

MonoDevelop is an open source integrated development environment for Linux, OS X, and Windows. Its primary focus is development of projects that use Mono and .NET frameworks. MonoDevelop integrates features similar to those of NetBeans and Microsoft Visual Studio, such as automatic code completion, source control, a graphical user interface (GUI) and Web designer. MonoDevelop integrates a Gtk# GUI designer called Stetic. It supports Boo, C, C++, C#, CIL, D, F#, Java, Oxygene, Vala, and Visual Basic.NET.

Autodesk Maya

Autodesk Maya features include character creation, texturing, animation, sculpting, lighting, particles, effects and motion graphics. Get powerful, integrated 3D tools on a robust, extensible CG pipeline core.

3D character modeling and sculpting

Maya® software offers production-proven tools for 3D character modeling, sculpting and environment modeling. Build and texture organic and hard-surface models with polygon, NURBS and subdivision surface modeling tools.

3D animation programmers and tools

Maya® 3D animation software offers a broad range of specialized tools for character creation, 3D editorial, and keyframe, procedural and scripted animation.

Make human

It is the free and open source software to create realistic 3d humans for:

- Illustrations
- Animations
- Games
- Zbrush/Mudbox sculpting

Easy and intuitive parameters, including

- Age, gender, height, weight
- Body proportions, face shapes
- Eyes, nose, mouth, chin, ears, neck...
- Hands details, feet

PURPOSE OF STUDY

When normal output channels of peripheral nerves and muscles are not working, (muscle paralysis condition), various rehabilitation techniques are often sought after. One of the latest reliable, exiting and proven ways of rehabilitation is by Brain computer Interface. Till date BCI had been used in aiding communication, interacting with environment, muscle training and rehabilitation of severe disabled persons. In BCI, signals from brain can be acquired by functional imaging devices like fNIRS, fMRI and EEG; states of brain classified (whether it is active or rest), and feedback can be given to the same subject via FES. This real time feedback based on classified activity of brain, foster neuroplasticity and motor rehabilitation.

fNIRS imaging modality will be deployed for BCI purpose due to its various advantages compared to other imaging modalities like portable, high temporal resolution, quick measurement, no safety issue and non-motion sensitive. Continuous wave type fNIRS was chosen over other types of fNIRS like time domain and frequency domain devices. CW fNIRS can measure optical properties of tissue, calculate absolute concentrations of chromophores.

Physical practice by patients is only therapy for stroke rehabilitation which partly recovers motor function by remodeling brain by synaptogenesis and neuroplasticity. But most of the time, it is difficult for stroke patients to move their impaired hands during rehabilitation. Motor imagery, the imagination of movements without physical action, presents alternative option for rehabilitation. Changes in cerebral activities can be observed because of MI training, which mirrored structural and functional reorganization due to neuroplasticity. MI neural correlation is shared with Physical practice or motor execution. By reestablishing juncture between cortical activity related to MI and feedback (FES), sensorimotor strength can be increased and ultimately motor recovery can be done. By considering motor imagery, it is possible to rehab patients with severe motor disabilities too.

Keeping in mind the advantages of training patients with motor execution and motor imagery, paradigms will be designed. NIRStim software will be used for designing paradigm. Block design found to advantageous over event related design, because it is adept to detect subtle hemodynamic responses across different tasks conditions. Three paradigms will be designed with block design.

Paradigm1:

- *Aim:* To classify brain states into active (ME) or rest states
- *Blocks:* 5 active and 5 Rest
- *Duration:* 10 seconds of Active and 10 seconds of Rest
- *Stimuli:* Visual (Text)

Paradigm2:

- *Aim:* To classify brain states into active (ME/MI) or rest states
- *Blocks:* 8 active (4 ME & 4MI) and 8 Rest
- *Duration:* 12 seconds of Active and 12 seconds of Rest
- *Stimuli:* Visual (Image)

Paradigm3:

- *Aim:* To classify brain states into active (MI) or rest states
- *Blocks:* 4 active (MI) and 4 Rest
- *Duration:* 10 seconds of Active and 10 seconds of Rest
- *Stimuli:* Visual (Virtual Reality)

Generally acquired fNIRS signal come with lot of noises like instrumental noise, experimental noise and physiological noises. PCA, ICA and band filtering have been till date used. Wavelet transformation is other attractive technique of removing noises by deconstructing signal into different frequencies and reconstructing required signals (brain signals) thereby removing other signals like physiological noises. Wavelet transformation will be used for noise removal and db7 will be investigated.

Various classification techniques like LDA, SVM, HMM have been used so far. Most of BCI researchers had used LDA because of it efficient run time (less than 0.01 sec) that best suits BCI. The success of classification best depends on discriminative power of features. Strategies like step wise reduction have been used for selected best features among set of features. Techniques like wrapper and recursive feature elimination had also been used for evaluation of feature set. Other way of selecting optimal feature combination is by classifying data with RF. Random forest is a classifier that quenches the major effort of researchers in figuring out the best optimal selection of

features for their classification. Owing to the ease at which it identifies best discriminate features for classification purpose and build good accurate model, we had decided to deploy RF for our offline BCI, finger tapping task.

Since RF is ensemble method of classifier, its run time of classification is usually higher. Therefore it would be best practice to best feature ranked by Random Forest, as optimal features of LDA. We hypothesize by using best ranked feature of RF with LDA; we could reduce run time of feature extraction and classification. Further RF could also be used for offline classification with even higher accuracies than LDA.

We plan to classify data as per

- 1) Active (Motor execution) vs Rest
- 2) Active (Motor imagery) vs Active (Motor execution)
- 3) Active (Motor execution) vs Active (Motor Imagery) vs Rest
- 4) Active (Virtual Reality stimuli for Motor Imagery) vs Rest

We hypothesize that by incorporating virtual reality into fNIRS- BCI, studies that include complex motor imagery tasks can be done with ease by subjects. We also aim at higher hemodynamic response for motor imagery that could only be achieved by virtual reality stimuli (visual stimuli). Comparative studies of classification will be done, and study will be conducted to estimate whether virtual reality stimuli based paradigms can replace 2D paradigms. Hemodynamic responses will be compared and further conclusions will be drawn.

GOALS OF STUDY

Goals of study can be briefly classified into following category based on priority:

- Noise removal from fNIRS
- Virtual reality application in BCI
- Formulating strategy for optimal features for classification
- Compare classification scores of classifiers (LDA & RF)
- Compare run time of classifiers
- Compare classification scores of VR stimuli vs non VR stimuli
- Identify optimal features for classifying different tasks

Traditional many techniques are available for signal noise removal. Techniques like PCA, ICA are been used widely. But in real time applications like BCI, a fast and accurate technique is need of hour. Wavelet transformation especially is found to be advantageous for non-stationary signal like brain activity.

Designing paradigms for motor imagery is a challenging task. The success of motor imagery study depends of the ability of subject to image a task thereby eliciting motor imagery signals. Static picture of execution and flexion task might not properly elicit Motor imagery, because it itself is a dynamic state during which an individual mentally simulates a given action. Thereby dynamic action of task will be simulating by increased frame rate of pictures of task (ie) extension and flexion of elbow. An alternate way of conducting motor imagery studies is to make use of virtual reality. Virtual reality visual 3D stimuli had been proved to simulate immersive effect that can elicit higher hemodynamic response than normal 2D visual stimuli. Therefore Virtual reality stimuli based paradigms will be the primary goal. An app will be developed having exact time duration and block design of NIRstim paradigm. This app would have active block where 3D stimuli of extension and flexion is displayed and at rest block a static blank image is displayed. Total run time of VR app and NIRStim paradigm will be same, and both NIRstim paradigm and VR would be manually launched, so that approximately run time of both is same with error less than 0.5 second.

Data would be acquired and classification will be done. A novel strategy of improving 2D feature space by differentiating signal will be tested. Features would be extracted and best features would

be selected. Feature selection has been effectively applied to different problems and shown to have excellent strength in making machine learning algorithms robust. Picking best feature set among a pool of features is important for maximizing classification. We formulate new strategy for feature selection and classification. Methods like step wise feature selection are not considered.

LDA classifier will be used for classifying data with all seven features. But inclusion of nondiscriminatory features will bring down classification scores. Therefore Random feature based features ranking would be calculated and best three ranked features among seven features would be considered as optimal feature combination for LDA (LDA_optimal). We hypothesis that if features ranked by RF are in fact the features with best discriminatory power, LDA_optimal model should yield higher accuracy than LDA model which is having more feature space or yield same classification accuracy.

Classification scores of RF, LDA, LDA_optimal would be compared and conclusions will be made. Run time would also be calculated for the above models, and best strategy would be adopted.

The strategy thus derived, would also be used for VR fNIRS studies. VR stimuli if at better should elicit more hemodynamic response when compared to counterpart paradigm.

CHAPTER 2: REVIEW OF LITERATURE

BCI FOR STROKE REHABILITATION

Current rehabilitation therapies for stroke rely on physical practice (PP) by the patients. Motor imagery (MI), the imagination of movements without physical action, presents alternate neuro rehabilitation for stroke patients without relying on residue movements. However, MI is an endogenous mental process that is not physically observable.

Task-specific and repetitive exercise appears to be key factors in promoting synaptogenesis and is central elements in rehabilitation of motor weakness following stroke. Therefore stroke survivors can partially recover their lost motor function with remodeling of brain that could be achieved by rehabilitation that involved repetitive and task-specific physical practice (PP) (M. W. O'Dell et al., 2009). Since it is difficult or impossible for some stroke survivors to move the stroke-impaired limb during rehabilitation, motor imagery (MI), which is the mental process of imagination of movements without PP, represents an alternate rehabilitation approach (N. Sharma et al., 2006). Specific changes in cerebral activities were recorded during MI training, which mirrored the structural and functional reorganization due to neuroplasticity (F. Di Rienzo et al., 2014). Early studies of BCI devices being used for rehabilitation have suggested the potential for meaningful gains in motor function to be achieved even after traditional therapies have failed to facilitate full recovery (Liu et al., 2012; Ono et al., 2014; Young et al., 2014).

The rationale of performing MI arises from the neural correlation it shared with PP (M. Jeannerod et al., 1995). The main advantage of MI in rehabilitation is that stroke survivors who have difficulty in performing PP can still perform MI. However, while PP is observable, MI is an endogenous mental process.

Recent advances in analysis of brain signals and improvements in computing capabilities have enabled people with motor disabilities to use their brain signals for communication and control without using their impaired neuromuscular system (J. R. Wolpaw et al., 2002). This technology, brain-computer interface (BCI), is useful in helping people who have suffered a nervous system injury by providing them with an alternative means of communication, mobility, and rehabilitation (J. J. Daly et al., 2008, A. Burns et al., 2014).

By reestablishing connectivity between cortical activity related to MI and feedback, the use of BCI might strengthen the sensorimotor loop and foster neuroplasticity that facilitates motor recovery (M. A. Dimyan et al., 2011). Control of cortical signals could be employed for the rehabilitation of motor and cognitive impairments of patients by offering on-line feedback in form of FES, about cortical activity associated with mental practice, motor intention, and other neural recruitment strategies during task-oriented practice (B. H. Dobkin et al., 2007). Hence, the use of BCI facilitates the alternate MI approach for neurorehabilitation in stroke.

Buch et al., 2008, first used a magneto encephalography (MEG)-based BCI to detect mu rhythm (9– 12 Hz) to provide visual feedback in which a screen cursor was raised or lowered toward the direction of a target displayed on the screen. Once MI was detected, an orthosis attached to the stroke impaired hand was triggered to provide a sensorimotor feedback.

Mihara et al., 2013, studied ten patients who received near-infrared spectroscopy (NIRS)-based BCI with visual feedback versus ten other patients who received NIRS-based BCI with irrelevant feedback. The results showed that the former group yielded averaged motor improvements of 5.0 measured by Fugl-Meyer motor assessment (FMMA) (A. R. Fugl-Meyer et al., 1975) compared to 2.3 in the latter group, proving MI training can be helping for stroke rehabilitation. The Fugl-Meyer Assessment (FMA) is a stroke-specific, performance-based impairment index that's designed to assess motor functioning, balance, sensation and joint functioning in patients with post-stroke hemiplegia.

Ramos-Murguialday et al., 2013, performed a randomized control trial on 16 patients who used EEG-based BCI to detect motor intention with hand and arm orthosis feedback versus 14 other patients who used EEG-based BCI with random orthosis feedback. Both groups received physiotherapy. The results showed that the group trained with MI, yielded averaged motor improvements of 3.4 measured by combined hand and modified arm FMMA compared to 0.4 in the non-MI group. This also proved the efficiency of MI, when compared to random feedback

Rayegani et al., 2014, studied ten patients who received occupational therapy (OT) with additional neurofeedback therapy for improving hand function versus ten patients who received OT with additional biofeedback therapy and ten patients who received only OT. The spectral power density of the sensorimotor rhythm band in the neurofeedback group significantly increased after mental motor imagery.

Ono et al., 2014, studied six patients who received EEG-based BCI with simple visual feedback of the open and grasp animated picture of the hand versus six patients who received EEG-based BCI with somatosensory feedback using motor-driven orthosis to extend the fingers of the stroke-impaired hand. The results showed that three out of six patients in the latter group had motor improvements measured by the Stroke Impairment Assessment Set (N. Chino et al., 1994).

The studies of using BCI in (A. Ramos-Murguialday et al., 2013; S. Rayegani et al., 2014; T. Ono et al., 2014) had demonstrated clinical improvements. One of the studies showed significant motor improvements in using BCI and PP compared to random feedback and PP (A. Ramos-Murguialday et al., 2013).

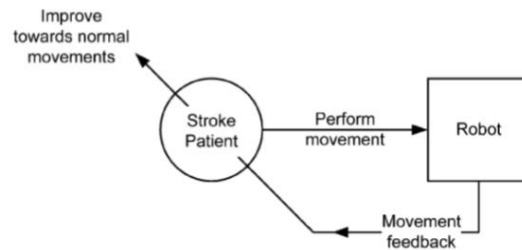


Figure 9: BCI to detect PP (Kai KengAng and Cuntai Guan 2015)

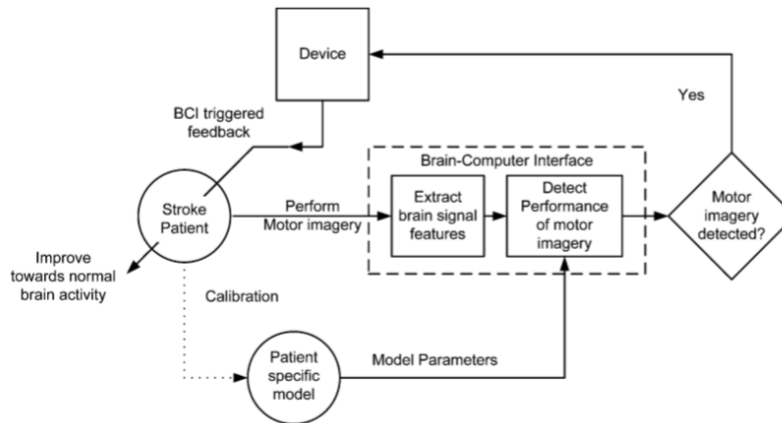


Figure 10: BCI to detect MI (Kai KengAng and Cuntai Guan 2015)

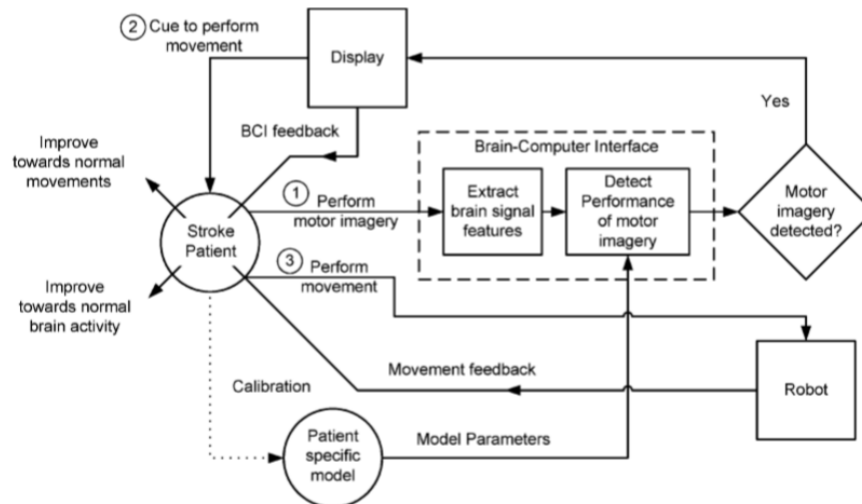


Figure 11: BCI to detect MI and provide concomitant of MI and PP (Kai KengAng and Cuntai Guan 2015)

The development of BCI devices to address persistent motor impairment after stroke may hold promise for additional meaningful recovery in stroke survivors (Young et al., 2014). Some studies of emerging therapies such as robot assisted therapy have suggested similar relationships in which increased therapy dose or intensity is associated with improved outcomes (Burgar et al., 2011; Hsieh et al., 2012). Some studies with neuromuscular electrical stimulation or constraint-induced movement therapy (CIMT) have found that increased therapy time is not always superior (Hsu et al., 2010), and in some cases higher intensity therapy has produced less improvement than lower intensity therapy administration (Dromerick et al., 2009). Hence it is advisable to use calibrate therapy intensity and time before implementation on patients.

Early neuroimaging studies in stroke survivors receiving rehabilitative therapies using BCI systems have also shown brain changes concurrent with the use of these therapies (Varkuti et al., 2013), and in some cases these markers of neuroplastic reorganization also correlate with individual behavioral gains (Varkuti et al., 2013)

One quantitative measure of neural activity is Laterality Index (LI), which reflects the degree to which a particular function is lateralized between the two hemispheres of the brain. LI can therefore be used as a marker of functional brain organization and has been applied in studies of stroke rehabilitation to examine relationships between changes in brain activation laterality and behavioral improvements using a variety of newer rehabilitative therapies (Johansen-Berg et al.,

2002; Bhasin et al., 2012) including approaches incorporating BCI technology (Young et al., 2014).

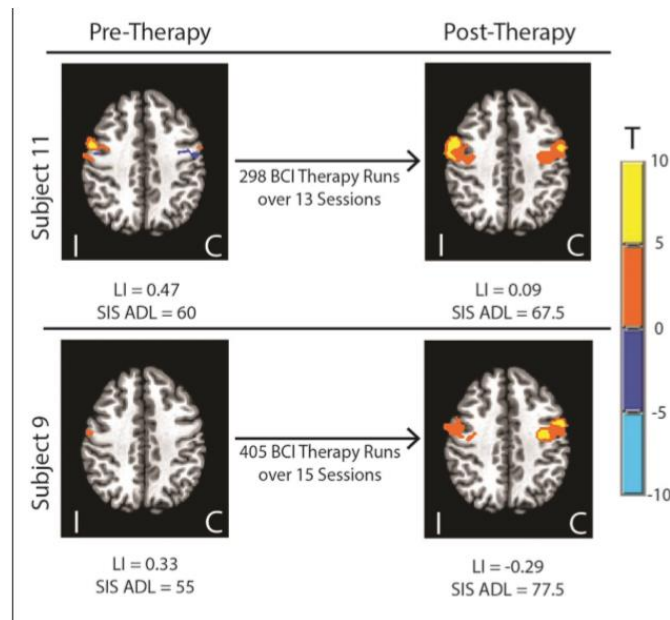


Figure 12: Laterality Index in Pre and Post therapy (Brittany M Young et al., 2014)

MOTOR IMAGERY

Motor imagery can be defined as a covert cognitive process of kinesthetic imagining of the movement of one's own body part without the involvement of muscular tension, contraction or flexion. Since the primary objective of BCI is to form a communication pathway for motor-disabled people, motor imagery is one of the most commonly utilized tasks in fNIRS-BCI. The motor imagery tasks include imagination of the squeezing of a soft ball, covert imagery of a simple or complex sequence of finger tapping, imagination of feet tapping, imagination of hand grasping/gripping, imagination of wrist flexion, imagination of flexion and extension of elbow, and folding and unfolding of specific fingers. Unlike motor execution tasks, the motor imagery signals are free of proprioception feedback.

Motor imagery (MI) is the mental simulation of a motor act, without any overt motor execution and thus refers to the capacity to produce kinesthetic representations of motor actions (Decety et al 1989). It is a complex cognitive operation (Jeannerod M et al., 1995) that is window into

representational stages of action. It is also perceptual information accessed from memory giving rise to experience of seeing with mind's eye (Kosslyn SM et al., 2001). MI would be used by brain, to predict the proprioceptive consequences of an action and then contribute to movement planning. The duration of task taken by motor imagery and motor execution were found to almost same. This underlies the similar cognitive process are activated for planning and control of movements, in both imagery and execution (Papaxanthis et al., 2002).

Michelon P et al., 2006 stated that MI is self-generated using sensory and perceptual processes, enabling the reactivation of specific motor actions within working memory. Therefore, sensory-perceptual, memory, and motor mechanisms are included in broader definition of the term.

For effective MI, Driskell JC et al., 1994, defined five conditions of interest: 1) type of task, 2) retention interval, 3) experience level of trainees, 4) length of practice and 5) type of control group.

MOTOR IMAGERY FOR REHABILITATION

The application of mental practice to rehabilitation began slowly in the late 1980s (FanslerCL et al., 1985, Warner L et al., 1988), and early 1990s (Decety J et al., 1990). Motor imagery practice refers specifically to the mental rehearsal of MI contents with the goal of improving motor performance (Braun SM et al., 2006, Malouin F et al., 2004). Evidence for neural reorganization as a result of MI training is emerging as well. It is conceivable to train using imagery which could further facilitate organization of central motor command (Lotze M et al., 2006).

Li S et al., 2004, had showed evidence of the existence of common brain area that is engaged in the performance and imagery of movements, by finger interactions in motor execution and motor imagery. Sharma et al., 2006, characterized motor imagery as a “backdoor” to accessing the motor system and rehabilitation at all stages of stroke recovery because “it is not dependent on residual functions yet still incorporates voluntary drive.”

Motor imagery required activation of brain regions, involved in movement preparation and execution accompanied with motor movement inhibition. Because MI is inexpensive and accessible and because of the increasing number of reports about the benefits of MI in improving motor performance.

Abundant evidence on the positive effects of MI practice on motor performance and learning has been published. Mental practice is found to improve athletics performance and is suggesting as an alternative to motor practice. As motor practice for a longer period of time leads to fatigue, motor imagery practice could replace motor execution practice for better results with athletic subjected to fatigue (Suinn RM et al., 1997). Nyberg L et al 2006 had conducted fMRI studies to decipher neural correlation between motor execution and motor imagery. He had concluded that motor imagery training could be used instead of motor execution training for improving motor activity of brain.

Mental practice was found to be effective in stroke rehabilitation (Braun SM et al., 2006). Braun had hypothesized that by combining covert and overt motor practice, linking of kinesthetic information with mental representations is possible and that would be more suitable for stroke patients received physiotherapy. For individuals who are healthy or those who have health-related problems, the rehearsal or practice of imagery tasks has been proven to be either beneficial by itself or in addition to physical motor practice (Sharma N et al., 2006).

Enhancements of performance with motor imagery include gains in strength (Sidaway B et al., 2005), improved speed in arm pointing capacity,(Gentili R et al., 2006) increased range of motion of the hip joint when MI was added to proprioceptive neuromuscular facilitation, and improved postural control in elderly people (Hamel MF et al., 2005). MI practice to facilitate the mastering of perceptive motor professional skills such as nursing and surgery has been demonstrated (Bachman K et al., 1990). For imagery applied in the sports context, positive effects have been reported in speed, (Blair A et al., 1993, Boschker MS et al., 2000), performance accuracy (Yue G and Cole KJ 1992), muscle strength, movement dynamics (Yaguez L et al., 1998) and motor skill performance (Taktek K et al., 2004).These studies consistently found that the greatest improvements in motor performance occurred with interventions that combined physical and mental practice, followed by physical practice alone, and then by MI practice alone, which was superior to no practice at all (Page SJ et al., 2001, Malouin F et al., 2004).The ability of individuals with chronic hemiplegia to achieve functional gains through imagery practice has further been supported by reports of significant, long-standing improvement in wrist movements and object manipulation in 2 patients⁵⁰ as well as in the improvement in line tracing in 3 patients with right post-stroke hemiparesis (Yoo E et al., 2001). In patients with chronic stroke, daily home practice

of moving tokens with the affected hand for a total period of 4 weeks was associated with significance improvement in task performance compared with the progress made by control group subjects (Dijkerman HC et al., 2004). Cramer and colleagues (Cramer SC et al., 2006) also found activation of cortical networks in accordance with imagery of specific movements, which suggested to them that brain motor system function can be modulated independently of voluntary motor control and peripheral feedback. They concluded that motor imagery training might have value as an adjunct to restorative interventions targeting post-SCI deficits (Cramer SC et al., 2006).

Some authors have claimed that familiarity is a prerequisite for successful use of MI practice. Mulder and associates (Mulder T et al., 2004) found that after mental practice, motor performance of a new motor task (big toe abduction) improved substantially in a group of people who had previously mastered the task compared with the group with no previous practice

VR FOR REHABILITATION

VR is the interaction of the person in the real world with a virtual environment (VE), generated by a computer. VR is defined as a “high-end-computer interface that involves real time simulation and interactions through multiple sensorial channels”. VR when augmented with exercise can be used for motor rehabilitation training and further for restoring postural balance and walking function (de Bruin ED et al., 2010).

VR had recently found tremendous interest in health care industry. It acts as a good communicative interface and learning technique which had been used in medicine education, surgical simulation and planning, virtual endoscopy, neuropsychological assessment and rehabilitation (Riva G et al., 2003).

Visual, auditory, vibrotactile, proprioceptive, haptic, knowledge of performance and knowledge of results can be given as feed to users with VR. This feedback about performance can enhance motor learning and permits individuals to safely explore their environments independently, which in turn increasing their sense of autonomy and independence in high-intensity training protocols (Deutsch JE et al., 2007). Keshner EA et al., 2007 had given both visual and motor stimuli as feedback in his study with VR, for differentiate between patients experiencing visual vertigo.

MI and VR have in common a cognitive significance on movement. MI requires sensory and perceptual processes, (Lequerica A et al., 2002) and interactions in VR engage participants in

cognitive and motor activities simultaneously, MI is requiring for planning, attention, sensory integration, and information processing of stimuli provided by the VE (Cole SW et al., 2012, Jacoby M et al., 2013). Both MI- and VR-based therapies were shown to have merit in rehabilitation of walking.

The application of MI and VR to assess sensorimotor and cognitive processes and to remediate balance and mobility for people with Parkinson disease is slowly emerging. The main reason for using such techniques is their ability to deliver a combined motor-cognitive experience in a safe, ecologically valid therapeutic environment, using a variety of tests or stimuli, which can be manipulated and personalized to the user. Virtual reality had proved to be effective for mental health. The rehabilitation techniques of physical exercise and mental exercise are beneficial to neurological disorders patients affected by parkinsons disease, alzheimers disease and various cognitive impairments (Matta Mello Portugal E et al., 2013).

Jungjin Kim et al., 2015 had tested feasibility of VR program for improving upper motor functions and activities of chronic stroke patients. Activities of chronic stroke affected patients are affected due to deficiencies in muscle strength, fine motor control, somatosensory perception and motion range. VR based rehabilitation has been suggested as alternative therapy for improving motor activities for stroke patients. Jungjin Kim et al., 2015 had embedded exercise direction, movement velocity, movement pattern, visual feedback and auditory feedback. VR based trained was proved to improve motor functional abilities in upper limb and activities of daily life. Virtual Reality-Based Approaches had also been studied for enabling walking for people post stroke.

VR coupled with physical exercises are proved to improve physical performance and cognitive abilities, thanks to neuroplasticity of brain.

During training of patients in VR, subject is immersed in virtual environment, which stimulates sensory system, thereby stimulating virtual environment in subject mind, and producing mental responses to that environment which is virtual. This immersion technique can actually alter cognitive and motor responses. Immersion can also increase navigational abilities of patients. Especially activations in caudate nucleus, hippocampus, and parietal cortex are seen during VR training. You SH et al., 2005 proved, VR coupled exercise improved cortical reorganization in stroke patients. Maillot P et al., 2012 showed improvement of cognitive and motor abilities in old age adults with VR coupled exercises.

VR offers a relatively affordable rehabilitation environment for motor rehabilitation, which allows for the effective inclusion of repetition of task in exercise, post training evaluation of the effects, and flexibility to increase repetition of exercises. These features of VR make it attractive option for rehabilitation. In this respect, VR is used in the rehabilitation of post-stroke and brain injury patients, in the orthopedic rehabilitation of patients with Parkinson's disease, in balance exercises, and in practicing everyday activities.

McComas et al., 1998 had experimented on using VR for education and rehabilitation of children with autism. He had hypothesized by limiting number of stimuli in VR environment and by encouraging focusing on a particular task for duration of time, can actually helping in motivating and acting as learning tool for autism children. By breaking down complex tasks in simple tasks, and by giving training with respect to simple broken down tasks, can improve ability of autism patients. Therefore VR can be used a tool to help in learning difficult task for autistic and cerebral palsy patients. In other study by DariusA.Rohan et al., 2014, virtual reality class room environment was simulated for attention based BCI studies. This study high lightened that VR can be used for rehabilitation of Attention deficit hyperactivity disorder (ADHD) via BCI. Alon Kalron et al., 2016, had used CAREN virtual reality system for training on postural control in multiple sclerosis patients. His study concluded that VR based devices could be used as effective training method for balance training in multiple sclerosis patients. Patrice L. Weiss et al., 2014 had reviewed on role in virtual reality for cerebral plasy management.

Virtual reality had also been used for enhanced gait training. Subjects can be actively involved in gait training by VR, simulating motor pattern which resulted in greater motor learning and retention (Karin Brüttsch et al., 2011).

Jun Hwan Choi et al., 2014 had reviewed on commercial gaming virtual reality movement therapy on functional recovery of upper extremity in sub-acute stroke patients.

Valeria Manera et al., 2015 had studied on application of image based rendering virtual reality for increased focus and attention of training for cognitive impairment and dementia patients.

PHYSICS OF FNIRS

When a radiation of Intensity I_0 passes through a layer of length L of medium, part of radiation is absorbed by medium and rest is transmitted on the other side of medium. This phenomenon can be modeled by Lambert Beer law, where μ_a is absorption coefficient, z is radiation beam direction and I is radiation intensity.

$$dI = -\mu_a I dz \quad (1)$$

$$\int_{I_0}^I \frac{dI}{I} = \int_0^L (-\mu_a) dz \quad (2)$$

$$I = I_0 e^{-\mu_a L} \quad (3)$$

The absorption coefficient can be further decomposed into two factors: the absorbent medium concentration and molar extinction coefficient.

This equation doesn't take into account of the diffusion of radiation in the medium. Diffusion of radiation can either take place due to discontinuities in dielectric properties of medium or turbidity of medium. In living tissue like brain, diffusion of radiation is caused by the turbidity of the tissue.

The beer lambert law will be valid in case of radiation scattering, only when scattering coefficient is added to absorption coefficient.

$$I = I_0 e^{-(\mu_a + \mu_s)L} \quad (4)$$

Radiation can scatter in all directions, even in backward direction. It is then possible to collect radiation from the same side of the sample used for the radiation injection.

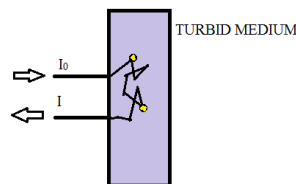


Figure 13: When using turbid media experiments in reflection geometry are possible. Scattering provides a positive probability to have radiation traveling backwards after encountering scattering centers in the medium.

The above corrected beer lambert law formula would be applicable for instances where chromophores concentrations $[c(t)]$ were constant over a period of time. But in real life scenario, chromophores concentrations would be changing over a period of time like in brain tissues. Hence concentrations changes with respect to time, too needs to be accounted in formula.

$$I(t_n) = I_0 e^{-([c(t_n)]\epsilon DL + G)} \quad (5)$$

Where scattering coefficients ($\mu_s L$) has been grouped together into term G . *Differential path length factor* D introduced to take into total random length travelled by light (ie) total length of travel is usually lengthier than the distance between source and detector, it reflects multiple times before reflecting completely back and reaching detector. Total of scattering coefficients doesn't change with respect to time.

Absorbance (A) can be calculated by

$$A = \ln \frac{I_0}{I} = -([c(t_n)]\epsilon DL + G) \quad (6)$$

The concentration changes of chromophores over a period of time can be calculated from the difference of absorbance (A) observed.

$$\Delta A_{mn} = A_m - A_n \quad (7)$$

$$= -([c_m(t_n)]\epsilon DL + G) - ([c_n(t_n)]\epsilon DL + G) \quad (8)$$

$$= \Delta C_{mn} \epsilon DL \quad (9)$$

The net concentration change of chromophores during time period of t_m and t_n is

$$\Delta C_{mn} = \frac{\Delta A_{mn}}{\epsilon DL} \quad (10)$$

ΔC_{mn} in equation (10), can be written as sum of $\Delta[\text{Hb}]$ and $\Delta[\text{HbO}_2]$. By Collecting data at different times and then computing the absorbance variation values ΔA_{λ_1} and ΔA_{λ_2} , it is possible to write the following system of equations:

$$\Delta A_{\lambda_1} = (\epsilon_{\text{Hb},\lambda_1} \Delta[\text{Hb}] + \epsilon_{\text{HbO}_2,\lambda_1} \Delta[\text{HbO}_2]) D_{\lambda_1} L \quad (11)$$

$$\Delta A_{\lambda_2} = (\epsilon_{\text{Hb},\lambda_2} \Delta[\text{Hb}] + \epsilon_{\text{HbO}_2,\lambda_2} \Delta[\text{HbO}_2]) D_{\lambda_2} L \quad (12)$$

Two equations (11 & 12) and two unknown values can be solved and values of $\Delta[\text{HbO}_2]$ and $\Delta[\text{Hb}]$ can be calculated. When data is collected for every time frame solving linear equations for each time frame would give concentration values over time frame.

For increased light penetration and better view of inner brain activity, source detector separation of 3-4 cm is recommended. But this compromises the spatial resolution and sampling volume. These limitations can be avoided by multiple source and detector topography systems which give better spatial resolution (Boas et al., 2004; Strangman et al., 2002)

$$\begin{pmatrix} \frac{\Delta A_{\lambda_1}}{D_{\lambda_1} L} \\ \frac{\Delta A_{\lambda_2}}{D_{\lambda_2} L} \end{pmatrix} = \begin{bmatrix} \epsilon_{\text{Hb}, \lambda_1} & \epsilon_{\text{HbO}_2, \lambda_1} \\ \epsilon_{\text{Hb}, \lambda_2} & \epsilon_{\text{HbO}_2, \lambda_2} \end{bmatrix} \begin{pmatrix} \Delta[\text{Hb}] \\ \Delta[\text{HbO}_2] \end{pmatrix} \quad (13)$$

$$\begin{pmatrix} \Delta[\text{Hb}] \\ \Delta[\text{HbO}_2] \end{pmatrix} = \begin{bmatrix} \epsilon_{\text{Hb}, \lambda_1} & \epsilon_{\text{HbO}_2, \lambda_1} \\ \epsilon_{\text{Hb}, \lambda_2} & \epsilon_{\text{HbO}_2, \lambda_2} \end{bmatrix}^{-1} \begin{pmatrix} \frac{\Delta A_{\lambda_1}}{D_{\lambda_1} L} \\ \frac{\Delta A_{\lambda_2}}{D_{\lambda_2} L} \end{pmatrix} \quad (14)$$

Hemoglobin saturation can also be calculated from fNIRS since it is simply the ratio of ox hemoglobin and total hemoglobin.

NOISE REMOVAL

Low pass filters have been generally used for the filtering of high frequency instrumental noise. Experimental errors like motion artifacts can result in a spike-like noise. Several methods like Wiener filtering-based method (Izzetoglu et al., 2005), eigenvector-based spatial filtering (PCA-based filtering) (Zhang et al., 2005), wavelet-analysis-based methods (Power et al., 2010), Savitzky-Golay type filters (Shin and Jeong et al., 2014), and others (Cooper et al., 2012) have been proposed for motion artifacts correction. In Cooper et al., 2012, Principle component analysis, spline interpolation, wavelet analysis, and Kalman filtering approaches are compared to one another and to standard approaches using the accuracy of the recovered, simulated hemodynamic response function (HRF).

Physiological noises like heartbeat (1~1.5 Hz), respiration (0.2~0.5 Hz), Mayer waves (~0.1 Hz), and blood pressure fluctuations (Boas et al., 2004; Zhang et al., 2005; Franceschini et al., 2006; Huppert et al., 2009).

Spatial filters like Laplacian derivation or common average reference (CAR) was used for physiological noise removal from EEG signal (Q. Zhang et al., 2009). CAR on fNIRS was reported by Bauernfiend G et al., 2003, in which they had calculated mean of all channels and subtracted from each single channel and for every time point of deoxy-Hb signal. One researcher tried removing physiological noises from respiratory sinus arrhythmia R-R interval series using transfer function model. Bauernfiend G et al., 2003 again applied TF model to remove physiological influence from deoxy-Hb signal. Zhang et al used adaptive filtering (AF) for estimating changes in overlaying tissue using additional detectors, thus obtained signals are used by AF to estimate global interference and later remove them from target signal.

FOURIER TRANSFORMATION

Recently interest in using transformation methods like Fourier transformation, Short time Fourier transformation, Continuous wavelet transformation and discrete wavelet transformation for bio-signal processing have increased. Most of bio signals recorded are in compact time domain, and the important data is hidden in frequency domain. Fourier transformation, transforms time domain signal to frequency domain. FT gives only information about frequency but not time. But for signals like bio signals which are non-stationary FT is not an attractive option. When time localization of spectral components on non-stationary signals is needed, a transformation giving time – frequency representation is need of hour. Short time Fourier Transform and Wavelet Transform are capable of giving time and frequency representation of signal at the same time.

The uncertainty principle states that momentum and position of moving particle can't be found at the same time. In signal transformation too, time and frequency information of signal can't be found at the same time. In other words, spectral component at time instant can't be found. Instead we can investigate spectral component for a time interval. STFT yields fixed resolution at the time, and window is of finite length and has no finite frequency resolution.

WAVELET TRANSFORMATION

The continuous wavelet transformation was developed as an alternative approach to short term Fourier transform to overcome resolution problem in STFT. The width of window is changed as the transformation is calculated at every single spectral component.

The Wavelet Transform is defined by:

$$W_f(s, \tau) = \int f(t) \psi_{(s,\tau)}^*(t) dt \quad (15)$$

The transformed signal is a function of two variables, tau and s, the translation and scale parameters. The wavelets are generated from a wavelet function $\psi(t)$, called “mother wavelet”, which is defined as:

$$\psi_{(s,\tau)}(t) = \frac{1}{\sqrt{s}} \psi\left(\frac{t-\tau}{s}\right) \quad (16)$$

The term wavelet means small wave which is an oscillatory function window that is of finite small length. The term mother implies that the functions with different region of support that are used in the transformation process are derived from one main function, or the mother wavelet. These wavelets were the first to make discrete analysis practical. Ingrid Daubechies constructed these models with a maximum orthogonal relationship in the frequency response and half of the sampling rate, imposing a restriction on the amount of decay in a certain range, thereby obtaining a better resolution in the time domain. (Burrus et al., 1998).

A time history $S(t)$ is decomposed into some detailed (high-frequency) components and an approximated (low-frequency) component. The original signal $S(t)$ given by:

$$f(x) = Sm_0(t) + \sum_{m=-\infty}^{\infty} (d_m(t)) \quad (17)$$

Where d_m are detailed components:

$$d_m(t) = \sum_{n=-\infty}^{\infty} D_{m,n} \psi_{m,n}(t) \quad (18)$$

In the wavelet transform, the choice of a mother wavelet $\psi(t)$ is important.

Once the mother wavelet is chosen, computation starts with $s=1$ and continuous wavelet transformation is calculated for all the values of s greater than 1. Usually s values are band limited.

The analysis starts from higher frequencies and later move towards smaller frequencies. Analysis with smaller s value yields compressed wavelets, and with larger s value yields diluted wavelets. As the analysis proceeds forward, s value and τ value is also increases continuously.

If signal has spectral component at some value of s , the product of wavelet with signal will yield large value at the exact location where spectral component exist. Likewise if signal doesn't have spectral component for a value s , then product of wavelet with signal will yield small value.

Continuous wavelet transformation is time taking, and the information it provides is completely redundant and its tough task for reconstruction of signal. Discrete wavelet transform on the other hand is easy to work out, less time taking and provide sufficient information for analysis and reconstruction of signal.

In the discrete case, filters of different cutoff frequencies are used to analyze the signal at different scales. The signal is passed through a series of high pass filters to analyze the high frequencies, and it is passed through a series of low pass filters to analyze the low frequencies.

The resolution of the signal, which is a measure of the amount of detail information in the signal, is changed by the filtering operations, and the scale is changed by up sampling and down sampling. The procedure of DWT starts with passing signal through half band low pass filter, which removes all frequencies that are above half of highest frequency in signal. After passing through half of samples can be eliminated according to Nyquist's rule, thereby subsampling signal by 2. By subsampling signal by 2, the scale of signal is doubled, and resolution is halved. This procedure can be mathematically expressed as

$$y[n] = \sum_{-\infty}^{\infty} \phi[k].x[2n - k] \quad (19)$$

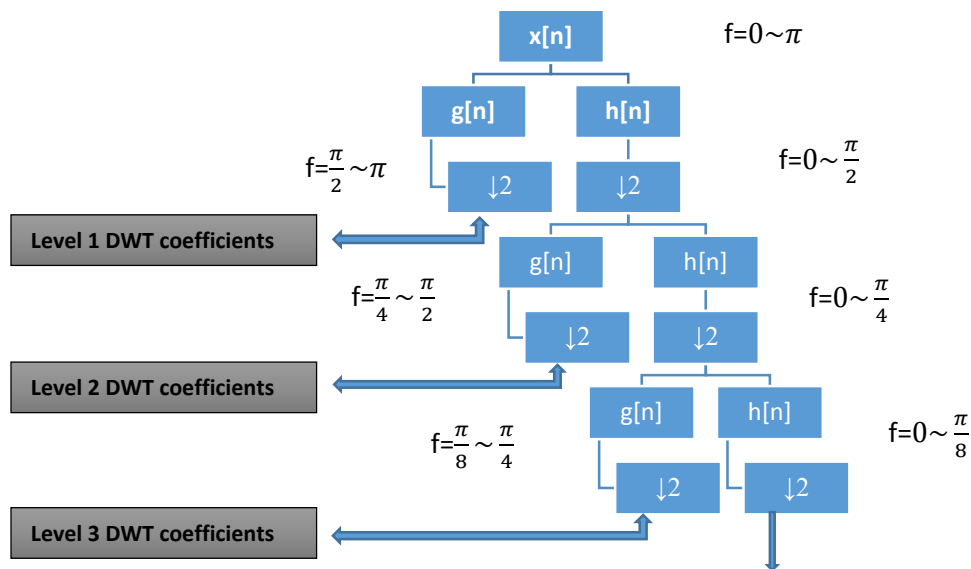
Sub sampling signal by 2, constitutes one level of decomposition and can be expressed as

$$y_{ig}[k] = \sum_n x[n].g[2k - n] \quad (20)$$

$$y_{low}[k] = \sum_n x[n].\phi[2k - n] \quad (21)$$

Where $y_{ig}[k]$ and $y_{low}[k]$ are the outputs of high pass and low pass filters after subsampling by 2.

DWT analyses signal at different frequency band with different resolutions, by decomposing signal to coarse approximations and detail information. The decomposition of signal can be done by successively filtering in high pass and low pass filters in time domain. It employs two set of functions called scaling function which can be associated with low pass filter, and wavelet function which can be associated with high pass filter. The decomposition halves time resolution and doubles frequency resolution. This procedure can be called as sub-band coding. At every level, filtering and subsampling will reduce time resolution by half and double frequency resolution.



Decomposition continues until two samples are left. The prominent frequencies will appear as high amplitude regions in DWT signal. If the prominent information lies in high frequencies, time localization of these frequencies is more precise. If prominent information lies in low frequencies, time localization is not precise as few signals are expressed at these frequencies. The net procedure is effect, offering good time resolution at high frequencies and good frequency resolution at low frequencies. Most of the biological signals are of this type. The frequency band that are not very prominent or the band that are associated with noises can be removed and net signal can be obtained by reconstructing DWT coefficients, thereby which data reduction without loss of signal and with reduction of noise is obtained.

Brain signals are non-stationary and have trends and repeated patterns, and with conventional methods of frequency analysis it is not possible for successful diagnostic classification (Subasi &

Erçelebi et al 2005). Wavelet transformation was found to be appropriate for time-frequency analysis, especially for non-stationary signals like brain signals (Asaduzzaman et al., 2010).

To evaluate brain activity in detail and to remove physiological noises, fNIRS signals are subjected to MRA (Tsunashima et al., 2009) through discrete wavelet transformation to decompose and reconfigure the signals.

CLASSIFICATION TECHNIQUES

Classification techniques are used to establish different brain states of subject. These classified signals output can be given as input of control commands for application interface like Functional muscle stimulator (FES). Classification of signal can done by machine learning techniques. Various classifiers have been used so far for fNIRS classification task. LDA is the most commonly used classifier for fNIRS BCI study. It makes use of Discriminant hyperplanes to separate data in classes. Due to its process simplicity and less computational requirement, it is highly suitable for real time BCI studies. LDA finds a vector in feature space (v), that maximum separates classes in ' v ' direction, maintaining less variance for each.

Classifier	Paper
LDA	Luu and Chau et al., 2009
LDA	Bauerfeind et al., 2011
LDA	Nasser and Hong 2013
LDA	Kaiser et al., 2014
LDA	Hong et al., 2015

Table 4: LDA classifier used for classification purpose in fNIRS BCI

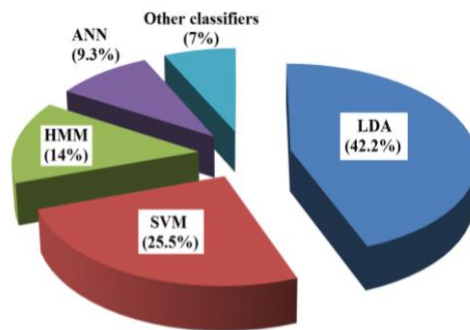


Figure 14: Distribution of classifiers used in fNIRS BCI

SVM classifiers had also been used for classification of fNIRS signals. It tries to maximize distance between separating hyper plane and nearest training points (otherwise called support vectors). Since it maximizes distance from nearest training points, it is known to enhance generalization capacities. SVM is a linear classifier but it can be made nonlinear by introducing kernel functions in it. Nonlinear SVM provides more flexible decision boundary that can aid in increased classification accuracy.

Classifier	Paper
SVM	Sitaram et al., 2007
SVM	Tai and Chau 2011
SVM	Tanaka and Katura 2013
SVM	Abibullalev and An 2012
SVM	Naseer et al., 2014

Table 5: SVM classifier used for classification purpose in fNIRS BCI

ANN is nonlinear classifiers that had recently been used for fNIRS BCI studies. ANN mimics brain activity and consists of assembles of artificial neurons that allows drawing of nonlinear decision boundary. It has been used for different architectures like multiple layer perception, Gaussian classifier, RBF neural networks.

Classifier	Paper
ANN	Abibullalev et al., 2012
ANN	Chan et al., 2012
ANN	Hai et al., 2013
ANN	Anthony and Bartlett 2009

Table 6: ANN classifier used for classification purpose in fNIRS BCI

HMM is nonlinear probabilistic classifier that provides probability of observing a given set of features that are suitable for classification of time series.

Classifier	Paper
HMM	Sitaram et al., 2007
HMM	Power et al., 2010
ANN	Zimmermann et al., 2013
ANN	Chan et al., 2012

Table 7: HMM classifier used for classification purpose in fNIRS BCI

FEATURE EXTRACTION AND SELECTION

Feature extraction and feature selection are two important steps that determine the accuracy of brain state classification. In BCI studies, statistical properties of time-domain signals like mean, variance, and peak, no of peaks, sum of peaks, skewness and kurtosis have been used so far.

In previous studies, Naseer et al., 2013 classified motor imaginary activity with mean accuracy of 83% using mean and slope of $\Delta cHbR$ as features. Naseer et al (2014) classified mental arithmetic vs rest with accuracy of 74.2% using mean values of values of $\Delta cHbO(t)$ and $\Delta cHbR(t)$.

In M. Jawad Khan et al., 2015, drowsiness state was classified with mean accuracy of about 83% using mean $\Delta cHbO$, signal peak and sum of peaks as features.

In other study to determine optimal feature combination, Naseer et al., 2016 classified mental arithmetic task with accuracy upto 93% using optimal feature combination.

- In Naseer et al., 2014, binary decision decoding was done with mean accuracy of 74% with LDA, and 82% with SVM using mean $\Delta cHbR$ and mean $\Delta cHbO$.
- In Naseer et al., 2014, binary decision decoding was done with mean accuracy of 86% with SVM using signal slope of $\Delta cHbR$ and $\Delta cHbO$.
- In Sitaram et al., 2007 motor imagery was classified using mean amplitude changes of $\Delta cHbR$ and $\Delta cHbO$ with maximum accuracy of 89% using HMM.
- Coyle et al., 2007, classified binary switch control with accuracy of 50-85% using mean $\Delta cHbO$ as feature.
- Naito et al., 2007 classified mental task with accyrcy of 80% using maximum and mean $\Delta cHbO$ as features with LDA.

- Tai and chau et al., 2009, classified visualised cued positive and negative emotional induction tasks with accuracy of 75% using mean, variance, skewness, kurtosis as features combined with LDA and SVM.
- Luu and chau et al., 2009, classified neural correlates of decision making with accuracy of 80% using mean $\Delta cHbO$ as feature with FLDA. In Shin and Jeong et al 2014, motor execution was classified with accuracy of 95% using Mean, amplitude, slope, delay, variance and median as features with Naive Bayes classifier.
- In Zimmermann et al., 2013, motor execution was classified with accuracy of 88.5% using combination of $\Delta cHbR$, $\Delta cHbO$ and biosignals as features with HMM.
- In Liu et al., 2013, nueral correlation of visual stimuli was classified with accuracy of 90% using mean $\Delta cHbR$, $\Delta cHbO$ and EEG amplitude as features with step wise classifier.
- In Abibullaev and An 2012, Object rotation, letter padding and multiplication was classified with accuracy of 90% using filter coefficients from wavelet transformation as features with SVM.
- In Chan et al., 2012, mental signaling was classified with accuracy of 63% using $\Delta cHbR$ and $\Delta cHbO$ as features with ANN.
- In Hong et al., 2015, motor imagery and mental arithmetic was classified with accuracy of 75% using mean and slope of $\Delta cHbO$ as features with multi class LDA.
- In Hwang et al., 2014, Motor Imagery, mental singing, mental arithmetic, mental rotation and mental character writing was classified with accuracy of 70% using mean $\Delta cHbR$, $\Delta cHbO$, $\Delta cHbT$ and $\Delta cHbR$ as features with LDA.

Feature	Reference
Mean	Sitaram et al., 2007; Power et al., 2010; Holper and Wolf, 2011; Faress and Chau, 2013; Naseer and Hong, 2013, 2015b; Power and Chau, 2013; Hong et al., 2014
Variance	Tai and Chau, 2009; Holper and Wolf, 2011), slope (Tai and Chau, 2009; Power et al., 2011; Naseer and Hong, 2013, 2015b; Hong et al., 2014
Kurtosis	Holper and Wolf, 2011
Skewness	Tai and Chau, 2009; Holper and Wolf, 2011
Number of peaks	M Jawed khan et al 2015
Sum of peaks	M Jawed khan et al 2015

Peak value	Tai and Chau, 2009; Cui et al., 2010; Bauernfeind et al., 2011; Holper and Wolf, 2011
-------------------	---

Table 8: List of features used for classification purpose

Mean, variance, and peak, no of peaks, sum of peaks, skewness and kurtosis of delta HbO are compute

Previous studies like Naseer Noman et al., 2015 had focused on determining optimal feature combination for LDA classification. Various feature combinations are studied and concluded that mean and peak features would be best for classification, owing to their highest classification accuracies.

Common strategy for reduction in number of features in LDA and other algorithms is step wise method. In step wise method, prediction scores are estimated for combinations of two features from all available features. This procedure can be repeated for combinations of three and more features too. Finally a list of prediction scores is made, and the combination which gives maximum score is considered to have best discriminatory power, which can classify data with more precision and accuracy than all other feature combinations.

Sometimes the optimized feature selected might not give maximum classification accuracy for all the subjects. But the above mentioned strategy of optimal feature selection is tardy, and if there is some way that can evade from manually optimizing features, that would be of great use.

But often feature reduction procedure is criticized as not being a logical one for elimination of features and its time consuming too.

Therefore in our project, we had decided to deploy random forest algorithm, and take advantage of its feature selection module, which considerably reduces our time in identifying best optimal features.

In our project, the features extracted were Mean, Variance, Skewness, Kurtosis, Peak, Number of Peaks and Sum of Peaks. Instead of picking up best features among available features by traditional method, we left the task of identification of best features based on its importance score to Random forest.

RANDOM FOREST

Random forests are type of ensemble methods in machine learning. Random forest is most successful ensemble methods which sometimes had exhibited performance better than boosting and support vector machines. Random Forests are the brain child of Breiman (Breiman, L et al., 2001) and It out performs to other classifiers like Support Vector Machines, Neural Networks and Discriminant Analysis in terms of accuracy, and overcomes the problem of over fitting. It is also proved to be effective classifier for classification of big data in biomedical, biotechnology, and medical imaging fields. Many competitions in kaggle had been won by using Random Forest classifier. When other classifier is hard to interpret, Random forest offers more intuitive illustrations (Strobl et al., 2009).

Two well know ensemble methods are boosting (Shapire et al., 1998) and bagging (Breiman et al., 1996). In boosting method, successive tree give weight for score that is incorrectly predicted by previous trees, and finally a weighted vote is taken. Where as in bagging method each tree is independent, where it classifies a bootstrap sample of dataset and finally simple majority of votes is taken. Breiman had proposed random forest which had rectified the defects of bagging and boosting. He added extra layer of randomness to bagging, thereby significantly improving classification accuracy. The random sampling and ensemble strategies utilized in RF enable it to achieve accurate predictions as well as better generalizations. This generalization property comes from the bagging scheme which improves the generalization by decreasing variance, while similar methods like boosting achieve this by decreasing bias (Yang et al., 2010). Breiman had defined random forest as “a classifier consisting of a collection of tree structured classifiers $\{h(x, \Theta_k), k=1, \dots\}$ where the $\{\Theta_k\}$ are independent identically distributed random vectors and each tree casts a unit vote for the most popular class at input x .

Randomization for increasing diversity is proved to be efficient method of classification. Forests have gained a substantial interest in machine learning because of its efficient discriminative classification (Amit, Y et al., 1997). Decision tree is provided with random subspaces which have both random selected set of features and subset of data which is taken by random sampling of training data. Features are randomly selected at each decision node, which greatly reduces the correlation between trees; thereby increase its classification accuracy. This somewhat counterintuitive strategy turns out to perform very well compared to many other classifiers,

including Discriminant analysis, support vector machines and neural networks, and is robust against overfitting (Breiman et al., 2001).

Random forest outperforms decision trees, thanks to inclusion of its unique voting scheme, where every tree vote for most popular class and majority of votes are taken, from which accuracy is predicted.

Thereby RF classification accuracies are best than Adaboost, bagging and boosting; relatively faster than bagging and boosting; robust to noise; gives estimates of error, strength, correlation and variable selection; don't overfit and offers better understanding of how classification is done.

As such the advantages of Random Forest are (N Horning et al., 2013)

- overcoming the problem of over fitting
- In training data, they are less sensitive to outlier data
- Parameters can be set easily and therefore, eliminates the need for pruning the trees
- variable importance and accuracy is generated automatically

RF FEATURE RANKING

In most of BCI the main aim is to make accurate prediction with maximum prediction accuracy. Various researchers had experimented on various available time series features for their predictive analysis. It is obvious that the success of classification best depend on discriminative power of features. Most of features calculated may not contribute positively towards classification decision of algorithm. For robust model, features having best discriminative power are chosen among a pool of features by feature selection.

Feature selection (also called variable or attribute selection) is the process of choosing a subset of features that best represent a model.

Feature selection has been effectively applied to different problems and shown to have excellent strength in making machine learning algorithms robust. Feature selection has been investigated in different machine learning fields such as image retrieval (S. Yu et al., 2010), bioinformatics, and medical imaging (J.C.Fu et al., 2005, L).

Wrapper methods use predictive models for the evaluation of feature subset and are more demanding than filter methods (Deng H et al., 2012). Sequential backward Selection (SBS) (Cotter SF et al., 2001) is one of the most commonly used wrapper methods which is based on greedy hill-climbing search method. Support vector machine with recursive feature elimination (SVM-RFE) (Guyon I et al., 2002) is a well-known example of embedded methods. SVM-RFE eliminates those features which have lowest weight obtained from a trained SVM.

Thereby optimally selected features, also increases performance of classification when compared to high dimensional feature space (Bhattacharyya S et al 2014)

But keeping in view on real time feedback requirement in online BCI, researchers have struck with the fast and reliable classifiers like LDA, HMM and SVM. Ensemble methods of classification haven't been done on fNIRS so far as our knowledge is concerned. We had classifying our signal with popular ensemble called Random Forest. Random forest is a classifier that quenches the major effort of researchers in figuring out the best optimal selection of features for their classification. Owing to the ease at which it identifies best discriminate features for classification purpose and build good accurate model, we had decided to deploy RF for our offline BCI, finger tapping task.

In Bagging (Breiman 1996), trees are built on random bootstrap copies of the original data, there producing different decision trees. In Random Forests (Breiman 2001), Bagging is extended and combined with a randomization of the input features that are used while splitting internal nodes. Instead of looking for the best split among all features, the Random Forest algorithm selects, at each node, a random subset of features K and then determines the best split among K set of features.

The features are scored with Mean Decrease Impurity importance (MDI) which uses Gini index as impurity function. Other way of getting feature importance score was proposed by Breiman (2001, 2002), He proposed to evaluate the importance of a variable X_m by measuring the Mean Decrease Accuracy (MDA) of the forest when the values of X are randomly permuted in the out-of-bag samples.

Strobl et al., 2007 compare both MDI and MDA and show experimentally that the former is biased towards some predictor variables. Strobl et al., 2008 later showed that MDA too is biased, and that it overestimates the importance of correlated variables.

In a study by Gilles Louppe et al., 2013 they had demonstrated that MDI importances as computed by totally randomized trees exhibit desirable properties for assessing the relevance of a variable: it is equal to zero if and only if the variable is irrelevant and it depends only on the relevant variables.

CHAPTER 3: METHODOLOGIES

fNIRS DATA ACQUISITION

The brain signals for classification were obtained using a 20 channel continuous wave system (NIRSPORT 8x8 by NIRX LLC). The NIRX system is equipped with LED illuminators and photo diode detectors. The two wave lengths used in the device are 760 nm and 850 nm. A scan rate of 7.81 Hz is used for the acquisition of optical signals. The signals were acquired using a motor montage (Figure 15) which covers motor cortex of both the hemispheres. Approach of utilizing the standard 10-20 international electrode system for EEG in the fNIRS optode placement is popular due to the simplicity. This method will measure the standard reference locations of the head as in 10-20 system like C_z . The C_z location, defined as the intersection point of two lines formed by 50% of the distance between the left and right tragus and 50% of the distance between the nasion andinion, will be calculated for each subject individually based on anatomical measurements obtained during data collection.

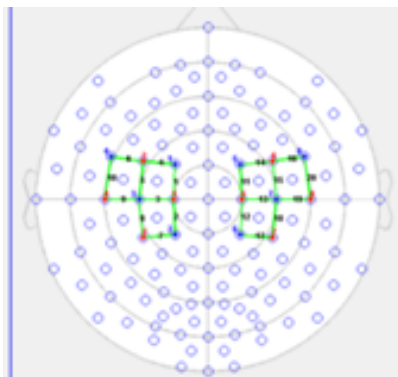


Figure 15: Motor montage

The inter-optode distance was fixed at 3 cm. The subjects were seated in a comfortable chair facing a computer screen and were asked to relax and restrict their head movement to minimize any variations in the hemodynamic response due to the motion artifacts. Once subject seated in a

comfortable position, head cap is fitted over subject head. Optodes are fitted over motor cortex montage of head cap and connected to fNIRS system. NIRStar, multi-platform controlling environment software has been used to investigate paradigms designed in NIRStim.

Built-in features such as automatic calibration and diagnostics are put to work to assure that your experiment begins by collecting the best data possible. The NIRStar signal quality indicator allows you to effortlessly review the integrity of any incoming data.



Figure 16: Signal quality

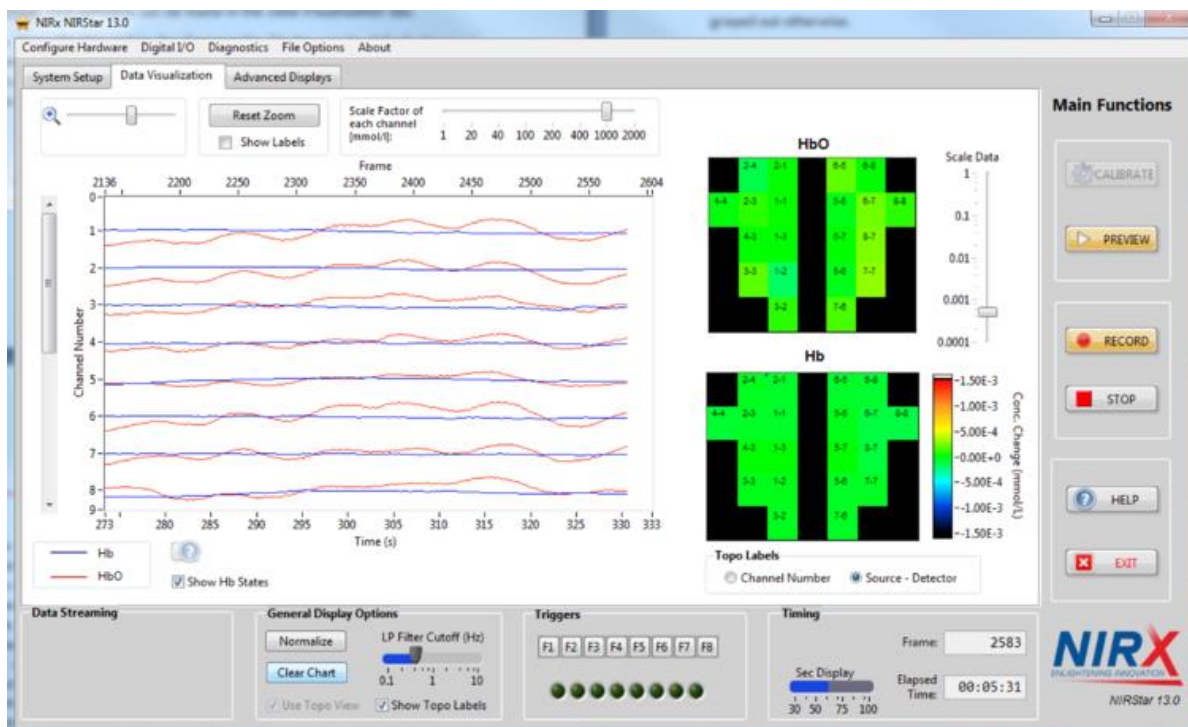


Figure 17: NIRStar Screenshot

Subjects were given prior instructions about task to be undertaken. Before every recording single trail run was done, to get subject acquiesced with task.

Experiment	Number of subjects
Experiment1	16
Experiment 2.1	3
Experiment 2.2	3
Experiment 3	5

Table 9: Number of subjects recruited per experiment

Experiment	Task	Classification	Paradigm
Experiment1	Motor execution (finger tapping)	Motor execution vs Rest	Paradigm 1
Experiment 2.1	Motor execution (Flexion and extension) and Motor imagery (Flexion and extension)	Motor Imagery vs Motor execution	Paradigm 2
Experiment 2.2	Motor execution (Flexion and extension) and Motor imagery (Flexion and extension)	Motor Imagery vs Motor execution vs Rest	Paradigm 2
Experiment 3	Motor imagery ((Flexion and extension) with VR	Motor imagery vs Rest	Paradigm 3

Table 10: List of experiments and details about task, classification and paradigm

For fNIRS acquired with VR stimuli, subject was fitted with VR headset with head strap and care was taken not to disrupt optode location. Android phone was fitted in phone holder compartment, and aligned proper with phone aligner clamp. Once VR app was launched, magnetic flip is closed. Subject was asked to readout countdown time, once countdown time falls to zero, NIRStim was started, thereby manually synchronizing NIRStim paradigm total run time with VR app run time.



Figure 18: NIRX fNIRS system

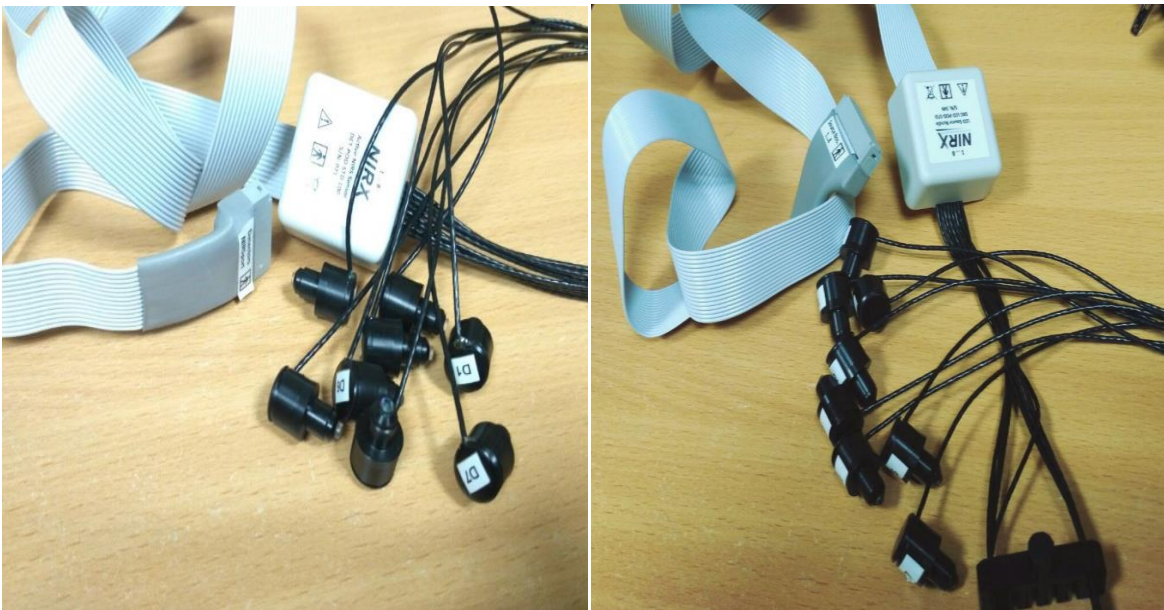


Figure 19: Source optodes (eight) and Detector optodes (eight)



Figure 20: Optodes fitted to cap, over motor cortex



Figure 21: Subject doing finger tapping task



Figure 22: VR headset



Figure 23: Subject with VR and fNIRs (Front view and top view)



Figure 24: Subject doing motor execution



Figure 25: Android phone with VR app mounted on VR headset

PARADIGMS DESIGN

A paradigm is a temporal allocation of stimuli to acquire functional responses from subject. Various paradigms with stimuli or events are used to evoke hemodynamic activation of subject. The precise design and effective duration of stimuli, is carefully designed and executed for good results (Jija S James et al., 2014). The commonly used experimental designs for functional studies are Block Design and Event Related Design.

Block design is first designed and widely used paradigm for functional studies. Block design consists of discrete on/off or active/rest periods. Active period represents period of stimulus presentations and rest period represents to state of rest or baseline of brain activity. Especially for classification of brain states that needs discriminating oxy hemoglobin concentration for different brain state, block design is best option.

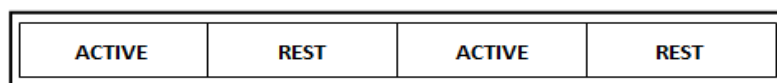


Figure 26: Block design

Advantages of Block Design:

- Single block design adequate for early exploratory stages of research
- Block design allows for experimental flexibility
- Multiple epochs can be given in single block design by including epochs in active phase
- Block design is adept for experiments pertaining to detect subtle hemodynamic response differences across test conditions
- The temporal design of Block design allows easy detection of non-fluctuating noises like physiological noises.

Disadvantages of Block Design:

- Can be predictable and has potential confounds like anticipation and rapid habituation
- Difficult to control specific cognitive state for relative long period
- Hemodynamic response might be constant across epoch
- Hemodynamic response might change from active block to active block

Rehabilitation techniques with help of BCI, usually classifies brain signal to either rest or active phase. Tasks like motor execution and motor imagery are widely used for BCI. We too employed motor and motor imagery in our project. Finger tapping task was done for motor execution task and elbow extension and flexion for motor imagery task.

Three Paradigms are designed, catering our need of classifying brain states. We concluded at classifying motor active vs rest, motor imagery vs rest, VR motor imagery vs rest and motor vs motor imagery vs rest.

PARADIGM 1

This paradigm was designed for the purpose of classifying brain states in motor active and rest states. Visual stimuli were given to guide subject in tapping his right and left hand alternatively in the paradigm, and subject was to execute finger tapping for active block duration of paradigm and be in rest for rest phase of paradigm.

Purpose: Classify brain states to active and rest

Task: Tapping hand left and right in alternative active blocks

Total duration: 125 seconds

Total blocks: five active and five rest

ACTIVE	REST	ACTIVE	REST	ACTIVE	REST	ACTIVE	REST	ACTIVE	REST
--------	------	--------	------	--------	------	--------	------	--------	------

Phase	Task	Duration	Tapping hand	Stimuli
ACTIVE 1	Finger Tapping (Motor execution)	10 seconds	Right	Visual (Text)
REST 1	Resting state	15 seconds	Nil	Nil
ACTIVE 2	Finger Tapping (Motor execution)	10 seconds	Left	Visual (Text)
REST 2	Resting state	15 seconds	Nil	Nil
ACTIVE 3	Finger Tapping (Motor execution)	10 seconds	Right	Visual (Text)
REST 3	Resting state	15 seconds	Nil	Nil
ACTIVE 4	Finger Tapping (Motor execution)	10 seconds	Left	Visual (Text)
REST4	Resting state	15 seconds	Nil	Nil
ACTIVE 5	Finger Tapping (Motor execution)	10 seconds	Right	Visual (Text)
REST 5	Resting state	15 seconds	Nil	Nil

Table 11: Paradigm 1 details

PARADIGM 2

This paradigm was designed for the purpose of classifying brain states into motor imagery or motor execution. Brain state can also be classified into motor imagery or motor execution or rest states. Visual stimuli were given in form of motor execution images to guide subject regarding tasks to be done in active and rest blocks. Subject was to execute motor execution for active block duration of paradigm, be in rest for rest phase of paradigm and motor imagery for the next active block duration of paradigm. Rest phase is followed after each active block and the motor execution and motor imagery are repeated alternatively

Purpose: Classify brain states to motor state, motor imagery and rest states

Task: Elbow flexion (motor execution) for active block series (1, 3, 5 and 7) and elbow flexion imagery for block series (2, 4, 6 and 8)

Total duration: 192 seconds

Total blocks: eight active and eight rest

Figure 27: Extension and flexion images

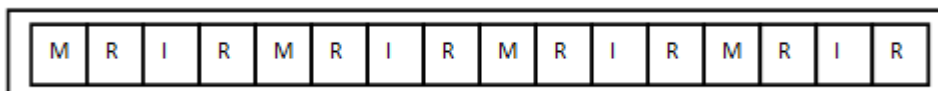
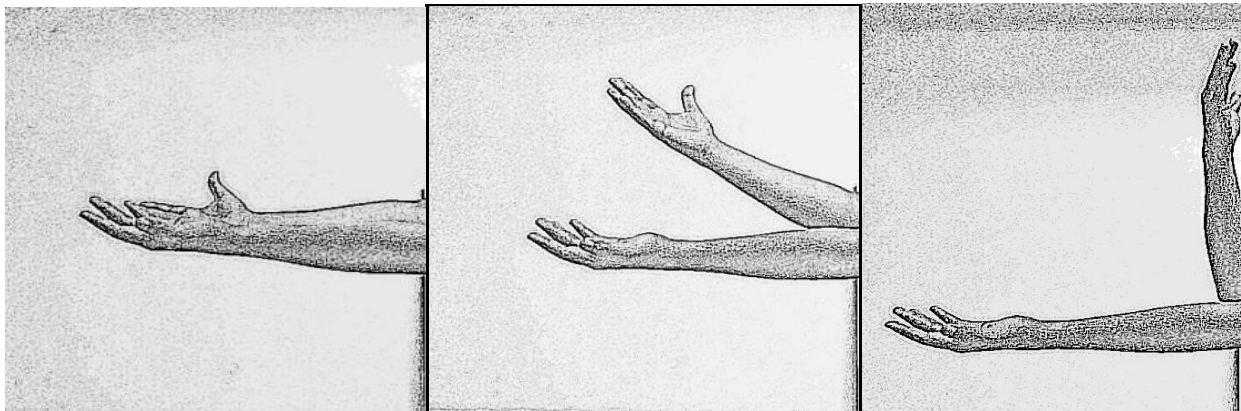


Figure 28: Block design, where M is motor execution, R is rest and I is motor imagery. Each block is of 12 seconds

Phase	Task	Duration	Elbow Movement	Stimuli
ACTIVE 1	Elbow extension & flexion (Motor execution)	12 seconds	Both hands	Visual (Images)
REST 1	Resting state	12 seconds	Nil	Nil
ACTIVE 2	Elbow extension & flexion (Motor Imagery)	12 seconds	Both hands	Visual (Images)
REST 2	Resting state	12 seconds	Nil	Nil
ACTIVE 3	Elbow extension & flexion (Motor execution)	12 seconds	Both hands	Visual (Images)
REST 3	Resting state	12 seconds	Nil	Nil
ACTIVE 4	Elbow extension & flexion (Motor Imagery)	12 seconds	Both hands	Visual (Images)
REST4	Resting state	12 seconds	Nil	Nil
ACTIVE 5	Elbow extension & flexion (Motor execution)	12 seconds	Both hands	Visual (Images)
REST 5	Resting state	12 seconds	Nil	Nil
ACTIVE 6	Elbow extension & flexion (Motor Imagery)	12 seconds	Both hands	Visual (Images)
REST 6	Resting state	12 seconds	Nil	Nil
ACTIVE 7	Elbow extension & flexion (Motor execution)	12 seconds	Both hands	Visual (Images)
REST 7	Resting state	12 seconds	Nil	Nil
ACTIVE 8	Elbow extension & flexion (Motor Imagery)	12 seconds	Both hands	Visual (Images)
REST 8	Resting state	12 seconds	Nil	Nil

Table 12: Paradigm2 details

PARADIGM 3

This paradigm was designed for the purpose of classifying brain states into motor imagery or rest states. Stimuli were given in form of Virtual Reality where a subject views motor execution task in virtual reality. Subject was to execute motor imagery for active block duration of paradigm, be in rest for rest phase of paradigm.

Virtual reality based motor imagery android app

The virtual reality motor imagery android app was developed for replacing standard image based paradigm design. Due to inability to incorporate GIF pictures in paradigm and increased difficulty in representing task with pictures we had sought help of virtual reality based android app.

Human character was developed in ‘The make human software’. Animation of human character was developed in “Autodesk Maya”. The further scenarios for active block and rest block were designed in “Unity game engine”. Later the project in unity was exported as VR android app.

Implementation:

VR app was made keeping in mind that it gives only motor imagery stimuli. The NIRStim paradigm was designed with five active and five rest block, each block having duration of 10 seconds. The VR app when launched displays countdown timer of 10 seconds, and the active session starts where motor execution is displayed in VR and subject is required to image as if doing the same task thus activating motor imagery. After active block, rest block starts and it lasts for 10 seconds where subjects are expected to rest to bring back their hemodynamic response to baseline. A plain black image was projected in VR for 10 seconds to imitate rest phase. Likewise total of 10 blocks were designed, active followed by rest alternatively. But the problem in implementation lies in synchronizing initiation/ launching of NIRstim and VR app. This was tackled by manually synchronizing NIRStim and VR app by clicking start button on NIRstim, when countdown time displayed in VR app falls to zero as read out by subject.

Purpose: Classify brain states to motor imagery and rest state

Task: Elbow flexion (motor imagery) for active block, resting in rest block

Total duration: 100 seconds

Total blocks: 5 active and 5 rests

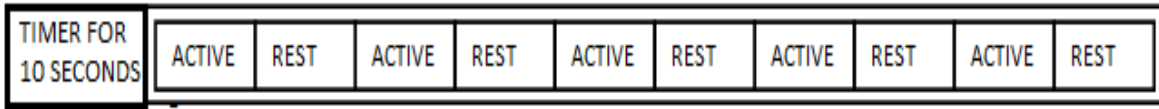


Figure 29: Block design of Paradigm 3



Figure 30: Screenshot of homepage of custom made VR motor imagery android app

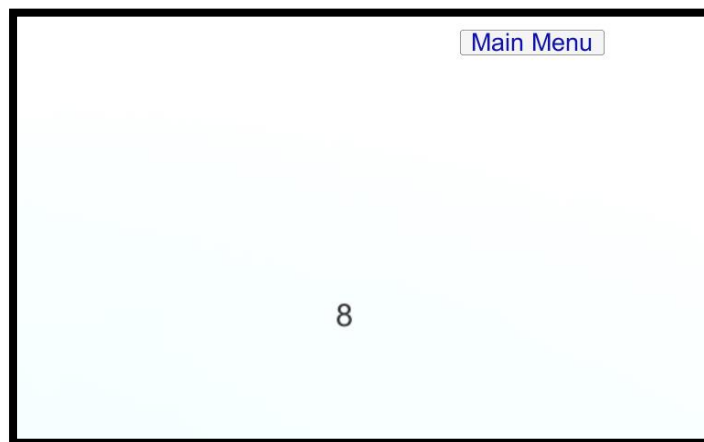


Figure 31: Countdown timer

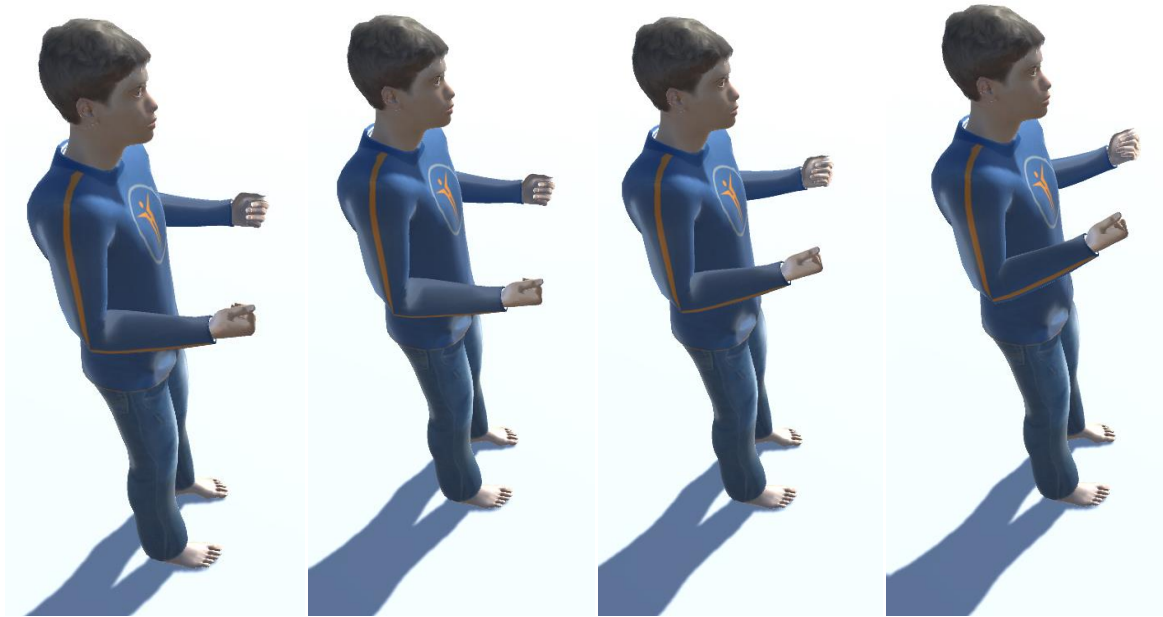


Figure 32: Extension and flexion as seen in VR

Phase	Task	Duration	Motor Imagery	Stimuli
ACTIVE 1	Motor Imagery	10 seconds	Both hands	Visual (VR)
REST 1	Resting state	10 seconds	Nil	Nil
ACTIVE 2	Motor Imagery	10 seconds	Both hands	Visual (VR)
REST 2	Resting state	10 seconds	Nil	Nil
ACTIVE 3	Motor Imagery	10 seconds	Both hands	Visual (VR)
REST 3	Resting state	10 seconds	Nil	Nil
ACTIVE 4	Motor Imagery	10 seconds	Both hands	Visual (VR)
REST4	Resting state	10 seconds	Nil	Nil
ACTIVE 5	Motor Imagery	10 seconds	Both hands	Visual (VR)
REST 5	Resting state	10 seconds	Nil	Nil

Table 13: Paradigm 3 details

WAVELET TRANSFORM

Due to its tremendous advantages as discussed in literature survey, we had used wavelet transformation for physiological noise removal from data. We had deployed wavlet toolbox of matlab for analyzing frequency content of time varying patterns in signal.

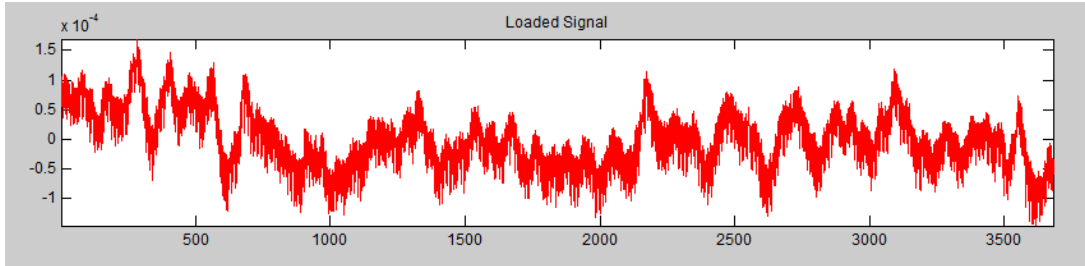


Figure 33: Single channel loaded in wavelet toolbox (Signal with noise)

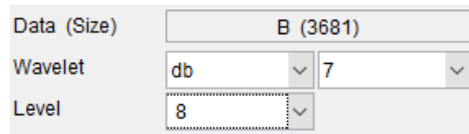


Figure 34: Db7 wavelet with level of 8 selected for multiresolution analysis

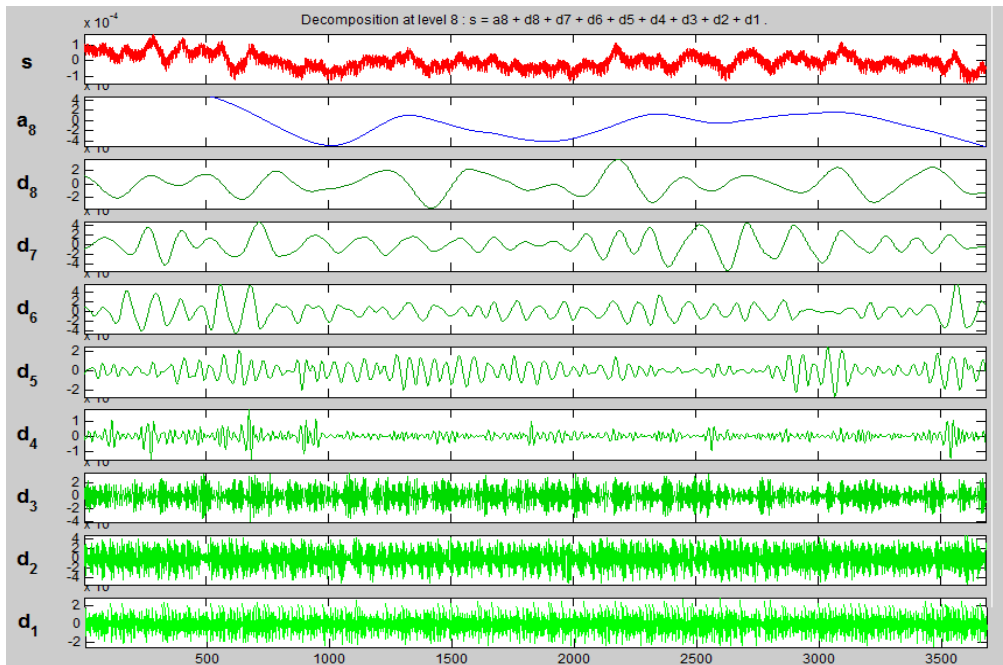


Figure 35: Multiresolution analysis of single channel data

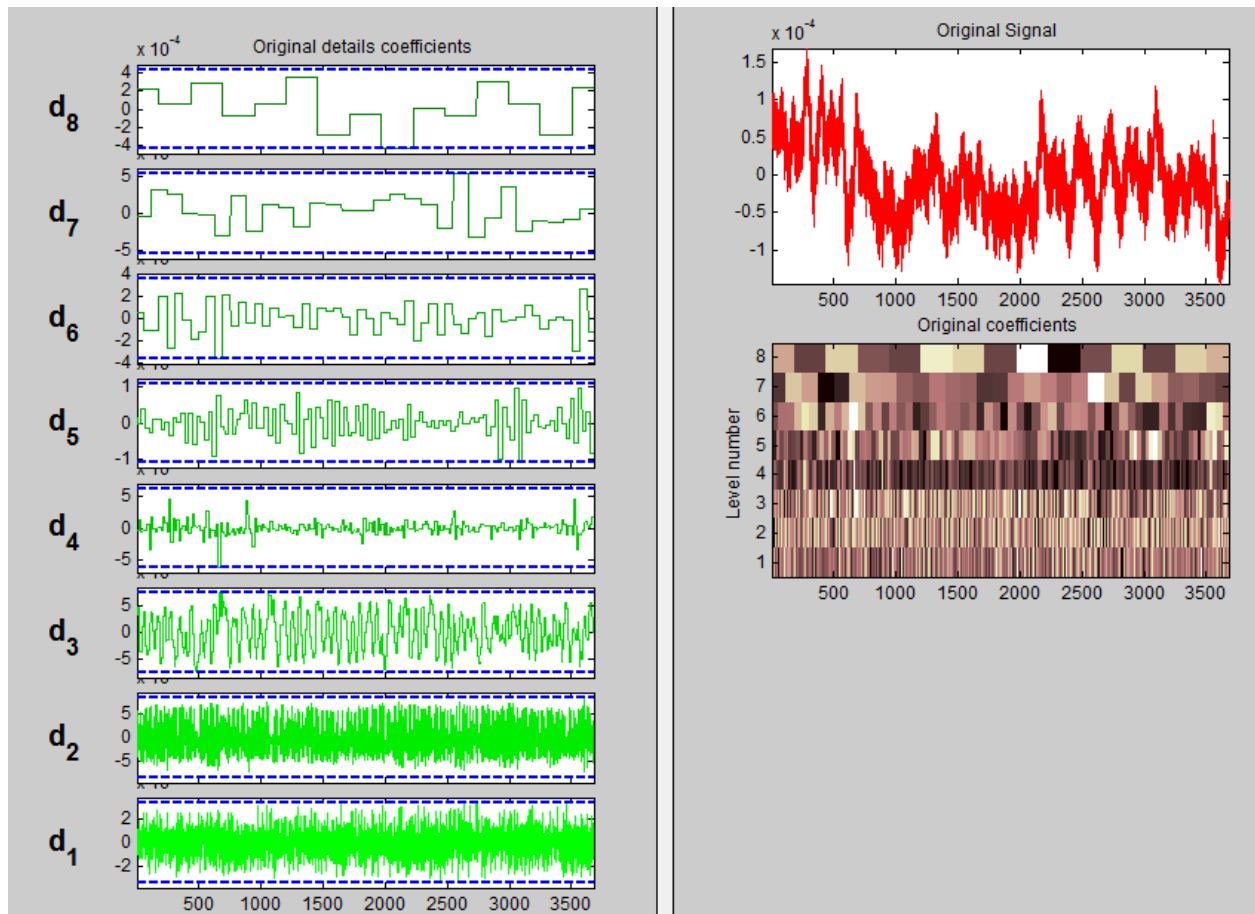


Figure 36: Coefficient details

We had used Daubechies wavelet (Daubechies et al., 1998) of seventh order which is orthonormal base and compactly supported wavelet. The level of diminishing wavelet can be changed by index N . We had used relatively high order generating index $N=8$.

Components d_1 – d_3 had comparatively large amplitudes, which we considered were caused by heartbeat-related blood flow and measurement noise. Large changes were observed in components d_9 and d_{10} . These were considered to be task-related changes, because the repetition interval of the starting and stopping, which is in the frequency band of component d_8 .

Since our data has 20 channels we had used the following code for MRA of all the channels. D_6 , d_7 and d_8 and a_8 are selected for reconstruction of signal assuming the other coefficients (d_1 , d_2 , d_3 , d_4 and d_5) are contributed by noise.

```

load('G:\project\Motor_BCI_Class\sub18\NIRS.mat')
oxy=Y.hbo;
mra=mdwtdec('c',oxy,8,'db7');
[XD,mraDEN,THRESH] = mswden('den',mra,'sqrtwolog','sln');
a8=mdwtrec(mraDEN,'a',8);
d8=mdwtrec(mraDEN,'d',8);
d7=mdwtrec(mraDEN,'d',7);
d6=mdwtrec(mraDEN,'d',6);
ss=d8+d7+d6+a8;

```

Figure 37: Matlab code for wavelet transformation (20 channels)

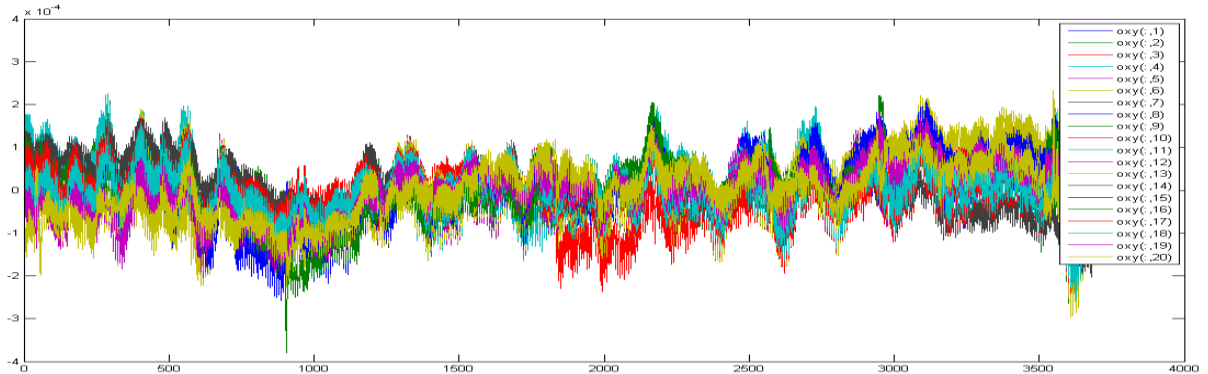


Figure 38: Raw signal (20 channels)

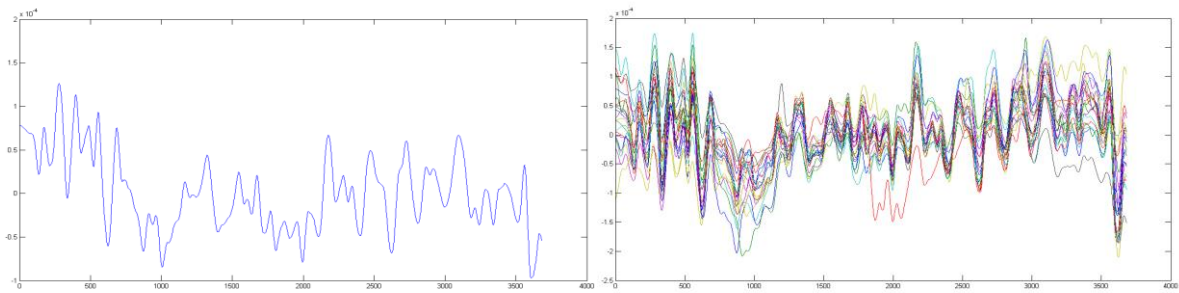


Figure 39: De-noised signal (left- 1 channel, right- 20 channels)

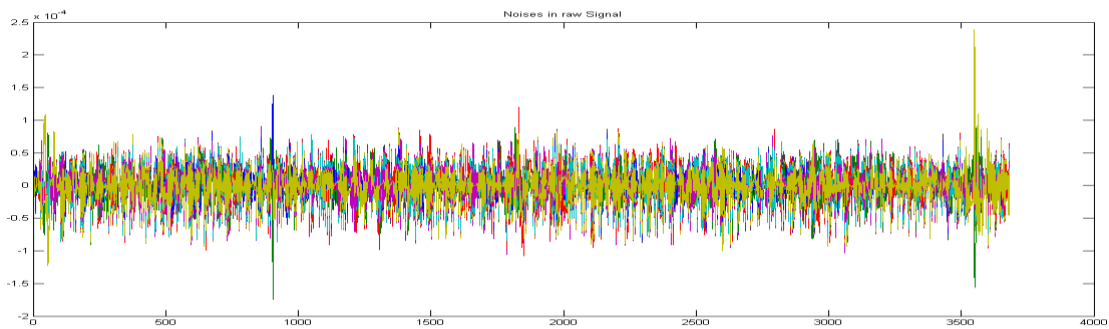


Figure 40: Noise in signal

DIFFERENTIATION OF SIGNAL

Important property of differentiation of peak type signal is its effect on peak width on amplitude of derivatives. It also discriminates against wider peaks, and higher the differentiation the greater the discrimination. This has been helpful in quantitative analytical applications like detecting peaks which are superimposed. Differentiation of curve was found to be useful in Discriminant analysis of titration curve and differential thermal analysis. Therefore it was decided to differentiate the signal and check its impact on 2D feature space which gives correlation of features. Differentiation of signals had increased correlation between features as shown in scatter plot (2D feature space). Width of peak reduction and increase in sharpness of peak are hypothesized to increase correlation among features which further can give improved classification accuracies.

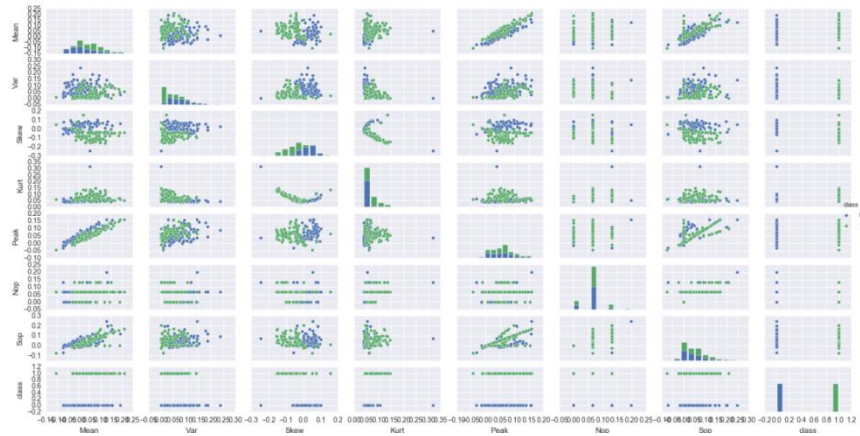


Figure 41: Non-diff signal scatter plot (subject 16)

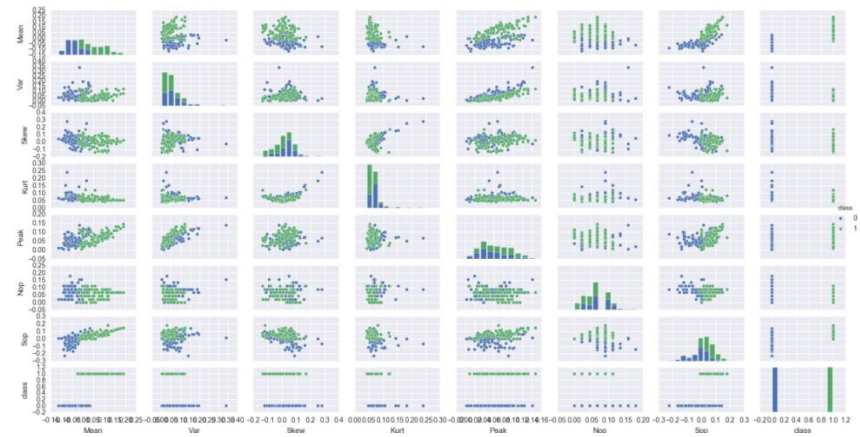


Figure 42: Diff signal scatter plot (subject 16)

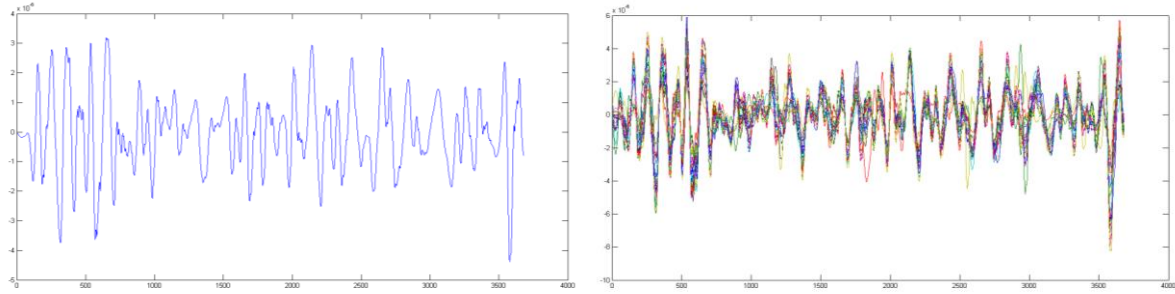


Figure 43: Diff signal (left- 1 channel, right- 20 channels)

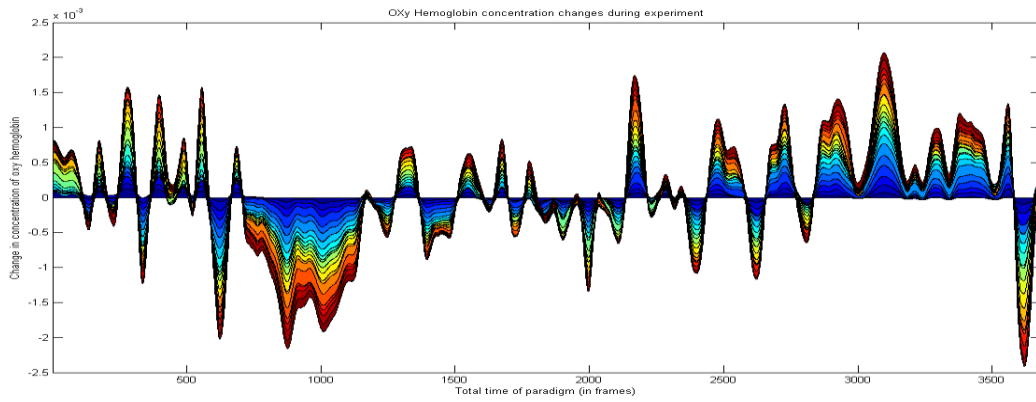


Figure 44: Area plot of non-diff signal

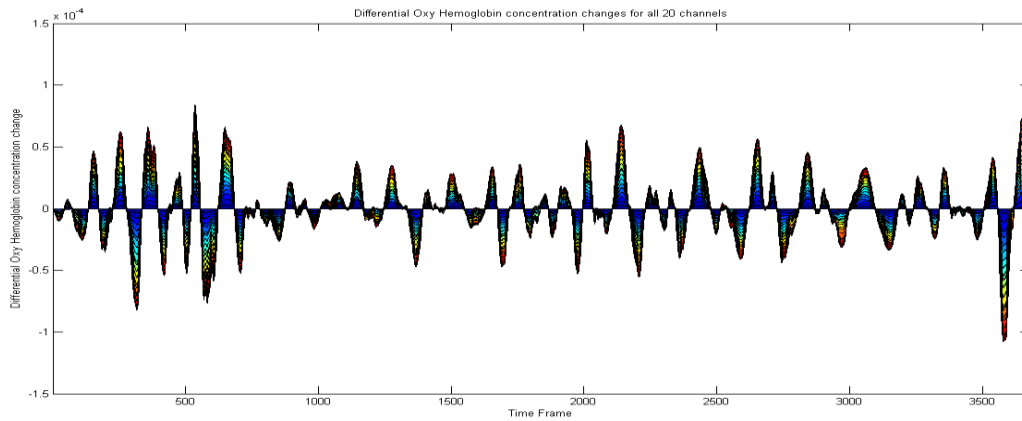


Figure 45: Area plot of diff signal

FEATURE EXTRACTION

Signal mean of HbO₂ are calculated as

$$M = \frac{1}{N} \sum_{i=1}^N X_i$$

Where M is mean value and N is number of observations and X_i represents data.

Signal variance of HbO₂ are calculated as

$$Var = \frac{\sum (X - \mu)^2}{N}$$

Where var is variance and μ is mean value of X

Signal skewness of HbO₂ are calculated as

$$Skew = E \left[\frac{X - \mu}{\sigma} \right]^3$$

Where skew is skewness and σ is standard deviation of X

Signal kurtosis of HbO₂ are calculated as

$$Skew = E \left[\frac{X - \mu}{\sigma} \right]^4$$

Sum of peaks and number of peaks is estimated by `sum(findpeaks(X))` function and `numel(findpeaks(X))` function of Matlab

After the eight features discussed above are calculated for each time window, their values are then normalized and rescaled between 0 and 1 by the following equation.

$$a' = \frac{a - \min a}{\max a - \min a}$$

Where $a \in \mathbb{R}^n$ represents the feature value, a' is the re-scaled value between 0 and 1, $\max a$ denotes the largest value, and $\min a$ indicates the smallest value

FEATURE SELECTION

Feature selection (also called variable or attribute selection) is the process of choosing a subset of features that best represent a model. The features are scored with Mean Decrease Impurity importance (MDI) of RF, which uses Gini index as impurity function.

Thereby MDI variable importance is measured with the optimized parameters predicted by GridSearch CV module of python, and best three ranked features are tabulated. Frequencies of features that are ranked best are tabulated. Frequencies of features that are ranked first, second and third by RF are also tabulated.

CLASSIFICATION

Random forest a ensemble method, which had exhibited performance better than boosting and SVM was chosen for classification task (RF model). Classification of data was done, and best three features among seven features were selected based on MDI scores. Data was once again classified with LDA (LDA model). The acquired optimal feature combination (ie) top three ranked features were used for classification by LDA and this model was named as LDA_optimal. Run time of LDA and LDA_optimal was also calculated.

For RF, data was split into training (60%) and testing (40%). Randomness of state four was introduced. Pipeline was used for chaining multiple estimators into one. This had served two purposes

- i) It was convenient to call fit and predict once on data to fit whole sequence of estimators
- ii) Grid search was used over parameters of all estimators in pipeline at once

The estimators used in pipeline parameters were n estimators, maximum depth, minimum sample split and minimum samples leaf.

Estimator	Parameters
n estimators	10,15,20
maximum depth	50,100,150
minimum samples leaf	1,2,3
minimum sample split	1,2,3

Table 14: Parameter tuning for estimator

This pipeline was run over Grid search CV with n jobs of -1, verbose of 1, scoring of F1 and cross validation of 5. This Grid search CV iterates over all possible combination of parameters of estimators and fits the best parameters of estimator for classification. By using Grid search CV, F1 scores can be maximized.

Further each subject data was classified with LDA (LDA model) with all seven features with cross validation of 15, and F1 scores are calculated. Each subject data was also classified with LDA (LDA_optimal) with optimal features (MDI RF) with cross validation of 15, and F1 scores were calculated.

The performance measure of classifiers is measured by accuracy, precision, recall, AUC score, ROC curve and F1 scores. Accuracy is ratio of correctly predicted observations. Precision is ratio of correct positive observations. Recall is true positive rate and is the ratio of correctly predicted positive events. F1 is weighted average of precision and recall. F1 score takes into account both false positive and false negatives. F1 is more useful than accuracy when there is uneven class distribution, and when false positive and false negative has similar cost function. F1 score had been selected to assess performance of classifier since it is weighted average of precision and recall.

CHAPTER 4: RESULTS

EXPERIMENT1

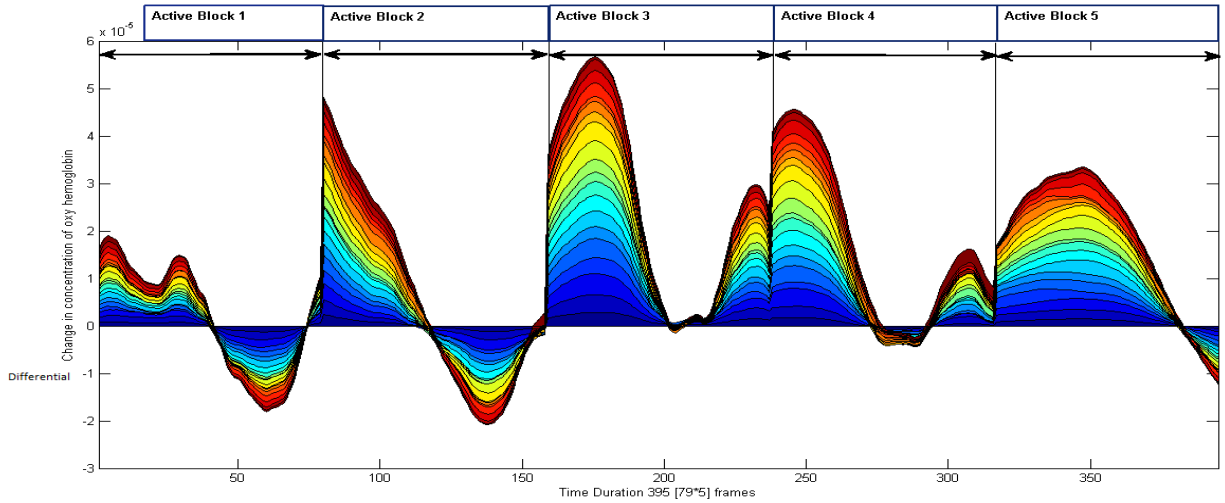


Figure 46: Active blocks

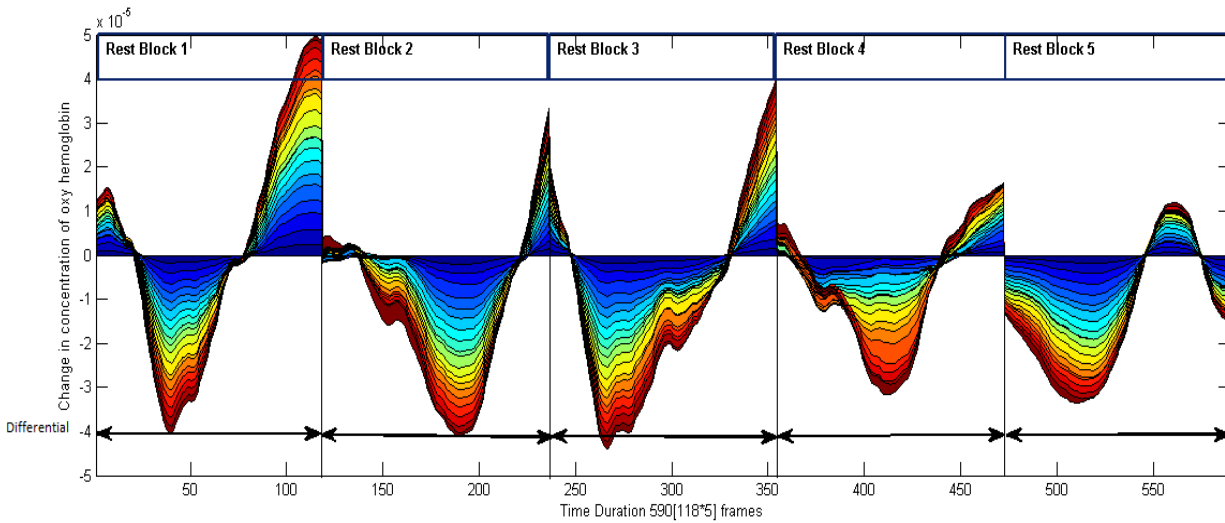


Figure 47: Rest blocks

Diff signals of Active blocks and Rest blocks of subject 16 in experiment 1 are shown in Figure 46 and Figure 47. HDR significantly increases in active blocks and HDR falls down in rest blocks.

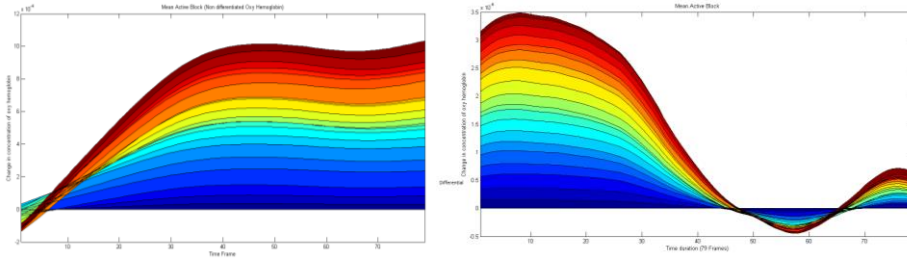


Figure 48: Active block (left- non diff signal, right- diff signal)

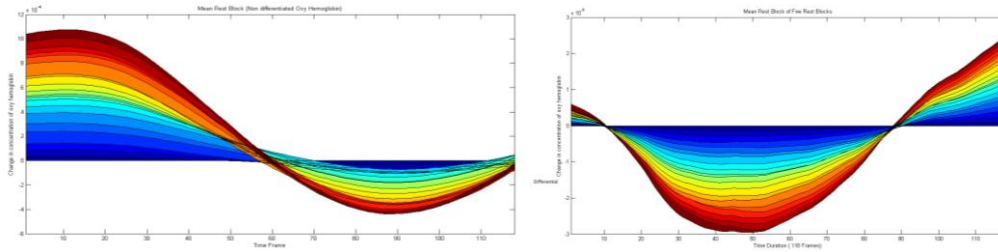


Figure 49: Rest block (left- non diff signal, right- diff signal)

Block averages of diff and non diff active blocks are shown in Figure 48. Block averages of diff and non diff rest blocks are shown in Figure 49. By closely inspecting Figure 48 and Figure 49, it is can be proved that differential denoised signal had sharp peaks and less width peaks. On the other hand non-differential denoised signal had blunt peaks and large width.

Figure 50 shows area plot of feature matrix extracted from differential denoised signal. A clear discrimination in features value between active and rest was seen.

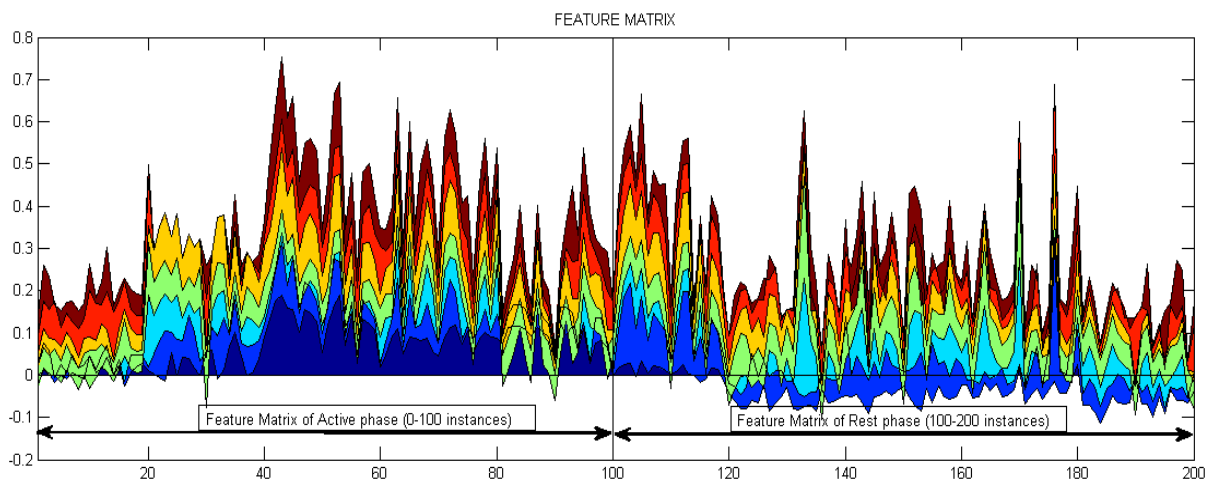


Figure 50: Feature matrix

Subject	Depth	M_leaf	M_split	N_estimator
1	50	3	2	15
2	50	3	3	10
3	50	2	1	10
4	50	3	2	20
5	50	3	1	15
6	50	2	2	15
7	50	2	3	10
9	50	3	1	15
11	50	3	1	15
12	50	1	1	15
13	50	2	1	20
14	50	2	2	15
15	50	3	2	10
16	50	1	2	10
17	50	3	1	10
18	50	3	1	20

Table 15: Optimal parameters estimated for estimators

Subject	RF_F1	Top three ranked features
1	0.819	Mean, Sop, Kurt
2	0.83	Mean, Kurt, Sop
3	0.825	Nop, Sop, Mean
4	0.763	Nop, Kurt, Peak
5	0.867	Kurt, Mean, Sop
6	0.848	Peak, Mean, Kurt
7	0.678	Skew, Var, Mean
9	0.86	Mean, Peak, Skew
11	0.778	Mean, Sop, Skew
12	0.854	Nop, Mean, Sop
13	0.849	Sop, Mean, Kurt
14	0.832	Nop, Peak, Kurt
15	0.818	Kurt, Mean, Sop
16	0.92	Mean, Sop, Peak
17	0.821	Kurt, Sop, Mean
18	0.871	Kurt, Nop, Var

Table 16: RF F1 scores and top three ranked features

Subject	First_ranked	Second_ranked	Third_ranked
1	Mean	Sop	Kurt
2	Mean	Kurt	Sop
3	Nop	Sop	Mean
4	Sop	Kurt	Mean
5	Kurt	Mean	Sop
6	Peak	Mean	Kurt
7	Skew	Var	Mean
9	Mean	Peak	Skew
11	Mean	Sop	Skew
12	Mean	Sop	Peak
13	Sop	Mean	Kurt
14	Mean	Kurt	Sop
15	Kurt	Mean	Sop
16	Mean	Sop	Peak
17	Kurt	Sop	Mean
18	Mean	Skew	Sop

Table 17: First ranked, second ranked and Third ranked features

Optimal parameters are estimated for estimators and tabulated in Table 15. The data was classified with Random Forest with optimal parameters estimated in Table 15, and tabulated in Table 16. Top three ranked features in each subject are also tabulated in Table 16. The top three ranked features are categorized into first rank, second rank and third rank with respect to subject in Table 17.

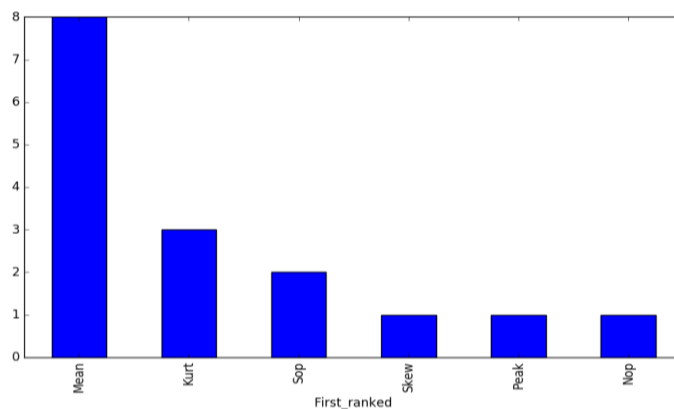


Figure 51: First ranked features

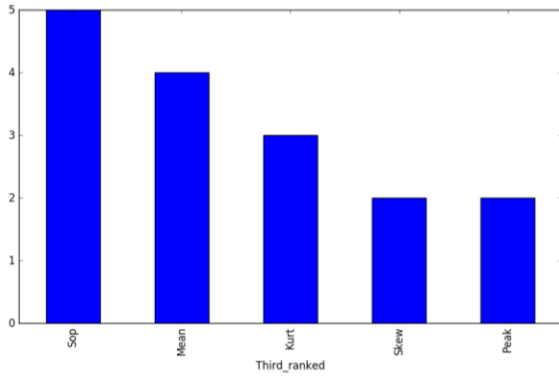


Figure 52: Second ranked features

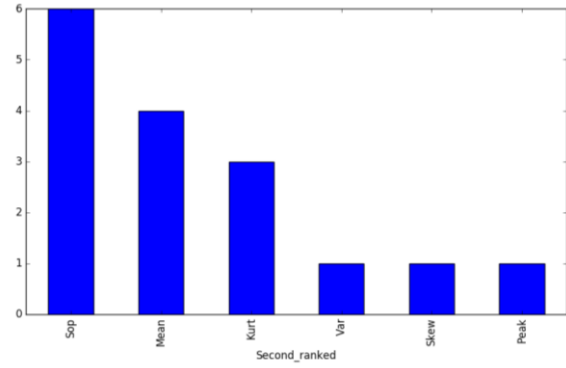


Figure 53: Third ranked features

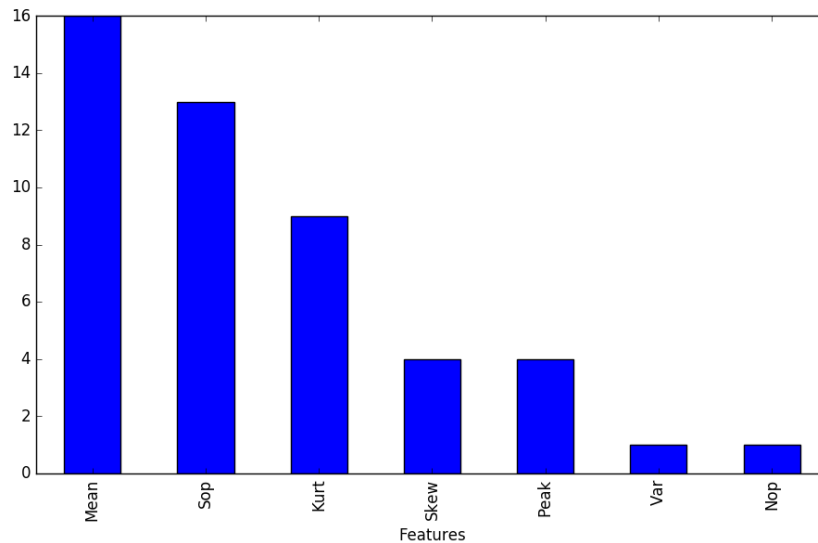


Figure 54: Frequencies of features

The frequency or occurrence of features among all the subjects are calculated and bar plots are drawn. This bar plots give a broader understanding about best features among top three ranked features ranked by RF. Frequency of features that are ranked first are bar plotted in Figure 51. Frequency of features that are ranked second are bar plotted in Figure 52 and the frequency of features that are ranked third are bar plotted in Figure 53. Finally the Frequency of top three features are bar plotted in Figure 53. The Figure 53, shows that Mean, Sop and Kurt are the best features to be considered for BCI experiments pertaining to motor execution tasks.

Features	Frequency
Mean	16
Sop	13
Kurt	9
Skew	4
Peak	4
Var	1
Nop	1

Table 18: Frequency of features

First Ranked	Frequency
Mean	8
Kurt	3
Sop	2
Skew	1
Peak	1
Nop	1

Table 19: Frequency of First ranked features

Second Ranked	Frequency
Sop	6
Mean	4
Kurt	3
Var	1
Skew	1
Peak	1

Table 20: Frequency of Second ranked features

Third Ranked	Frequency
Sop	5
Mean	4
Kurt	3
Skew	2
Peak	2

Table 21: Frequency of Third ranked features

	Sub	F1_Score (Random_Forest)	F1_Score (LDA)	LDA_time	F1_Score (LDA_optimal)	LDA_optimal time
0	Sub1	0.819	0.76260	0.0580	0.7810	0.05400
1	Sub2	0.830	0.71400	0.0560	0.7030	0.05100
2	Sub3	0.825	0.62900	0.0580	0.6660	0.05000
3	Sub4	0.763	0.68800	0.0550	0.6530	0.05300
4	Sub5	0.867	0.73100	0.0560	0.7360	0.04100
5	Sub6	0.848	0.76000	0.0554	0.7737	0.04900
6	Sub7	0.678	0.68360	0.0630	0.6700	0.05641
7	Sub9	0.860	0.70280	0.0560	0.6900	0.05310
8	Sub11	0.778	0.67714	0.0520	0.6700	0.05900
9	Sub12	0.854	0.77640	0.0570	0.7400	0.04800
10	Sub13	0.849	0.70200	0.0540	0.6900	0.05200
11	Sub14	0.832	0.77652	0.0550	0.7420	0.04700
12	Sub15	0.818	0.71562	0.0540	0.7450	0.06500
13	Sub16	0.920	0.89001	0.0510	0.8500	0.04800
14	Sub17	0.821	0.65314	0.0541	0.6200	0.04710
15	Sub18	0.871	0.82517	0.0620	0.8256	0.04800

Figure 55: Classification results

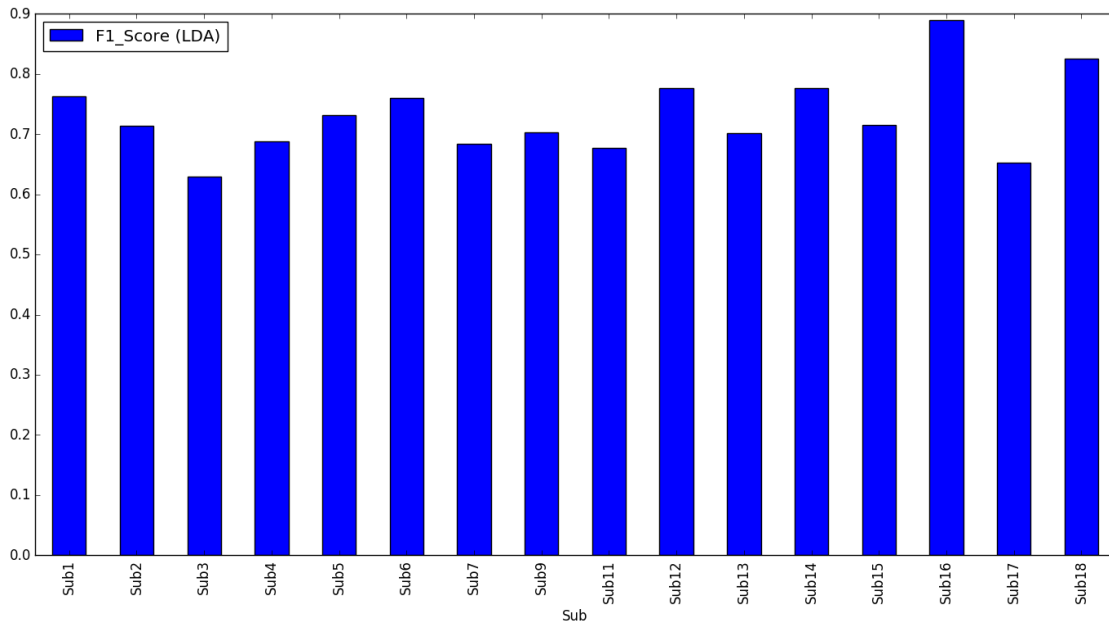


Figure 56: F1 scores of LDA

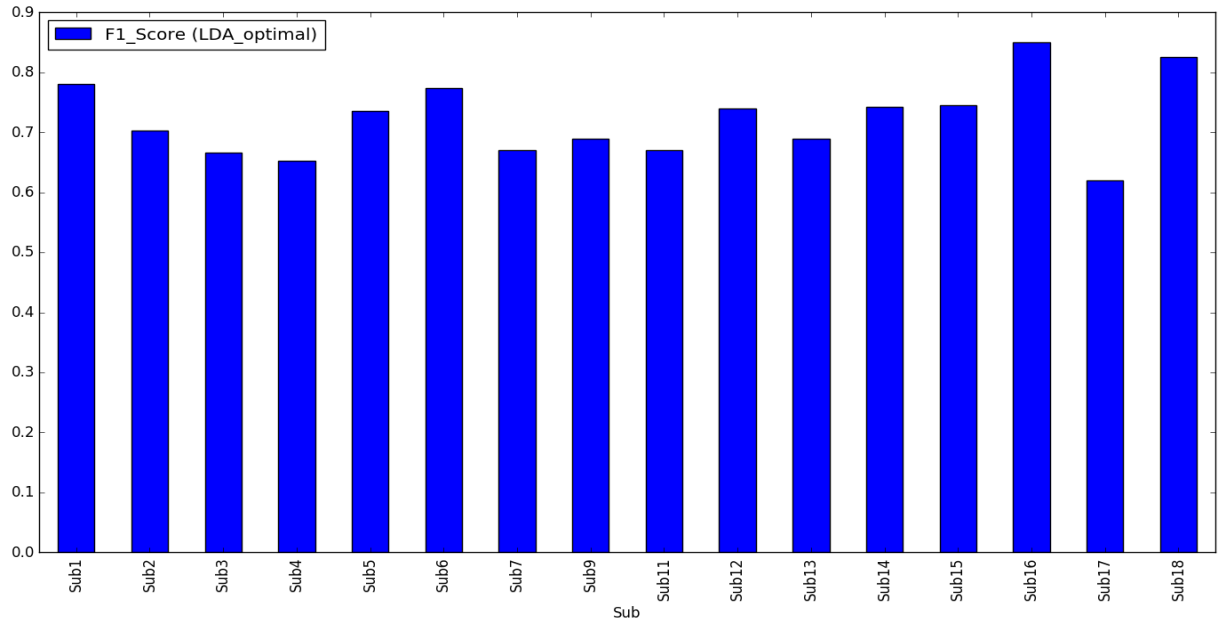


Figure 57: F1 scores of LDA_optimal

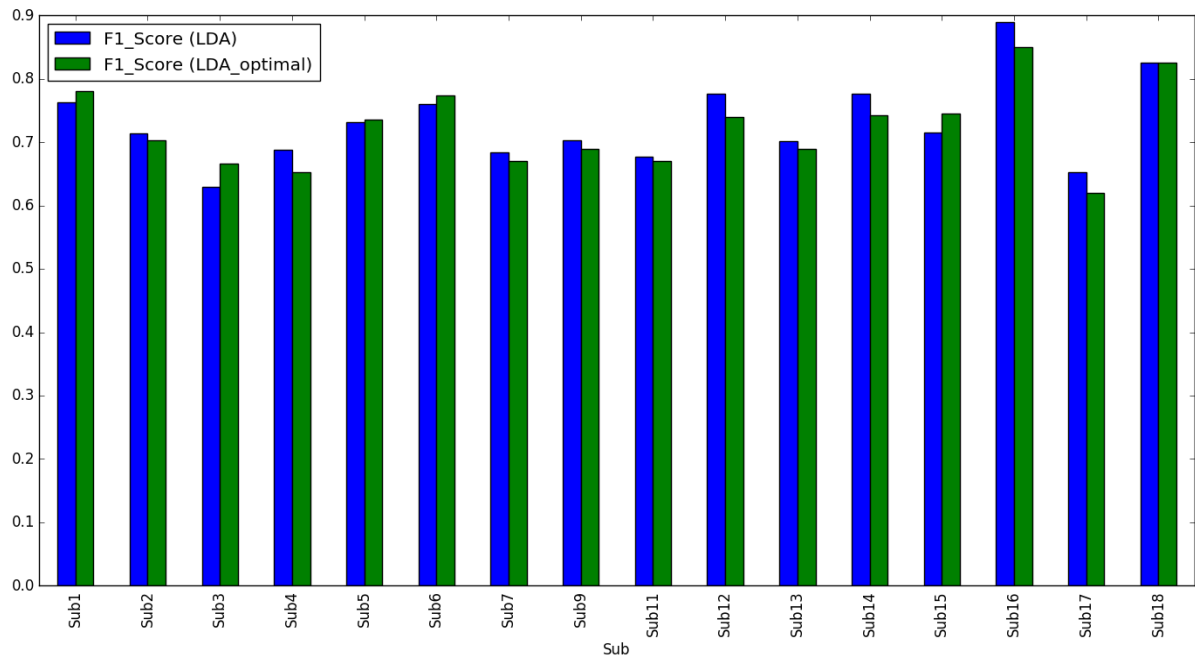


Figure 58: F1 scores of LDA and LDA_optimal

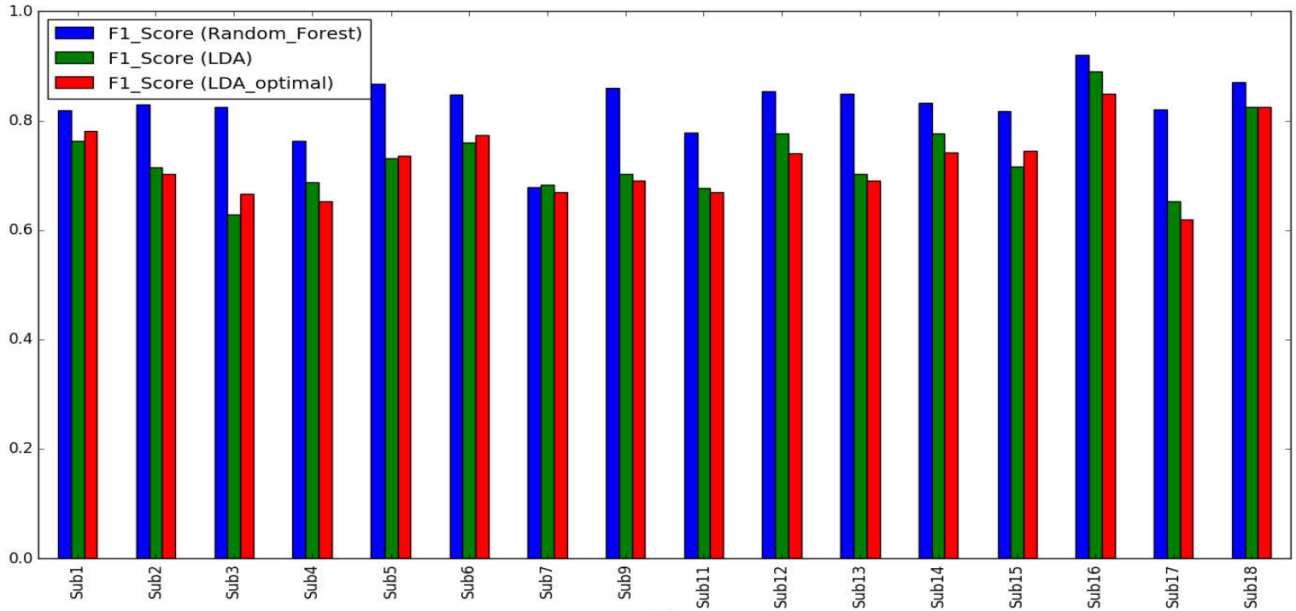


Figure 59: F1 scores of RF,LDA and LDA_optimal

F1 scores of LDA are bar plotted in Figure 56, F1 scores of LDA_optimal are bar plotted in Figure 57, F1 scores of LDA and LDA_optimal are bar plotted in Figure 58, and F1 scores of LDA, LDA_optimal and RF are bar plotted in Figure 59. Among three models, RF was having best F1 scores across all subjects, followed by LDA and LDA_optimal. LDA_optimal was having higher F1 scores than LDA in subject 1, subject 3, subject 5, subject 6 and subject 15. LDA_optimal was having same F1 score as LDA in subject 18. Where as in the rest of subjects LDA was having higher F1 scores than LDA_optimal. The overall statistics reveal that LDA F1 score achieved with all seven features can be achieved with LDA_optimal model having optimal features. This reduction of number of feature extraction would be important in real time BCI experiments.

EXPERIMENT 2.1 & 2.2

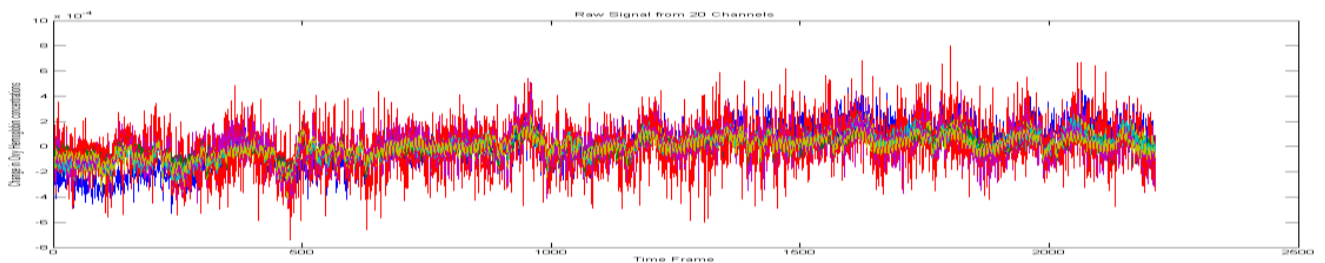


Figure 60: Raw signal

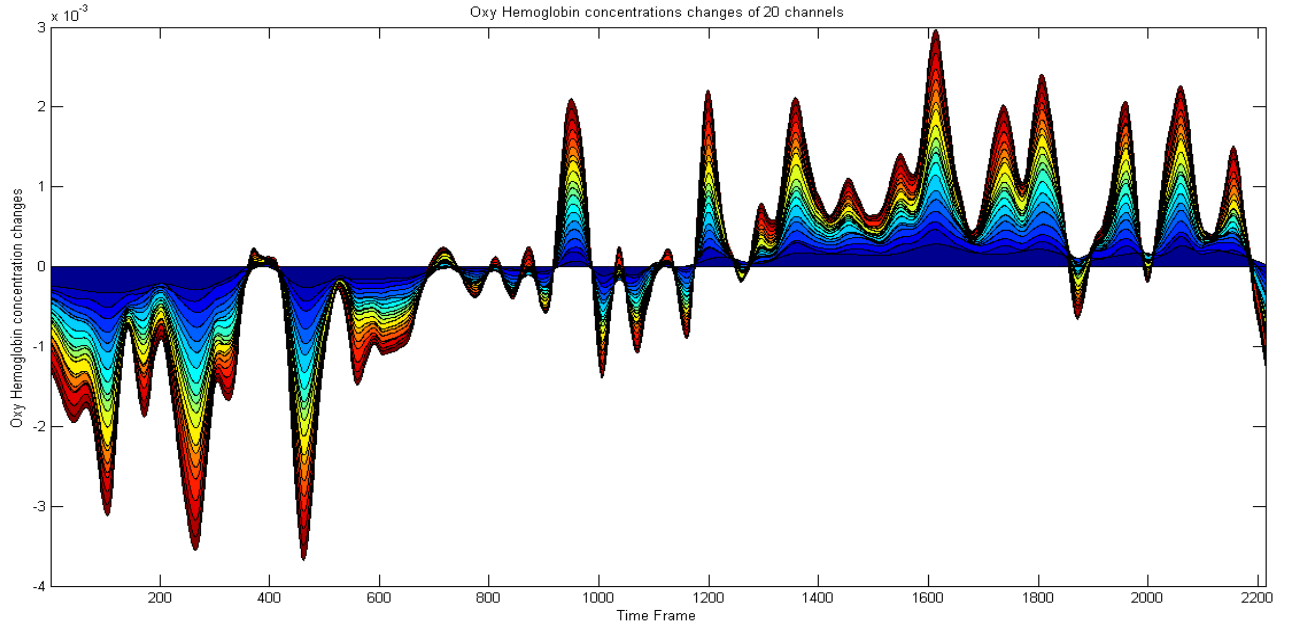


Figure 61: Area plot of non diff signals

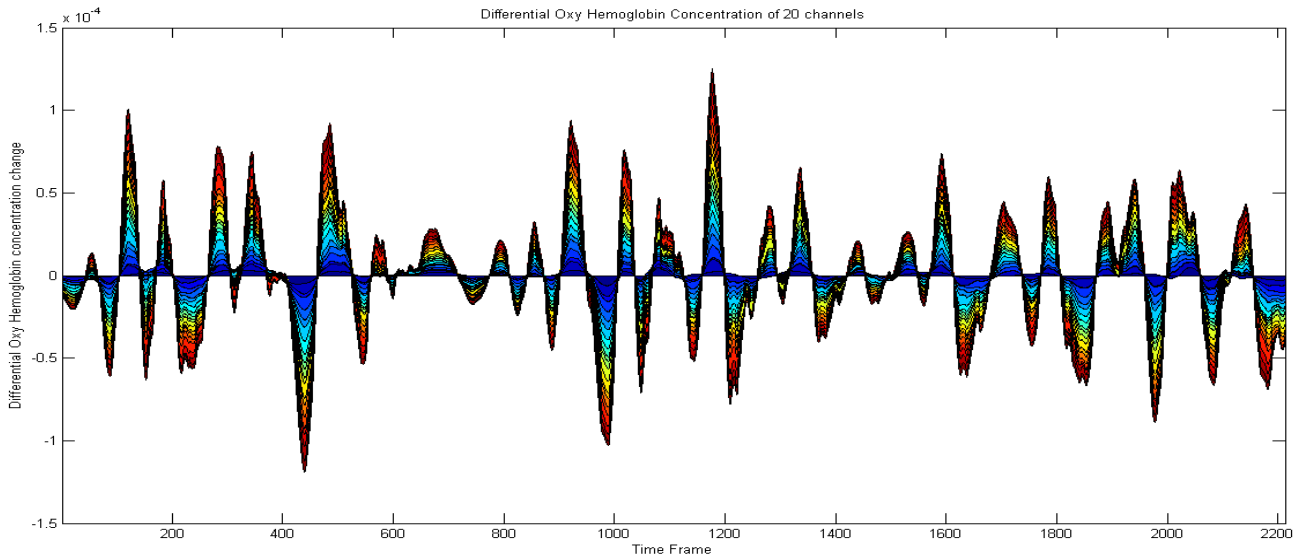


Figure 62: Area plot of diff signals

Area plot of non diff signal and diff signal are plotted in Figure 61 and Figure 62. Differentiated signals had increases peak sharpness and decreased the width of peak.



Figure 63: Scatter plot of diff signal



Figure 64: Scatter plot of non diff signal

Scatter plot of diff signal and non diff signal are shown in Figure 63 and Figure 64. Class 0 is motor imagery and class 1 is motor execution. Therefore when considering classification between motor imagery and motor execution, it is best to consider signals without differentiation as non diff signals were having better scatter plot (ie) significant correlation.

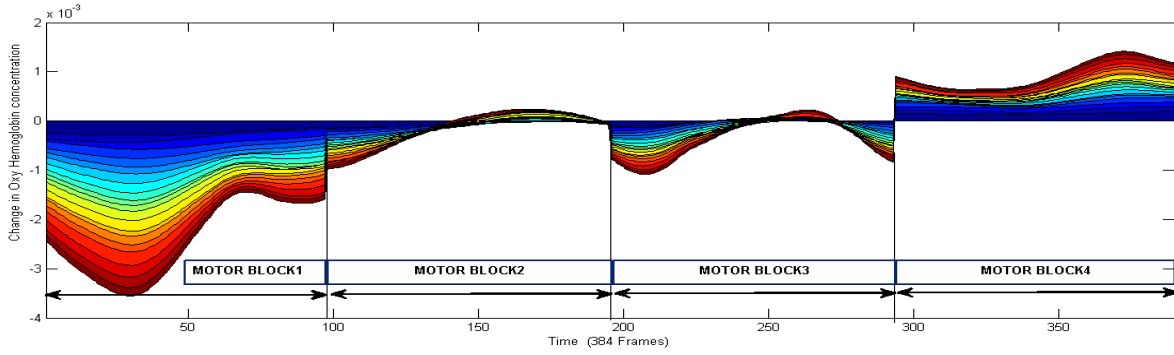


Figure 65: Motor blocks (non-diff signals)

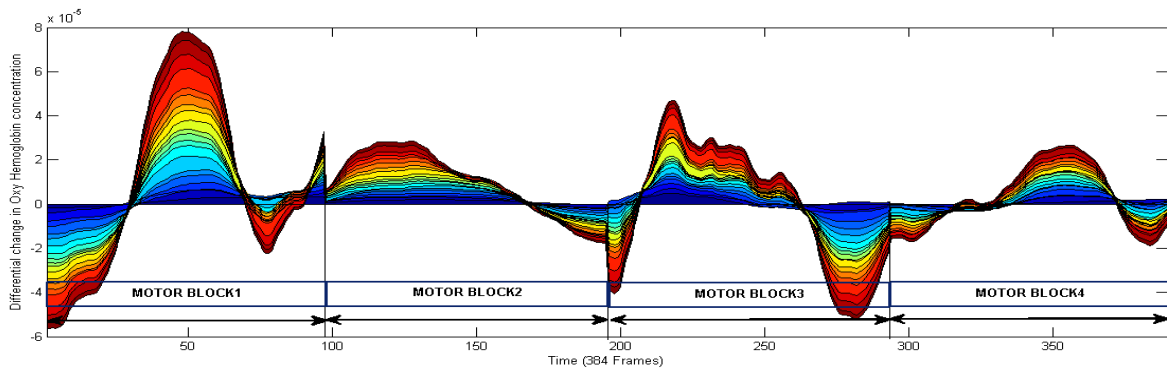


Figure 66: Motor blocks (diff signals)

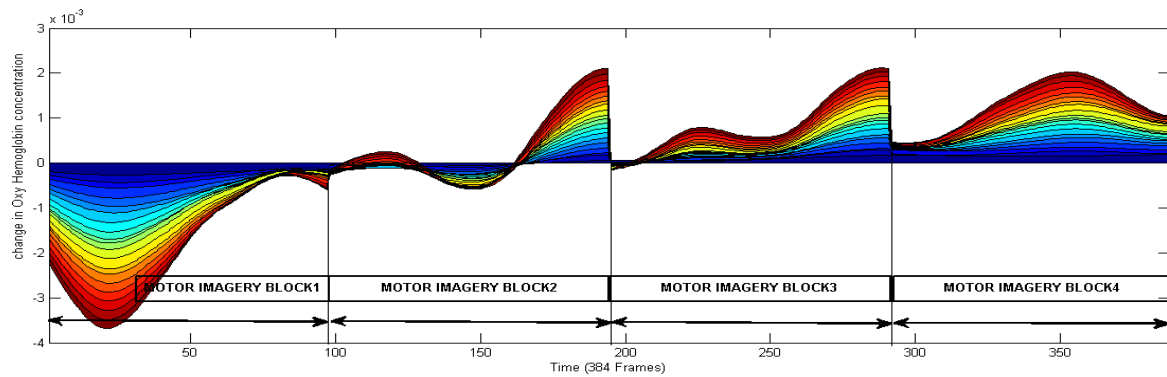


Figure 67: Motor imagery blocks (non-diff signals)

Motor blocks of four active sessions with non diff signals of experiment 2 are shown in Figure 65. Motor blocks of four active sessions with diff signals of experiment 2 are shown in Figure 66. Motor imagery blocks of four active sessions with non diff signals of experiment 2 are shown in Figure 67. Motor imagery blocks of four active sessions with diff signals of experiment 2 are shown in Figure 68. Rest blocks of four rest sessions with non diff signals of experiment 2 are shown in Figure 69.

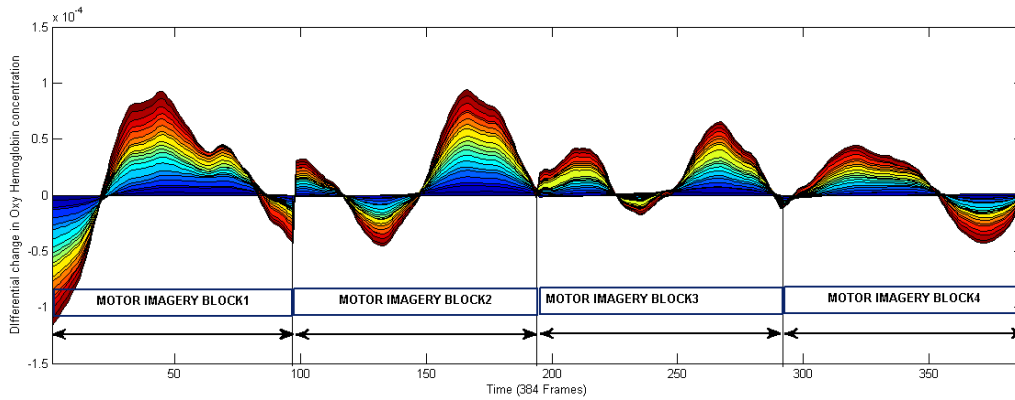


Figure 68: Motor imagery blocks (non-diff signals)

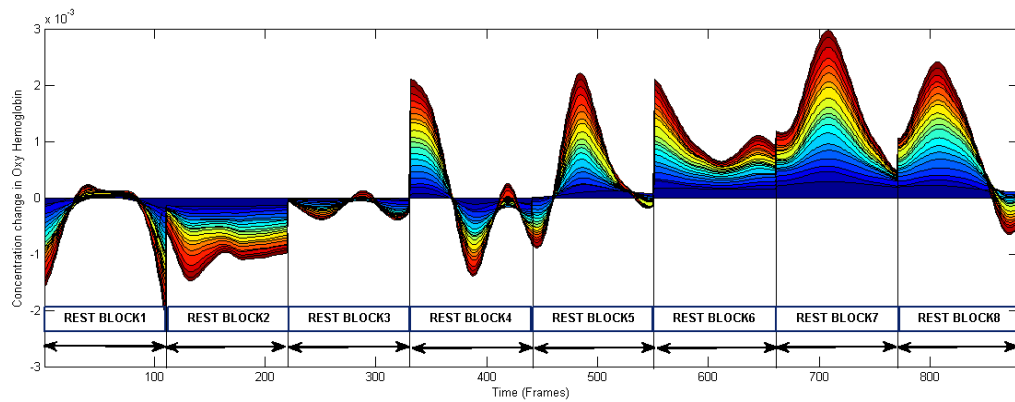


Figure 69: Rest blocks

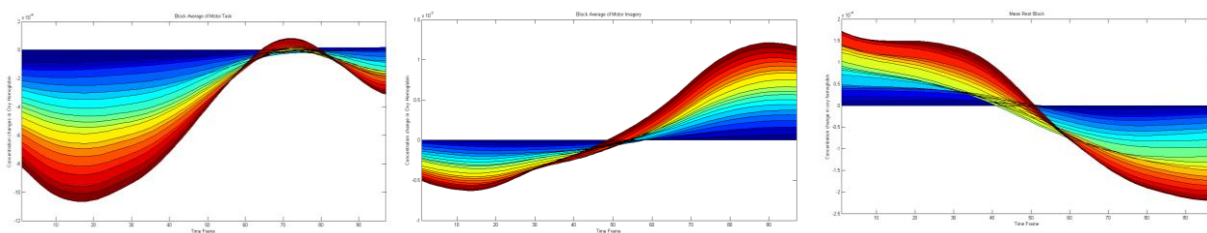


Figure 70: Block average of Motor, Motor Imagery and Rest (non-diff signals)

Block average of Motor, Motor imagery and Rest of experiment 2 are shown in Figure 70. Block average of Motor imagery was having less HDR than block average of Motor execution, and HDR of block average of rest, falls down, showing significant reduction of blood rush in rest phase.

Subject	RF_F1	Top three ranked features
1	0.84	Skew, Var, Peak
2	0.75	Peak, Nop, Kurt
3	0.808	Sop, Var, Skew

Table 22: RF F1 scores and Top three ranked features (Experiment 2.1)

Sub	First_ranked	Second_ranked	Third_ranked
sub1	Skew	Var	Peak
sub2	Peak	Nop	Kurt
sub3	Sop	Var	Skew

Table 23: First ranked, Second ranked and Third ranked (Experiment 2.1)

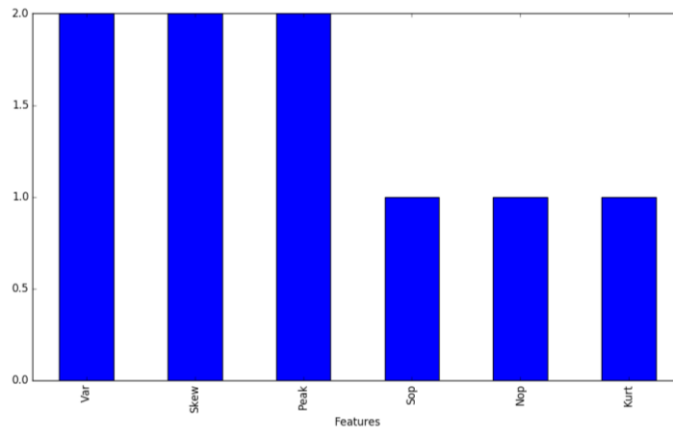


Figure 71: Frequency of features (Experiment 2.1)

Subject	LDA	LDA_time	LDA_opt	LDA_opt_time
1	0835	0.058	0.837	0.056
2	0.73	0.056	0.75	0.052
3	0.55	0.0557	0.69	0.050

Table 24: LDA, LDA_time, LDA_opt and LDA_opt_time (Experiment 2.1)

Subject	RF_F1	Top three ranked features
1	0.753	Peak, Var, Kurt
2	0.695	Peak, Sop, Kurt
3	0.724	Peak, Kurt, Sop

Table 25: RF F1 scores and Top three ranked features (Experiment 2.2)

Sub	First_ranked	Second_ranked	Third_ranked
sub1	Peak	Var	Kurt
sub2	Peak	Sop	Kurt
sub3	Peak	Kurt	Sop

Table 26: First ranked, Second ranked and Third ranked (Experiment 2.2)

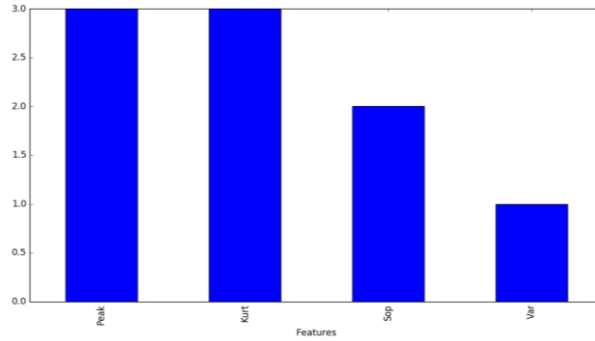


Figure 72: Frequency of features (Experiment 2.2)

Subject	LDA	LDA_time	LDA_opt	LDA_opt_time
1	0.4378	0.612	0.399	0.601
2	0.389	0.623	0.377	0.59
3	0.41344	0.531	0.388	0.520

Table 27: LDA, LDA_time, LDA_opt and LDA_opt_time (Experiment 2.2)

Experiment 2.1

RF, F1 scores are tabulated in Table 22. Top three ranked features from RF are categorized into first, second and third ranked features and tabulated in Table 23. Frequency of best ranked top three features of Table 22 are bar plotted in Figure 71. The Figure 71, shows that Var, Skew and Peak are the best features to be considered for BCI experiments discriminating motor execution and motor imagery tasks.

Experiment 2.2

RF, F1 scores are tabulated in Table 25. Top three ranked features from RF are categorized into first, second and third ranked features and tabulated in Table 26. Frequency of best ranked top three features of Table 25 are bar plotted in Figure 72. The Figure 72, shows that Peak, Kurt and Sop are the best features to be considered for BCI experiments discriminating motor execution, motor imagery tasks and rest phase.

EXPERIMENT 3

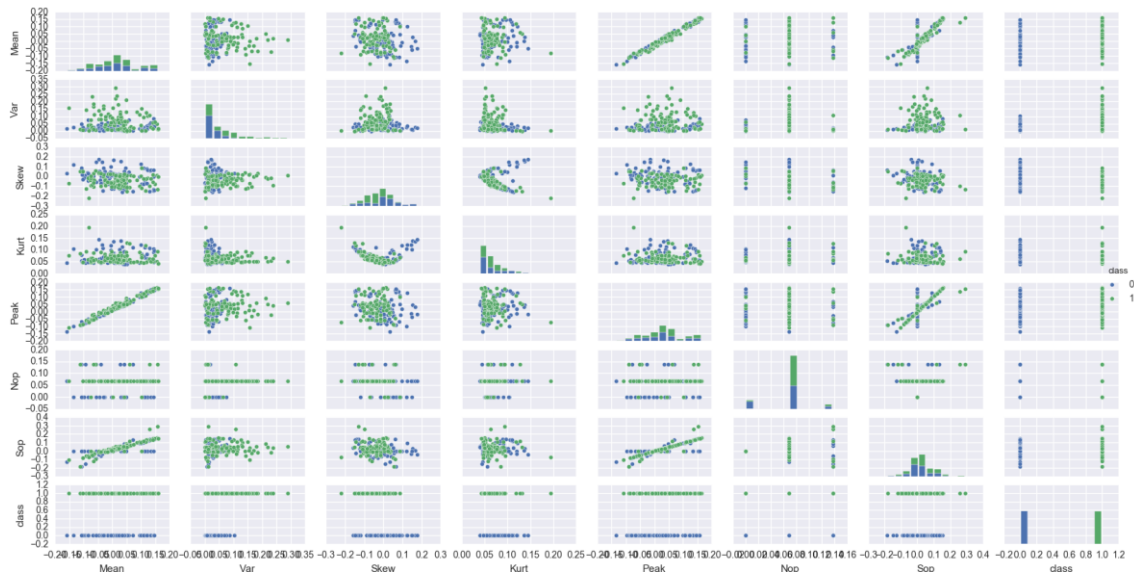


Figure 73: Scatter plot (non-diff signal)

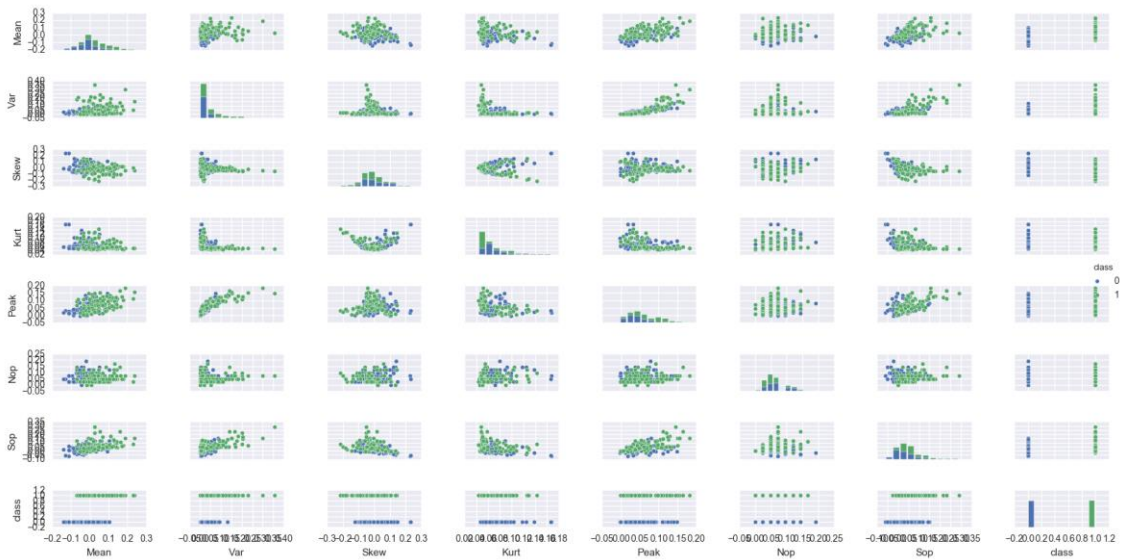


Figure 74: Scatter plot (diff signal)

Scatter plot of non diff signal and diff signal are shown in Figure 73 and Figure 74. Class 1 is motor imagery with VR and Class 0 is rest phase. Therefore when considering classification between motor imagery with VR and rest, it is best to consider signals with differentiation as diff signals were having better scatter plot (ie) significant correlation.

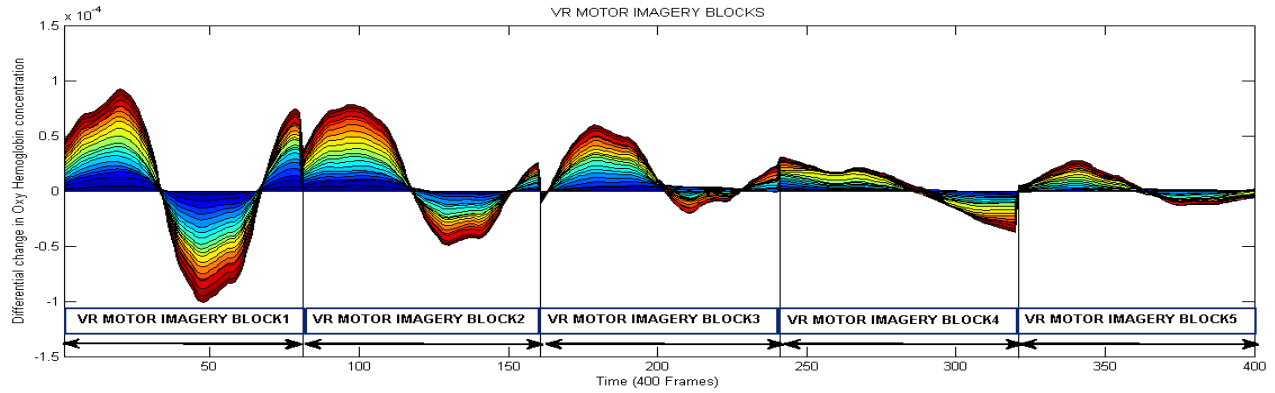


Figure 75: VR Motor Imagery blocks

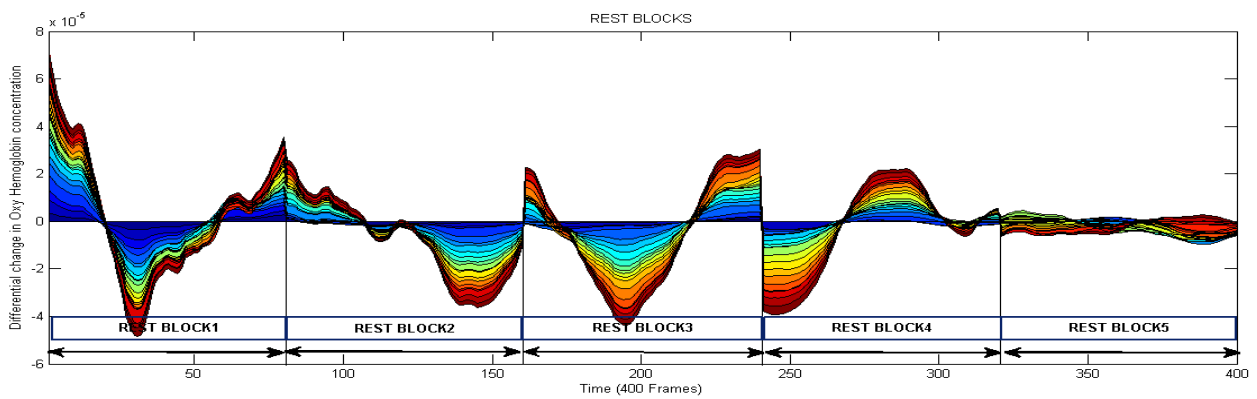


Figure 76: Rest blocks

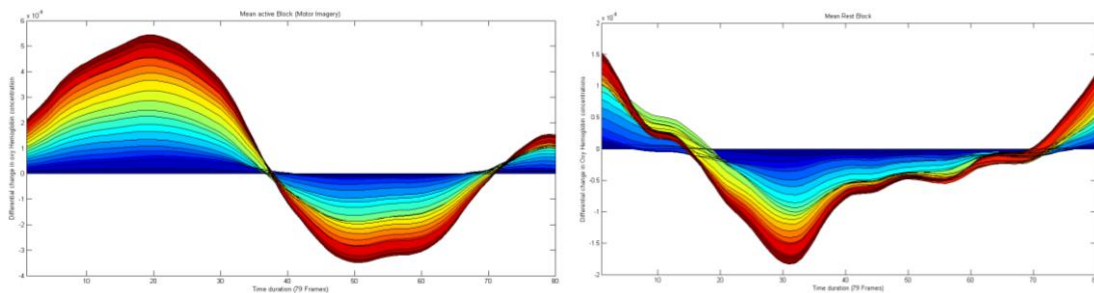


Figure 77: Block average of Active and Rest

VR Motor imagery blocks of five active sessions with diff signals of experiment 3 are shown in Figure 75. Rest blocks of five rest sessions with diff signals of experiment 3 are shown in Figure 76. Block average of Motor imagery and Rest phase of experiment 3 are shown in Figure 77. Block average of Motor imagery was having significantly higher HDR than block average of rest phase, and HDR of block average of rest, falls down, showing significant reduction of blood rush in rest phase.

Subject	Depth	M_leaf	M_split	N_estimator
1	50	3	2	15
2	50	1	2	10
3	50	2	1	10
4	50	3	2	15
5	50	1	3	20

Table 28: Optimal parameters estimated for estimators

Subject	RF_F1	Top three ranked features
1	0.777	Skew, Var, Kurt
2	0.757	Mean, Kurt, Var
3	0.810	Mean, Kurt, Sop
4	0.730	Kurt, Peak, Skew
5	0.907	Kurt, Mean, Skew

Table 29: RF F1 scores and Top three ranked features

Subject	First_ranked	Second_ranked	Third_ranked
1	Skew	Var	Kurt
2	Mean	Kurt	Var
3	Mean	Kurt	Sop
4	Kurt	Peak	Skew
5	Kurt	Mean	Skew

Table 30: First ranked, Second ranked and Third ranked features

Subject	LDA	LDA_time	LDA_opt	LDA_opt_time
1	0.63	0.0535	0.578	0.04402
2	0.6025	0.0590	0.59	0.056
3	0.71	0.0790	0.68	0.037
4	0.59	0.0618	0.61	0.051
5	0.73	0.0597	0.77	0.052

Table 31: LDA, LDA_time, LDA_opt and LDA_opt_time (Experiment 3)

RF, F1 scores are tabulated in Table 29. Top three ranked features from RF are categorized into first, second and third ranked features and tabulated in Table 30. Frequency of best ranked top three features of Table 29 are bar plotted in Figure 78.

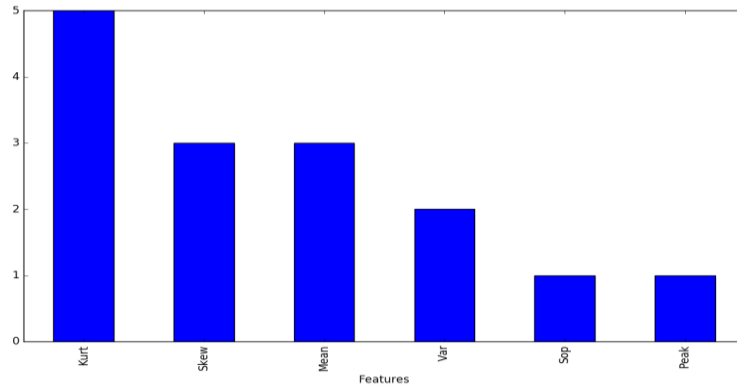


Figure 78: Frequency of features

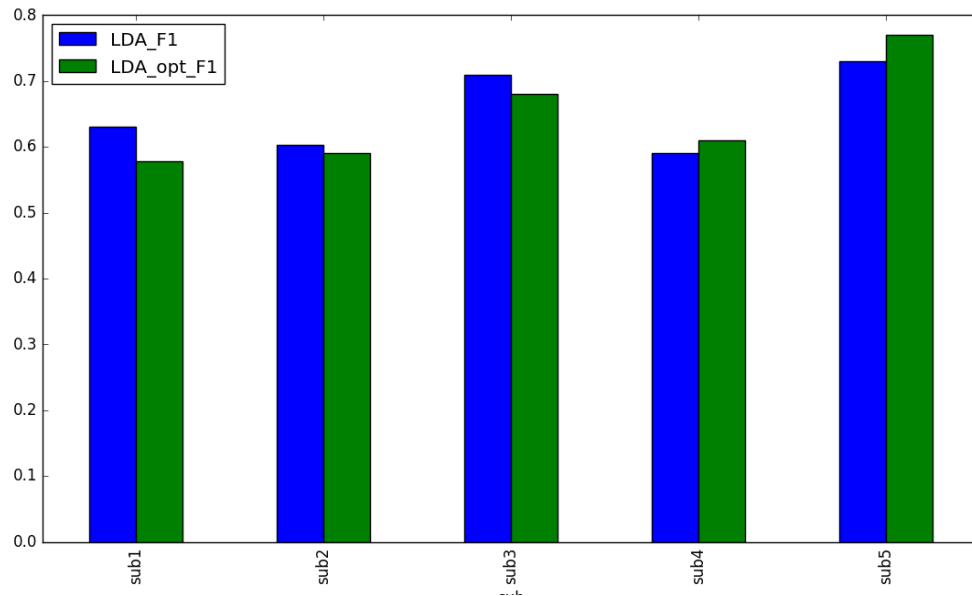


Figure 79: LDA and LDA_opt F1 scores

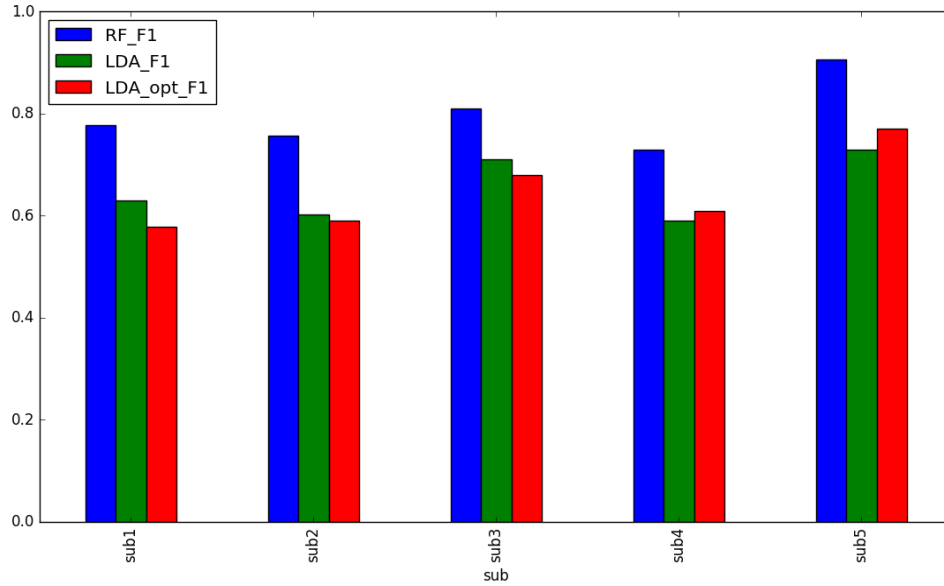


Figure 80: LDA, LDA_optimal and RF F1 scores

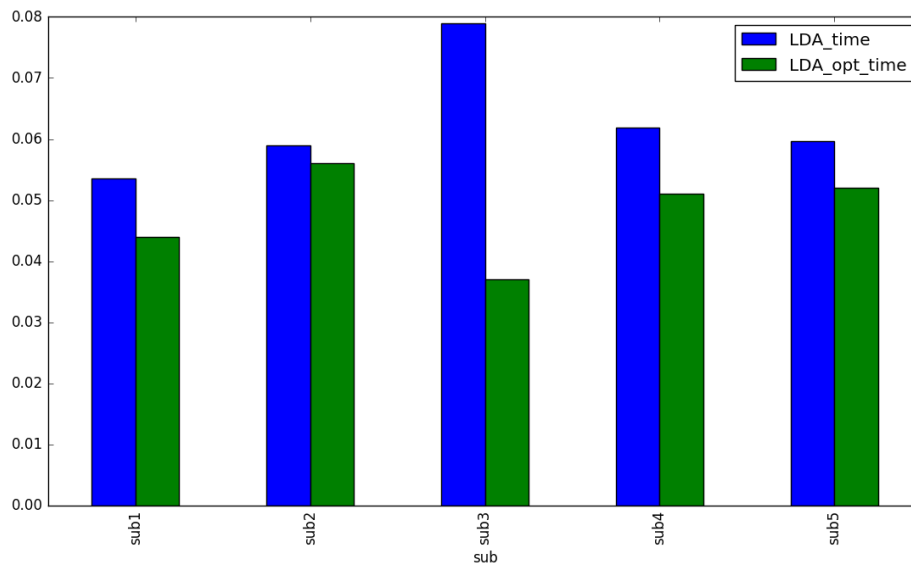


Figure 81: LDA and LDA_optimal run time

F1 scores of LDA and LDA_optimal were bar plotted in Figure 79, F1 scores of LDA, LDA_optimal and RF are bar plotted in Figure 80. Among three models, RF was having best F1 scores across all subjects, followed by LDA and LDA_optimal. LDA_optimal was having higher F1 scores than LDA in subject 4 and subject 5. Whereas in the rest of subjects LDA was having higher F1 scores than LDA_optimal. The overall statistics reveal that LDA F1 score achieved with

all seven features can be achieved with LDA_optimal model having optimal features. This reduction of number of feature extraction would be important in real time BCI experiments.

FEATURES WITH BEST DISCRIMINATIVE POWER

Features	Experiment1	Experiment 2.1	Experiment 2.2	Experiment 3
Mean	16	0	0	3
Sop	13	1	2	1
Kurt	9	1	3	5
Skew	4	2	0	3
Peak	4	2	3	1
Var	1	2	1	2
Nop	1	1	0	0

Table 32: Frequency of features in all experiments

This table yields an interesting insight.

- Mean, Sop and Kurt was ranked best across 16 subjects in experiment 1.
- Skew, Peak and Var was ranked best across 3 subjects in experiment 2.1.
- Peak, Kurt and Sop was ranked best across 3 subjects in experiment 2.2
- Mean, Sop and Kurt was ranked best across 5 subjects in experiment 3

Therefore for experiments, related to BCI, the following features can be extracted and used as optimal features for classification purposes

- Mean, Sop and Kurt could be used for classifying motor execution vs rest
- Skew, Peak and Var could be used for classifying motor execution vs motor imagery
- Peak, Kurt and Sop could be used for classifying motor execution vs motor imagery vs rest
- Mean, Sop and Kurt could be used for classifying VR motor imagery vs rest

CHAPTER 5: DISCUSSION AND CONCLUSIONS

Major finding using Wavelet transformation for noise reduction

Wavelet transformation was found to be best for noise removal for experiments pertaining to fNIRS BCI. Db7 of seven order was found to be best for deconstructing signal and d6, d7 and d8 levels were reconstructed back to get signal with noise removed. d1, d2, d3, d4 and d5 were identified to be noise signals especially physiological signals. This was consistency with previous studies like Tsunashima et al., 2009.

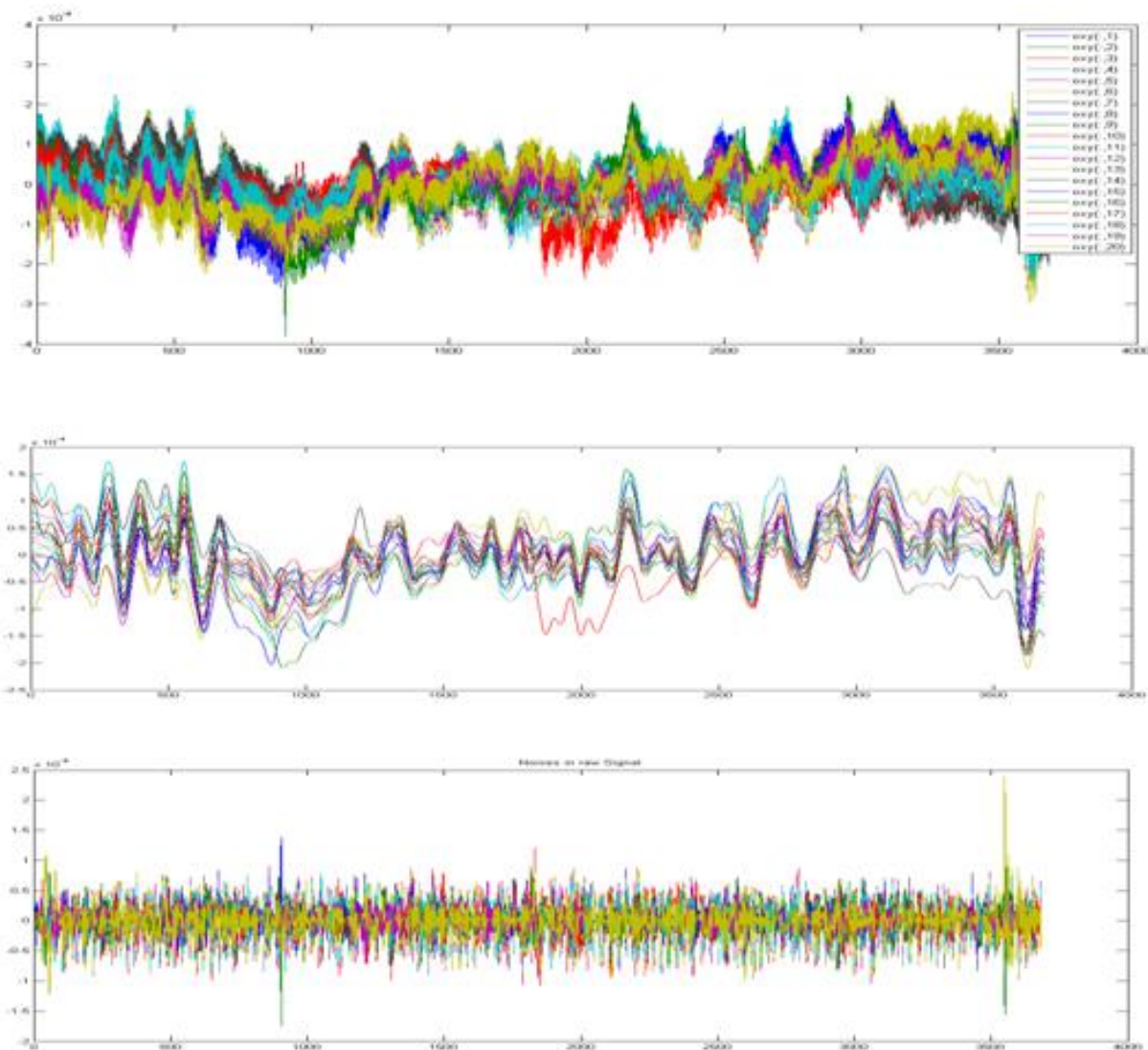


Figure 82: Wavelet transformation, Top picture: Raw signal, Middle picture: Signal denoised, Bottom picture: Noise in signal

Differentiation of signal

Differentiation of signal was also found to be advantageous and proved to contribute positively towards increasing classification scores of machine learning model. Correlation between 2D feature spaces had also increased by differentiation of signal. To our knowledge differentiation of fNIRS signal for increasing correlation among features had not been done before.

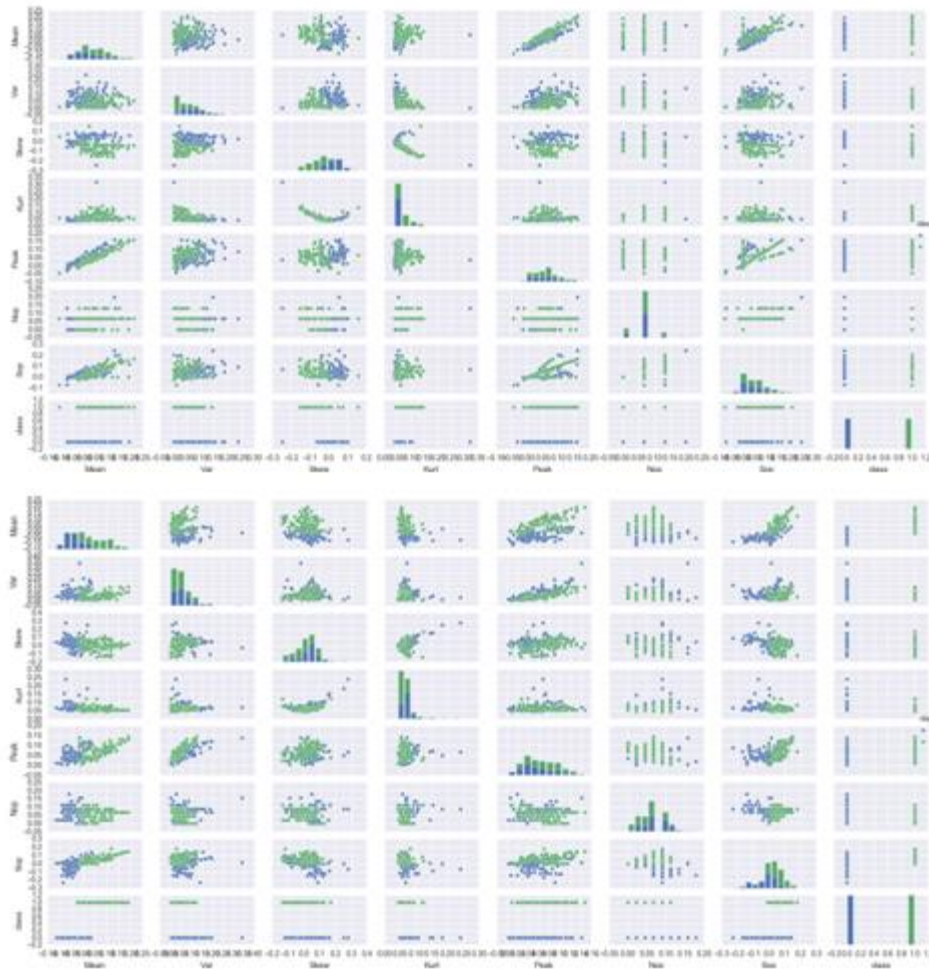


Figure 83: Differentiation of signal increasing correlation in 2D feature space

Major findings

Key finding in using differentiation of signal for four experiments was

Experiment 1: For all 16 subjects differentiation of signal (diff-signal) increased classification scores when compared with non-differentiation of signal.

Experiment 2.1: For all 3 subjects non-differentiation of signal (signal) was found to be better when compared with differentiation of signal (diff-signal).

Experiment 2.2: For all 3 subjects non-differentiation of signal (signal) was found to be better when compared with differentiation of signal (diff-signal).

Experiment 3: For all 3 subjects differentiation of signal (diff-signal) increased classification scores when compared with non-differentiation of signal.

Important facts to be noted here is, experiment 2.1 and experiment 2.2 involves classifying two active states. And since differentiation of signal increases sharpness of peak and decreases width of peak it is best to use non-differential signal for classification involving two active classes (ie) motor execution and motor imagery.

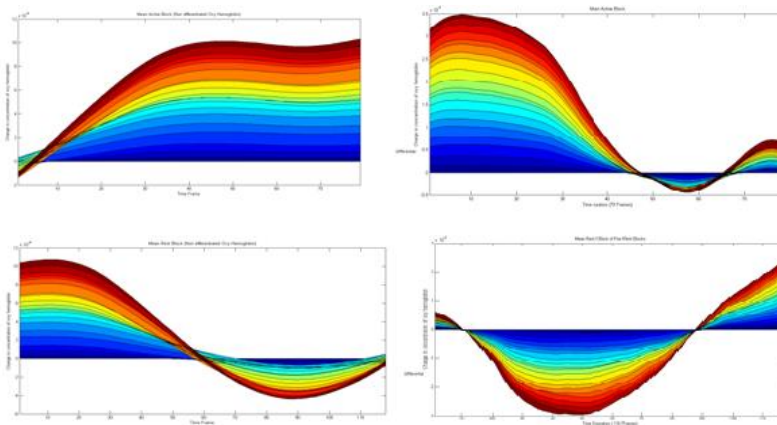


Figure 84: Experiment1: Left images are of active state (motor execution) and Right images are of rest state; Top images are of non diff signals and down images are of diff signals

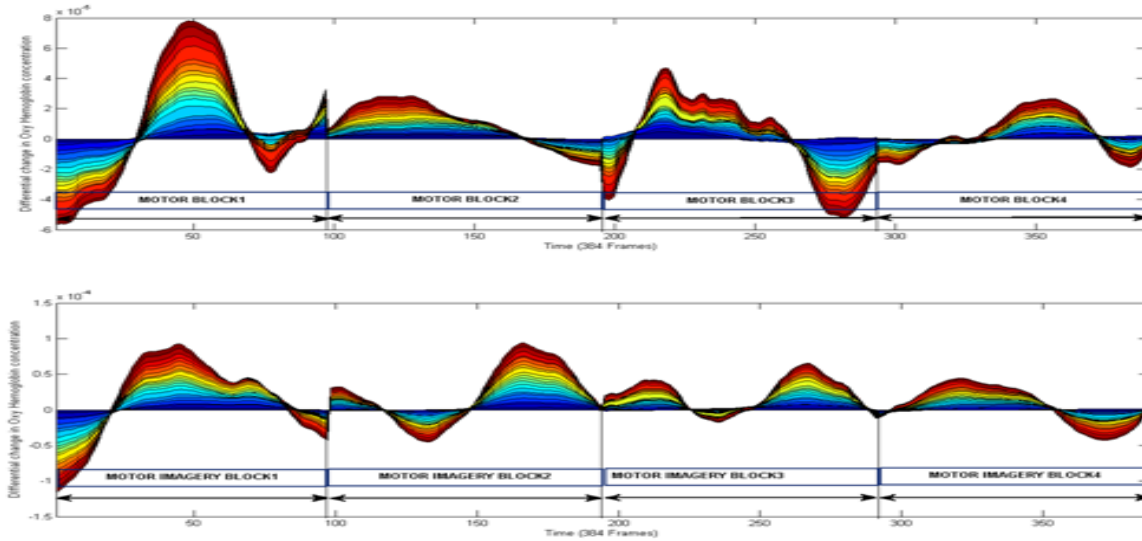


Figure 85: Experiment 2.1: Top image is of diff signals of motor task and down image is of diff signals of motor imagery

From the above figures it can be established that differentiation of signal had actually decreased width of signal and increased sharpness of peak. Active state peak was seen above the baseline and rest state peak was seen below the baseline. Hence it can be established for classification involving two active tasks; it is best to take non-differentiation data, because it is devoid of sharp peaks and reduced width which can undermine classification of two active states like motor execution and motor imagery.

Strategy for classification

As highlighted in literature survey, feature identification, selection and extraction plays a important role in classification task and good performance. Mean, Skewness, Variance, Kurtosis, Number of peaks, Sum of peaks and Peak were identified as necessary features to be inspected based on literature survey. Instead of feature reduction or feature selection with step wise method (Noman Naseer et al., 2016) or other wrapper techniques we had made use of RF classifier for ranking given set of features and top three ranked features were considered as ideal optimistic feature that can maximize classification scores and help us in building good classification model. The classification performance was assessed by F1 scores. We had cross checked the discriminative power of selected features from RF, by using them as features in LDA and compared F1 scores with LDA using all the seven features. It was proven beyond doubt that

features which were ranked by RF were indeed features with top discriminative power and LDA had yielded the same average F1 score as LDA_optimal.

Steps involved:

- Feature extraction (calculation of features from data)
- Classify with LDA (using all seven features)
- Identify best parameter estimator for RF by Grid search CV
- Use the identified parameter for estimator for MDI scores with RF
- Select top three ranked features
- Classify with LDA_optimal (using top three ranked features)

Feature selection

Mean, Sop and Kurt was ranked best across 16 subjects in experiment 1. Skew, Peak and Var was ranked best across 3 subjects in experiment 2.1. Peak, Kurt and Sop was ranked best across 3 subjects in experiment 2.2. Mean, Sop and Kurt was ranked best across 5 subjects in experiment 3.

The features selected are in consistent with the top features reported by various researchers.

Mean was used as best feature in Sitaram et al., 2007; Power et al., 2010; Holper and Wolf, 2011; Faress and Chau, 2013; Naseer and Hong, 2013, 2015b; Power and Chau, 2013; Hong et al., 2014. Kurtosis was used as best feature in Holper and Wolf, 2011. Peak value was used as best feature in Tai and Chau, 2009; Cui et al., 2010; Bauernfeind et al., 2011; Holper and Wolf, 2011.

Major findings

The following had been established regarding best features for respective tasks

- Mean, Sop and Kurt are the best features for classifying data into motor execution like finger tapping and rest state (2 class).
- Skew, Peak and Variance are the best features for classifying data into motor execution like extension and flexion and motor imagery of the same (2 class).

- Peak, Kurt and Sop are best features for classifying data into motor execution like extension and flexion, motor imagery of the same and rest state (3 class).
- Mean, Sop and Kurt are best features for classifying data into VR motor imagery like extension and rest state (2 class).

Comparison of classifiers

Classifier (Experiment1)	Average F1 score
RANDOM FOREST	0.8271
LDA	0.7304
LDA with Optimal features	0.7248

Table 33: Average F1 scores (Experiment 1)

Classifier (Experiment1)	Average run time (seconds)
LDA	0.0560
LDA with Optimal features	0.0514

Table 34: Average run time (Experiment 1)

Classifier (Experiment 2.1)	Average F1 score
RANDOM FOREST	0.7933
LDA	0.705
LDA with Optimal features	0.695

Table 35: Average F1 scores (Experiment 2.1)

Classifier (Experiment 2.1)	Average run time (seconds)
LDA	0.0572
LDA with Optimal features	0.0526

Table 36: Average run time (Experiment 2.1)

Classifier (Experiment 2.2)	Average F1 score
RANDOM FOREST	0.7234
LDA	0.4132
LDA with Optimal features	0.388

Table 37: Average F1 scores (Experiment 2.2)

Classifier (Experiment 2.2)	Average run time (seconds)
LDA	0.58867
LDA with Optimal features	0.57033

Table 38: Average run time (Experiment 2.2)

Classifier (Experiment 3)	Average F1 score
RANDOM FOREST	0.7962
LDA	0.6525
LDA with Optimal features	0.6456

Table 39: Average F1 scores (Experiment 3)

Classifier (Experiment 3)	Average run time (seconds)
LDA	0.06262
LDA with Optimal features	0.048004

Table 40: Average run time (Experiment 3)

Experiment	Average RF F1 scores
Experiment1	82.7%
Experiment 2.1	79%
Experiment 2.2	72%
Experiment 3	79%

Table 41: Average RF F1 scores

RF had given best F1 scores in all the experiments. Best F1 score was achieved in Experiment 1 (ie) finger tapping task which was 82.7%. Experiment 2.1 and experiment 3 gave almost equal F1 scores of 79%. Experiment 2.2 gave F1 score of 72%.

All the analysis was done offline. And RF would be best for offline analysis and if runtime of classifier is not an issue, RF would serve as best model.

Experiment	Average LDA F1 scores	Average LDA_optimal F1 scores	F1 scores difference
Experiment1	73.04 %	72.48%	0.56
Experiment 2.1	70.5%	69.5%	1
Experiment 2.2	41.3%	38.8%	2.5
Experiment 3	65.25%	64.56%	0.69

Table 42: Average LDA, LDA_optimal F1 scores

Average LDA F1 scores and average LDA_optimal F1 scores were tabulated in table 42. The difference between two F1 scores was least for experiment 1, highest for experiment 2.2. This table proves that MDI feature ranking of RF is best among a set of features.

Experiment	Average LDA run time (seconds)	Average LDA_optimal run time (seconds)	Run time difference (seconds)
Experiment1	0.0560	0.0514	0.046
Experiment 2.1	0.0572	0.0526	0.050
Experiment 2.2	0.588867	0.57033	0.01857
Experiment 3	0.0626	0.048004	0.01456

Table 43: Average LDA, LDA_optimal run time

Average run time of LDA_optimal had reduced in all experiments owing to reduction of features. Experiment 2.1 saw maximum difference and experiment 3 saw least difference.

Major findings

Keen observations are

- RF is best classifier compared to linear classifiers like LDA
- RF since it is ensemble method can be used for offline analysis
- LDA is the fastest classifier, hence best for online analysis
- RF feature selection works perfectly
- LDA_optimal has run time low compared to LDA
- LDA with seven features is also giving good classification but model is less perfect than RF
- In experiments involving three class classification, RF has classified exceptionally good compared to LDA and LDA_optimal

VIRTUAL REALITY FOR FNIRS BCI (VR fNIRS BCI)

Virtual reality had been previously used for restoring postural balance and walking function (de Bruin ED et al., 2010), neuropsychological assessment and rehabilitation (Riva G et al., 2003), rehabilitation for parkinsons disease, alzheimers disease and various cognitive impairments (Matta Mello Portugal E et al., 2013), education and rehabilitation of children with autism (McComas et al., 1998), rehabilitation of Attention deficit hyperactivity disorder (DariusA.Rohan et al., 2014), focus and attention of training for cognitive impairment and dementia patient (Valeria Manera et al., 2015).

Virtual reality use in BCI is of recent trend. Studies like DariusA.Rohan et al., 2014 used BCI inside a Virtual Reality Classroom for potential training tool for attention. QiBin Zhao et al., 2009 worked on EEG-based Asynchronous BCI Control of a Car in 3D Virtual Reality Environments. Duan F et al., 2015 had worked on Design of a Multimodal EEG-Based Hybrid BCI System with Visual Servo Module. Robert Leeb et al., 2007 had worked on Self-Paced (Asynchronous) BCI Control of a Wheelchair in Virtual Environments. G Cheron et al., 2012 had integrated BCI for walking rehabilitation from spinal cord pattern generator to cortical network.

On the lines of researchers who had previously worked on BCI with stimuli given in virtual reality, we too carried our work with VR for fNIRS BCI. Traditionally researchers had worked on VR headgears like oculus rift and Samsung gear. Till date no one had worked with VR android app based fNIRS BCI. We are first to report this type of feasibility study. The study yielded positive results and proved that for researchers devoid of high end VR technology devices, VR android apps could be made used of. By manually synchronizing VR app run time which includes block just like fNIRS paradigm with NIRStim paradigm, virtual reality stimuli was given for the active blocks of paradigm. F1 scores as high as 70% with LDA was achieved and as high as 80% was achieved with RF.

RECOMMENDATIONS OF STUDY

- Virtual Reality for BCI experiments pertaining to motor imagery
- Virtual Reality android application for fNIRS BCI studies
- Paradigms with complex stimuli can be easily given to subject with Virtual Reality
- Paradigms could be designed for classification of three states of brain
- Recommended to have motor imagery block duration between 8-10 seconds
- Use RF classifier for feature selection
- Top three ranked features from RF would serve as optimal feature combination for other linear classifiers
- LDA would best serve in terms of time run
- RF would best serve in terms of classification score
- LDA_optimal would be optimistic model, when compared to LDA and RF
- By using features selected by RF in LDA (LDA_optimal) number of features calculated can be reduced, reducing overall run time of BCI

RECOMMENDATIONS OF FURTHER STUDY

Since it is established that VR could be indeed used in fNIRS BCI studies for simulating artificial environment that in turn activates brain, the following can be recommended for further studies in VR fNIRS BCI

- Complex paradigm with auditory, visual, vibrotactile, haptic, knowledge of performance and knowledge of results and proprioceptive can designed easily in virtual reality
- Intrinsic feedback in Virtual Reality by external source that can facilitate in rehabilitation

Further Virtual Reality based training applications for the following can be developed.

- Cerebral Palsy
- Autism
- Stroke
- Attention deficit hyperactivity disorder (ADHD)
- multiple sclerosis

- GAIT training
- Anxiety disorders
- Phobias
- Contralateral hemispatialagnosia

Stroke rehabilitation:

Physical therapy is the most rehabilitation technique used so far. With advancement in technology, it is time to look for alternative techniques which are highly efficient in training and assessing stroke patients.

We plan to

Develop motor imagery VR app that includes tasks like

Simple tasks:

- Finger tapping
- Feet tapping
- Extension and flexion
- Elevation and depression
- Rotation
- Retrograde and circumduction
- Pronation and supination
- Inversion and eversion
- Protrusion and Retrusion
- Reciprocal motion

Fine motor skills like

- Threading with beads
- Rotating ball
- Picking up cup of coffee and placing it back
- Poking straws into holes
- Pasta necklaces

- Pipe cleaners and colanders
- Building 3D models

VR motor imagery apps could be used by patients at home. Daily training with motor imagery can show improvement in patient motor performance, and performance would be assessed by either fNIRS or GAIT analysis.

The same VR motor imagery apps could also be used for fNIRS BCI studies.

LIMITATIONS OF STUDY:

- No of subjects recruited in experiment 2 and experiment 3
- Manual synchronizing of VR app and NIRStim in experiment 3

These are some limitations. Other limitation includes inability to have online BCI in this project, due to lack to external communication device like Functional muscle stimulator.

REFERENCES

- Asaduzzaman, K., et al. "A study on discrete wavelet-based noise removal from EEG signals." *Advances in Computational Biology*. Springer New York, 2010. 593-599.
- A. Burns, H. Adeli, and J. A. Buford, "Brain-computer interface after nervous system injury," *Neuroscientist*, vol. 20, no. 6, pp. 639–651, Dec. 2014.
- A. R. Fugl-Meyer, L. Ja "a "sko ", I. Leyman, S. Olsson, and S. Steglind, "The post-stroke hemiplegic patient. 1. A method for evaluation of physical performance," *Scand. J. Rehab. Med.*, vol. 7, no. 1, pp. 13–31, 1975
- A. Ramos-Murguialday et al., "Brain-machine interface in chronic stroke rehabilitation: A controlled study," *Ann. Neurol.*, vol. 74, no. 1, pp. 100–108, Jul. 2013.
- Amit, Yali, and Donald Geman. "Shape quantization and recognition with randomized trees." *Neural computation* 9.7 (1997): 1545-1588.
- Abibullaev, B., and An, J. (2012). Classification of frontal cortex hemodynamic responses during cognitive tasks using wavelet transforms and machine learning algorithms. *Med. Eng. Phys.* 34, 1394–1410. doi: 10.1016/j.medengphy.2012.01.002
- Bhattacharyya S, Sengupta A, Chakraborti T, Konar A, Tibarewala D (2014) Automatic feature selection of motor imagery EEG signals using differential evolution and learning automata. *Med BiolEngComput* 52:131–139
- BART O, AGAM T, WEISS LP, KIZONY R. Using videocapture virtual reality for children with acquired brain injury. *Disabil Rehabil* 2011;33(17-18):1579-86
- Bachman K. Using mental imagery to practice a specific psychomotor skill. *J ContinEducNurs.* 1990;21:125–128.
- Breiman, Leo. "Bagging predictors." *Machine learning* 24.2 (1996): 123-140.
- Breiman, Leo. "Random forests." *Machine learning* 45.1 (2001): 5-32.
- Blair A, Hall C, Leyshon G. Imagery effects on the performance of skilled and novice soccer players. *J Sports Sci.* 1993; 11:95–101.
- Boschker MS, Bakker FC, Rietberg MB. Retroactive interference effects of mentally imagined movement speed. *J Sports Sci.* 2000;18:593–603.
- Birbaumer N, Cohen LG. Brain-computer interfaces: communication and restoration of movement in paralysis. *J Physiol.* 2007 Jan;579(3):621–36.
- Braun SM, Beurskens AJ, Borm PJ, et al. The effects of mental practice in stroke rehabilitation: a systematic review. *Arch Phys Med Rehabil.* 2006;87:842–852.

- Brütsch, Karin, et al. "Virtual reality for enhancement of robot-assisted gait training in children with neurological gait disorders." *Journal of rehabilitation medicine* 43.6 (2011): 493-499.
- Benoit, Michel, et al. "Is it possible to use highly realistic virtual reality in the elderly? A feasibility study with image-based rendering." *Neuropsychiatric disease and treatment* 11 (2015): 557-563.
- Bauernfeind, Günther, et al. "Development, set-up and first results for a one-channel near-infrared spectroscopy system/Entwicklung, Aufbau und vorläufige Ergebnisse eines Einkanal-Nahinfrarot-Spektroskopie-Systems." *Biomedizinische Technik* 53.1 (2008): 36-43.
- Burrus, C. Sidney, Ramesh A. Gopinath, and Haitao Guo. "Wavelets and wavelet transforms." *rice university, houston edition* 98 (1998).
- B. H. Dobkin, "Brain-computer interface technology as a tool to augment plasticity and outcomes for neurological rehabilitation," *J. Physiol.*, vol. 579, no. 3, pp. 637–642, 2007.
- Burgar, C. G., Lum, P. S., Scremin, A. M., Garber, S. L., Van der Loos, H. F., Kenney, D., et al. (2011). Robot-assisted upper-limb therapy in acute rehabilitation setting following stroke: department of Veterans Affairs multisite clinical trial. *J. Rehabil. Res. Dev.* 48, 445–458. doi: 10.1682/JRRD.2010.04.0062
- Bhasin, A., Padma Srivastava, M. V., Kumaran, S. S., Bhatia, R., and Mohanty, S. (2012). Neural interface of mirror therapy in chronic stroke patients: a functional magnetic resonance imaging study. *Neurol. India* 60, 570–576. doi: 10.4103/0028-3886.105188
- Boas, D. A., Dale, A. M. & Franceschini, M. A. (2004). Diffuse optical imaging of brain activation: approaches to optimizing image sensitivity, resolution, and accuracy, *NeuroImage* 23(Supplement 1): S275 – S288. *Mathematics in Brain Imaging*.
- Cotter SF, Kreutz-Delgado K, Rao BD (2001) Backward sequential elimination for sparse vector subset selection. *Signal Process* 81:1849–1864
- Chéron, Guy, et al. "From spinal central pattern generators to cortical network: integrated BCI for walking rehabilitation." *Neural plasticity* 2012 (2012).
- Chen YP, Kang LJ, Chuang TY, Doong JL, Lee SJ. Use of virtual reality to improve upper extremity control in children with cerebral palsy: a single subject design. *Phys Ther* 2007;87:1441-57.
- Chen et al 2007, showed post training of normal subjects with VR, increased motor performance, kinematics of object reaching, improved fine motor movement, and improved neuroplasticity
- Crosson, Bruce, et al. "Functional imaging and related techniques: An introduction for rehabilitation researchers." *Journal of rehabilitation research and development* 47.2 (2010)
- Cooper, R. J., Selb, J., Gagnon, L., Phillip, D., Schytz, H. W., Iversen, H. K., et al. (2012). A systematic comparison of motion artifact correction techniques for functional near-infrared spectroscopy. *Front. Neurosci.* 6:147. doi:10.3389/fnins.2012.00147

Coyle SM, Ward TE, Markham CM: Brain-computer interface using a simplified functional near-infrared spectroscopy system. *Journal of Neural Engineering* 2007, 4(3):219-226.

Calderon Arnulphi, Mateo, Ali Alaraj, and Konstantin V.Slavin. Near infrared technology in neuroscience: past, present and future. *Neurological research* 31.6 (2009): 605-614.

Cole SW, Yoo DJ, Knutson B. Interactivity and reward-related neural activation during a serious videogame. *PLoS One* 2012;7:e33909.

Choi, Young Jun, et al. "Differences in risk of malignancy and management recommendations in subcategories of thyroid nodules with atypia of undetermined significance or follicular lesion of undetermined significance: the role of ultrasound-guided core-needle biopsy." *Thyroid* 24.3 (2014): 494-501.

Cramer SC, Orr EL, Cohen MJ, Lacourse MG. Effects of motor imagery training after chronic, complete spinal cord injury. *Exp Brain Res.* 2006;177:233–242.

Chan, J., Power, S., and Chau, T. (2012). Investigating the need for modeling temporal dependencies in a brain-computer interface with real-time feedback based on near infrared spectra. *J. Near Infrared Spectrosc.* 20, 107–116. doi: 10.1255/jnirs.971

Deng H, Runger GC (2012) Feature selection via regularized trees, *CoRR*, vol. abs/1201.1587

Daly JJ, Wolpaw JR. Brain-computer interfaces in neurological rehabilitation. *LancetNeurol.* 2008;7(11):1032–43.

Dehghani, Hamid, et al. "Near infrared optical tomography using NIRFAST: Algorithm for numerical model and image reconstruction." *Communications in numerical methods in engineering* 25.6 (2009): 711-732.

Dobkin BH. Plasticity in the sensorimotor and cognitive networks. In: Dobkin BH, ed. *The Clinical Science of Neurologic Rehabilitation*. 2nd ed. New York, NY: Oxford University Press; 2003:16–18.

Dijkerman HC, Ietswaart M, Johnston M, MacWalter RS. Does motor imagery training improve hand function in chronic stroke patients? A pilot study. *ClinRehabil.* 2004;18:538–549.

Dromerick, A. W., Lang, C. E., Birkenmeier, R. L., Wagner, J. M., Miller, J. P., Videen, T. O., et al. (2009). Very early constraint-induced movement during stroke rehabilitation (VECTORS): a single-center RCT. *Neurology* 73, 195–201. doi:10.1212/WNL.0b013e3181ab2b27

Daubechies, I., Orthonormal bases of compactly supported wavelets, *Communications on Pure and Applied Mathematics*, 41(7), pp. 909–996, 1988

Daubechies, I., *Ten Lectures on Wavelets*, CBMS-NSF Regional Conference Series in Applied Mathematics: Society for Industrial and Applied Mathematics, (61), 1992

- Decety, J., Jeannerod, M., &Prablanc, C. (1989). The timing of mentally represented actions. *Behavioural Brain Research*, 34, 35–42.
- Driskell et al. summarized the effects of MP and determined under which conditions MI was most effective (Driskell JC et al 1994).
- Decety J, Ingvar DH. Brain structures participating in mental simulation of motor behavior: a neuropsychological interpretation. *ActaPsychol (Amst)*. 1990;73: 13–34.
- DesCoteaux JG, Leclere H. Learning surgical technical skills. *Can J Surg*. 1995; 38:33–38
- de Bruin ED, Schoene D, Pichierri G, Smith ST. Use of virtual reality technique for the training of motor control in the elderly. Some theoretical considerations. *Z GerontolGeriatr* 2010;43:229–234.
- Deutsch JE, Mirelman A. Virtual reality-based approaches to enable walking for people poststroke. *Top Stroke Rehabil* 2007;14:45–53.
- E. Buch et al., “Think to move: A neuromagnetic Brain-Computer Interface (BCI) system for chronic stroke,” *Stroke*, vol. 39, no. 3, pp. 910–917, Mar. 2008.
- Fansler CL, Poff CL, Shepard KF. Effects of mental practice on balance in elderly women. *PhysTher*. 1985;65:1332–1338.
- Guyon I, Weston J, Barnhill S, Vapnik V (2002) Gene selection for cancer classification using support vector machines. *Mach Learn* 46:389–422
- Gentili R, Papaxanthis C, Pozzo T. Improvement and generalization of arm motor performance through motor imagery practice. *Neuroscience*. 2006;137: 761–772.
- Hsieh, Y. W., Wu, C. Y., Lin, K. C., Yao G, Wu K. Y. and Chang, Y. J. (2012). Dose-response relationship of robot-assisted stroke motor rehabilitation: the impact of initial motor status. *Stroke* 43, 2729–2734. doi: 10.1161/STROKEAHA.112.658807
- Hsu S. S., Hu M. H., Wang, Y. H., Yip P K, Chiu J W and Hsieh, C. L. (2010). Dose-response relation between neuromuscular electrical stimulation and upper-extremity function in patients with stroke. *Stroke* 41, 821–824. doi: 10.1161/STROKEAHA.109.574160
- Hamel MF, Lajoie Y. Mental imagery: effects on static balance and attentional demands of the elderly. *Aging ClinExp Res*. 2005;17:223–228.
- Horning, Ned. "Introduction to decision trees and random forests." *American Museum of Natural History's* (2013).
- Hill, N. Jeremy, et al. "Classifying EEG and ECoG signals without subject training for fast BCI implementation: comparison of nonparalyzed and completely paralyzed subjects." *IEEE transactions on neural systems and rehabilitation engineering* 14.2 (2006): 183-186.

Izzetoglu, M., Devaraj, A., Bunce, S., and Onaral, B. (2005). Motion artifact cancellation in NIR spectroscopy using Wiener filtering. *IEEE Trans. Biomed. Eng.* 52, 934–938. doi: 10.1109/TBME.2005.845243

J.C.Fu, S.K.Lee, S.T.C.Wong, J.Y.Yeh, A.H.Wang, and H.K. Wu, “Image segmentation feature selection and pattern classification for mammographic microcalcifications,” *Comput. Med. Imag. Graph.*, vol. 29, no. 6, pp. 419–429, 2005..

Jeannerod M, Decety J. Mental motor imagery: a window into the representational stages of action. *Curr Opin Neurobiol.* 1995;5:727–732.

Jöbsis, F.F. (1977). Non-invasive infrared monitoring of cerebral and myocardial oxygen sufficiency and circulatory parameters. *Science*, Vol. 198, No. 4323, (December 1977), pp. 1264–7, ISSN 1095-9203

J. R. Wolpaw, N. Birbaumer, D. J. McFarland, G. Pfurtscheller, and T. M. Vaughan, “Brain-computer interfaces for communication and control,” *Clin Neurophysiol.*, vol. 113, no. 6, pp. 767–791, Jun. 2002.

J. J. Daly and J. R. Wolpaw, “Brain-computer interfaces in neurological rehabilitation,” *Lancet Neurol.*, vol. 7, no. 11, pp. 1032–1043, Nov. 2008.

J. Wolpaw and E. W. Wolpaw, *Brain-Computer Interfaces: Principles and Practice*. New York, USA: Oxford University Press, 2012

Johansen-Berg, H., Dawes, H., Guy, C., Smith, S.M., Wade, D. T., and Matthews, P. M. (2002). Correlation between motor improvements and altered fMRI activity after stroke. *Brain* 125, 2731–2742. doi:10.1093/brain/awf282

Jacoby M, Averbuch S, Sacher Y, Katz N, Weiss PL, Kizony R. Effectiveness of executive functions training within a virtual supermarket for adults with traumatic brain injury: a pilot study. *IEEE Trans Neural Syst Rehabil Eng* 2013;21:182–190.

Kalron, Alon, et al. "The effect of balance training on postural control in people with multiple sclerosis using the CAREN virtual reality system: a pilot randomized controlled trial." *Journal of neuroengineering and rehabilitation* 13.1 (2016)

Keshner EA, Streepey J, Dhaher Y, Hain T. Pairing virtual reality with dynamic posturography serves to differentiate between patients experiencing visual vertigo. *J Neuroeng Rehabil* 2007;4:24

Kosslyn SM, Ganis G, Thompson WL. Neural foundations of imagery. *Nat Rev Neurosci.* 2001;2:635–642.

Kai Keng Ang, Senior Member IEEE, and Cuntai Guan, Senior Member IEEE. Brain-Computer Interface for Neurorehabilitation of Upper Limb After Stroke. *Proceedings of the IEEE* | Vol. 103, No. 6, June 2015

- Kononen, M., Tarkka, I. M., Niskanen, E., Pihlajamaki, M., Mervaala, E., Pitkanen, K., et al. (2012). Functional MRI and motor behavioral changes obtained with constraint-induced movement therapy in chronic stroke. *Eur. J. Neurol.*19,578–586.doi:10.1111/j.1468-1331.2011.03572.
- Louppe, Gilles, et al. "Understanding variable importances in forests of randomized trees." *Advances in neural information processing systems*. 2013.
- Leeb, Robert, et al. "Self-paced (asynchronous) BCI control of a wheelchair in virtual environments: a case study with a tetraplegic." *Computational intelligence and neuroscience 2007* (2007).
- Lequerica A, Rapport L, Axelrod BN, Telmet K, Whitman RD. Subjective and objective assessment methods of mental imagery control: construct validation of self-report measures. *J ClinExpNeuropsychol* 2002;24:1103–1116.
- Liu, M., Fujiwara, T., Shindo, K., Kasashima, Y., Otaka, Y., Tsuji, T., et al. (2012). Newer challenges to restore hemiparetic upper extremity after stroke: HANDS therapy and BMIneurorehabilitation. *Hong Kong Physiother. J.* 30,83–92. doi: 10.1016/j.hkpj.2012.05.001
- Lotze M, Cohen LG. Volition and imagery in neurorehabilitation. *CognBehav Neurol.* 2006;19:135–140.
- Luu S, Chau T: Decoding subjective preference from single-trial nearinfrared spectroscopy signals. *Journal of Neural Engineering* 2009, 6(1):016003.
- Liu, Y., Ayaz, H., Curtin, A., and Onarall, B. (2013). "Towards a hybrid P300based BCI using simultaneous fNIR and EEG," in *Foundations of Augmented Cognition*, eds D. Schmorow and C. Fidopiastis (Heidelberg: Springer-Verlag), 335–344.
- Malouin F, Belleville S, Richards CL, et al. Working memory and mental practice outcomes after stroke. *Arch Phys Med Rehabil.* 2004;85:177–183.
- Matteo Caffini, DavideContini, Rebecca Re, Lucia M. Zucchelli, RinaldoCubeddu, Alessandro Torricelli and Lorenzo Spinelli (2012). *Functional Near Infrared Spectroscopy and Diffuse Optical Tomography in Neuroscience*, *Advances in Brain Imaging*, Dr. Vikas Chaudhary (Ed.), ISBN: 978-953-307-955-4.
- Maillot, Pauline, Alexandra Perrot, and Alan Hartley. "Effects of interactive physical-activity video-game training on physical and cognitive function in older adults." *Psychology and aging* 27.3 (2012): 589.
- McComas, Joan, Jayne Pivik, and Marc Laflamme. "Children's transfer of spatial learning from virtual reality to real environments." *CyberPsychology & Behavior* 1.2 (1998): 121-128.
- M. W. O'Dell, C.C. D. Lin, and V. Harrison, "Stroke rehabilitation: Strategies to enhance motor recovery," *Annu. Rev. Med.*, vol. 60, no. 1, Feb. 2009

- M. Jeannerod, "Mental imagery in the motor context," *Neuropsychologia*, vol. 33, no. 11, pp. 1419–1432, Nov. 1995
- M. A. Dimyan and L. G. Cohen, "Neuroplasticity in the context of motor rehabilitation after stroke," *Nat. Rev. Neurol.*, vol. 7, no. 2, pp. 76–85, 2011.
- M. Mihara et al., "Near-infrared spectroscopy-mediated neurofeedback enhances efficacy of motor imagery-based training in poststroke victims: A pilot study," *Stroke*, vol. 44, no. 4, pp. 1091–1098, Apr. 2013.
- Michelon P, Vettel JM, Zacks JM. Lateral somatotopic organization during imagined and prepared movements. *J Neurophysiol.* 2006;95:811–822.
- Maillot P, Perrot A, Hartley A: Effects of interactive physical-activity video-game training on physical and cognitive function in older adults. *Psychol Aging* 2012;27:589-600
- Mulder T, Zijlstra S, Zijlstra W, Hochstenbach J. The role of motor imagery in learning a totally novel movement. *Exp Brain Res.* 2004;154:211–217.
- Matta Mello Portugal E, Cevada T, Sobral Monteiro-Junior R, Teixeira Guimarães T, da Cruz Rubini E, Lattari E, Blois C, Camaz Deslandes A: Neuroscience of exercise: From neurobiology mechanisms to mental health. *Neuropsychobiology* 2013;68:1-14.
- McCOMAS J, PIVIK J, LaFLAMME M. Current uses of virtual reality for children with disabilities. In: RIVA G, WIEDERHOLD B, MOLINARI E, editors. *Virtual environments in clinical psychology and neuroscience*. Amsterdam: Ios Press, 1998;161-70.
- Naseer, Noman, and Keum-Shik Hong. "fNIRS-based brain-computer interfaces: a review." *Frontiers in human neuroscience* 9 (2015): 3.
- Naito M, et al: A Communication Means for Totally Locked-in ALS Patients Based on Changes in Cerebral Blood Volume Measured with Near-Infrared Light. *IEICE T InfSyst* 2007, 90(7):1028-1037.
- N. Sharma, V. M. Pomeroy, and J.-C. Baron, "Motor imagery: A backdoor to the motor system after stroke?" *Stroke*, vol. 37, no. 7, pp. 1941–1952, Jul. 2006.
- N. Chino, S. Sonoda, K. Domen, E. Saitoh, and A. Kimura, "Stroke Impairment Assessment Set (SIAS). A new evaluation instrument for stroke patients," *Jpn. J. Rehab. Med.*, vol. 31, no. 2, pp. 119–125, 1994.
- N. Langer, J. Hänggi, N.A. Müller, H.P. Simmen, and L. Jäncke. Effects of limb immobilization on brain plasticity. *Neurology*, 78 (2012), 182-188.
- Nyberg L, Eriksson J, Larsson A, Marklund P. Learning by doing versus learning by thinking: an fMRI study of motor and mental training. *Neuropsychologia.* 2006;44:711–717.
- Obrig, Hellmuth, et al. "Spontaneous low frequency oscillations of cerebral hemodynamics and metabolism in human adults." *Neuroimage* 12.6 (2000): 623-639.

- Pinter, D., Pegritz, S., Pargfrieder, C., Reiter, G., Wurm, W., Gattringer, T., et al. (2013). Exploratory study on the effects of a robot hand rehabilitation device on changes in grip strength and brain activity after stroke. *Top. Stroke Rehabil.* 20, 308–316. doi:10.1310/tsr2004-308
- Power, S., and Chau, T. (2013). Automatic single-trial classification of prefrontal hemodynamic activity in an individual with Duchenne muscular dystrophy. *Dev. Neurorehabil.* 16, 67–72. doi: 10.3109/17518423.2012.718293
- Papaxanthis, C., Pozzo, T., Skoura, X., & Schieppati, M. (2002). Does order and timing in performance of imagined and actual movements affect the motor imagery process? The duration of walking and writing task. *Behavioural Brain Research*, 134, 209–215.
- Page SJ, Levine P, Sisto SA, Johnston MV. Mental practice combined with physical practice for upper-limb motor deficit in subacute stroke. *PhysTher.* 2001;81: 1455–1462.
- Raichle, Marcus E. "Behind the scenes of functional brain imaging: a historical and physiological perspective." *Proceedings of the National Academy of Sciences* 95.3 (1998): 765-772.
- Rohani, Darius Adam, Helge BD Sorensen, and Sadasivan Puthusserypady. "Brain-computer interface using P300 and virtual reality: a gaming approach for treating ADHD." *2014 36th Annual International Conference of the IEEE Engineering in Medicine and Biology Society*. IEEE, 2014.
- Riva G. Applications of virtual environments in medicine. *Methods Inf Med* 2003;42:524–534.
- S. Yu and B. Bhanu, "Image retrieval with feature selection and relevance feedback," in Proc. 17th IEEE Int. Conf. Image Process., Oct. 2010, pp. 3209–3212.
- SINDER L, MAJNEMER A, DARSAKLIS V. Virtual reality as a therapeutic modality for children with cerebral palsy. *Dev Neurorehabil* 2010;13(2):120-8.
- Schmidt RA, Wrisberg CA. Mental rehearsal techniques. In: Schmidt RA, Wrisberg CA, eds. *Motor Learning and Performance*. 2nd ed. Champaign, Ill: Human Kinetics; 2000:22–225.
- Subasi, Abdulhamit. "Automatic detection of epileptic seizure using dynamic fuzzy neural networks." *Expert Systems with Applications* 31.2 (2006): 320-328.
- S. Rayegani et al., "Effect of neurofeedback and electromyographic-biofeedback therapy on improving hand function in stroke patients," *Top. Stroke Rehab.*, vol. 21, no. 2, pp. 137–151, Mar. 2014.
- Sitaram, Ranganatha, et al. "Temporal classification of multichannel near-infrared spectroscopy signals of motor imagery for developing a brain-computer interface." *NeuroImage* 34.4 (2007): 1416-1427.
- Shelton, F. N., and Reding, M. J. (2001). Effect of lesion location on upper limb motor recovery after stroke. *Stroke* 32, 107–112. doi:10.1161/01.STR.32.1.107
- Song, J., Young, B. M., Nigogosyan, Z., Walton, L. M., Nair, V. A., Grogan, S. W., et al. (2014). Characterizing relationships of DTI, fMRI, and motor recovery in stroke rehabilitation utilizing brain-computer interface technology. *Front. Neuroeng.* 7:31. doi:10.3389/fneng.2014.0003

Suinn RM. Mental practice in sport psychology: where have we been, where do we go? *Clinical Psychology: Science and Practice*. 1997;4:189–207.

Sreedharan, Sujesh, et al. "Brain-computer interfaces for neurorehabilitation." *Critical Reviews™ in Biomedical Engineering* 41.3 (2013).

Strangman, G., Boas, D. A. & Sutton, J. P. (2002). Non-invasive neuroimaging using near-infrared light, *Society of Biological Psychiatry* 52: 679–693.

Shin, J., and Jeong, J. (2014). Multiclass classification of hemodynamic responses for performance improvement of functional near-infrared spectroscopy-based brain-computer interface. *J. Biomed. Opt.* 19:067009. doi: 10.1117/1.JBO.19.6.067009

Sharma N, Pomeroy VM, Baron JC. Motor imagery: a backdoor to the motor system after stroke? *Stroke*. 2006;37:1941–1952

Sidaway B, Trzaska AR. Can mental practice increase ankle dorsiflexor torque? *PhysTher*. 2005;85:1053–1060.

Sinder et al 2010, studied applications of VR in cerebral palsy and concluded that post training, cerebral palsy patients had regained lost abilities of competence and self esteem in motor activities.

Strobl, Carolin, James Malley, and Gerhard Tutz. "An introduction to recursive partitioning: rationale, application, and characteristics of classification and regression trees, bagging, and random forests." *Psychological methods* 14.4 (2009): 323.

Schapire, Robert E., et al. "Boosting the margin: A new explanation for the effectiveness of voting methods." *Annals of statistics* (1998): 1651-1686.

T. Ono et al., "Brain-computer interface with somatosensory feedback improves functional recovery from severe hemiplegia due to chronic stroke," *Front. Neuroeng.*, vol. 7, Jul. 2014.

Tsunashima, Hitoshi, and Kazuki Yanagisawa. "Measurement of brain function of car driver using functional near-Infrared spectroscopy (fNIRS)." *Computational intelligence and neuroscience* 2009 (2009).

Taktek K. The effects of mental imagery on the acquisition of motor skills and performance: a literature review with theoretical implications. *Journal of Mental Imagery*. 2004;29:79–114

Tong, Yunjie. "Time lag dependent multimodal processing of concurrent fMRI and near-infrared spectroscopy (NIRS) data suggests a global circulatory origin for low-frequency oscillation signals in human brain." *Neuroimage* 53.2 (2010): 553-564.

Tai K, Chau T: Single-trial classification of NIRS signals during emotional induction tasks: towards a corporeal machine interface. *Journal of NeuroEngineering and Rehabilitation* 2009, 6(1):39.

- Varkuti, B., Guan, C., Pan, Y., Phua, K. S., Ang, K. K., Kuah, C. W., et al. (2013). Resting state changes in functional connectivity correlate with movement recovery for BCI and robot-assisted upper-extremity training after stroke. *Neurorehabil. Neural Repair* 27, 53–62. doi: 10.1177/1545968312445910
- Warner L, McNeill ME. Mental imagery and its potential for physical therapy. *PhysTher.* 1988; 68:516–521.
- Wolpaw, Jonathan R., et al. "Brain-computer interface technology: a review of the first international meeting." *IEEE transactions on rehabilitation engineering* 8.2 (2000): 164-173.
- Yamada, N., Kakuda, W., Senoo, A., Kondo, T., Mitani, S., Shimizu, M., et al. (2013). Functional cortical reorganization after low-frequency repetitive transcranial magnetic stimulation plus intensive occupational therapy for upper limb hemiparesis: evaluation by functional magnetic resonance imaging in poststroke patients. *Int. J. Stroke* 8, 422–429. doi: 10.1111/ijss. 12056
- You, Sung H., et al. "Virtual reality–induced cortical reorganization and associated locomotor recovery in chronic stroke an experimenter-blind randomized study." *Stroke* 36.6 (2005): 1166-1171.
- Young, B. M., Nigogosyan, Z., Walton, L. M., Song, J., Nair, V. A., Grogan, S. W., et al. (2014c). Changes in functional brain organization and behavioral correlations after rehabilitative therapy using a brain-computer interface. *Front. Neuroeng.*7:26.doi:10.3389/fneng.2014.00026
- Yue G, Cole KJ. Strength increases from the motor program: comparison of training with maximal voluntary and imagined muscle contractions. *J Neurophysiology.* 1992;67:1114–1123.
- Yaguez L, Nadel D, Hoffman H, et al. A mental route to motor learning: improving trajectorial kinematics through imagery training. *Behav Brain Res.* 1998;90: 95–106.
- Yoo E, Park E, Chung B. Mental practice effect on line-tracing accuracy in persons with hemiparetic stroke: a preliminary study. *Arch Phys Med Rehabil.* 2001;82: 1213–1218.
- You SH, Jang SH, Kim YH, Hallett M, Ahn SH, Kwon YH, Kim JH, Lee MY: Virtual reality-induced cortical reorganization and associated locomotor recovery in chronic stroke: An experimenter-blind randomized study. *Stroke* 2005;36:1166-1171.
- Yang, Pengyi, et al. "A review of ensemble methods in bioinformatics." *Current Bioinformatics* 5.4 (2010): 296-308.
- Zimmermann, R., Marchal-Crespo, L., Edelmann, J., Lamercy, O., Fluet, M.C., Riener, R., et al. (2013). Detection of motor execution using hybrid fNIRS-biosignal BCI: a feasibility study. *J. Neuroeng. Rehabil.* 10:4. doi: 10.1186/1743-0003-10-4
- Zhao, QiBin, LiQing Zhang, and Andrzej Cichocki. "EEG-based asynchronous BCI control of a car in 3D virtual reality environments." *Chinese Science Bulletin* 54.1 (2009): 78-87.

APPENDIX



Figure 86: Foot tapping



Figure 87: Finger tapping

```

import os
os.getcwd()
os.chdir('G:\project\Motor vs Motor Imagery\sub2')
#os.chdir('G:')

import pandas as pd
from sklearn.cross_validation import train_test_split
from sklearn.metrics import classification_report
from sklearn.pipeline import Pipeline
from sklearn.grid_search import GridSearchCV
import matplotlib.pyplot as plt
from matplotlib import style
import numpy as np
from sklearn import metrics
from sklearn.cross_validation import cross_val_score
style.use('ggplot')
file1=pd.read_csv('M_MI_2c_nd_2.csv')
df=pd.DataFrame(file1)
print(df)
df
X=np.array(df.drop(['class'],1))
print X
Y=np.array(df['class'])
print Y

```

Figure 88: Code for loading csv file having features and converting it into dataframe

```

import time
start = time.clock()

X=np.array(df.drop(['class'],1))
Y=np.array(df['class'])

from sklearn.lda import LDA
lda=LDA()

scores=cross_val_score(lda,X,Y,cv=15,scoring='f1')
print "F1_score_LDA", scores.mean()
print "Time taken:", time.clock() - start , "seconds"

F1_score_LDA 0.557868057868
Time taken: 0.050565506418 seconds

```

Figure 89: Code for LDA classifier

```

from sklearn.cross_validation import train_test_split
X_train,X_test,Y_train,Y_test=train_test_split(X,Y,test_size=0.4,random_state=4)

from sklearn.ensemble import RandomForestClassifier
import matplotlib.pyplot as plt
pipeline=Pipeline([('clf',RandomForestClassifier(criterion='gini'))])

parameters={'clf__n_estimators': (10,15,20), 'clf__max_depth':range(50,100,150),
            'clf__min_samples_split':(1,2,3),
            'clf__min_samples_leaf':(1,2,3)}

grid_search=GridSearchCV(pipeline,parameters,n_jobs=-1,verbose=1,scoring='f1',cv=5)
uio=grid_search.fit(X_train,Y_train)
print 'Best score:, %0.3f' %grid_search.best_score_
print 'Best Parameters set:'
best_parameters=grid_search.best_estimator_.get_params()
for param_name in sorted(parameters.keys()):
    print '\t%s: %r' % (param_name, best_parameters[param_name])

predictions=grid_search.predict(X_test)
print classification_report(Y_test, predictions)

```

Figure 90: Code for Random Forest classifier

Fitting 5 folds for each of 27 candidates, totalling 135 fits

```

[Parallel(n_jobs=-1)]: Done 42 tasks | elapsed: 19.5s
[Parallel(n_jobs=-1)]: Done 135 out of 135 | elapsed: 21.1s finished

```

Best score:, 0.808

Best Parameters set:

```

    clf__max_depth: 50
    clf__min_samples_leaf: 1
    clf__min_samples_split: 1
    clf__n_estimators: 15

```

	precision	recall	f1-score	support
1	0.61	0.85	0.71	26
2	0.86	0.63	0.73	38
avg / total	0.76	0.72	0.72	64

Time taken: 21.6142398542 seconds

Figure 91: RF Classification scores and Gridsearch CV results

```

clf = RandomForestClassifier(n_estimators=15,
                           max_depth=50,min_samples_leaf=1,
                           min_samples_split=1,oob_score=True)
clf=clf.fit(X_train,Y_train)

imp=clf.feature_importances_
names=df.columns
imp,names=zip(*sorted(zip(imp,names)))
print imp
print names

clf.set_params(n_estimators=15)

oob_error = 1 - clf.oob_score_
oob_error

(0.040910015430978865, 0.12243885222464182, 0.14126808350417783, 0.146423539890
45265, 0.14773692951013961, 0.19233644857327187, 0.20888613086633734)
('Nop', 'Kurt', 'Peak', 'Mean', 'Skew', 'Var', 'Sop')

0.34375

```

Figure 92: MDI scores of RF

```

import time
start = time.clock()

from sklearn.lda import LDA
lda=LDA()

X=np.array(df.drop(['class','Sop','Nop','Peak','Mean'],1))
#print X
Y=np.array(df['class'])

import time
start = time.clock()

scores=cross_val_score(lda,X,Y,cv=15,scoring='f1')
print "F1_score_LDA_optimal", scores.mean()

print "Time taken:", time.clock() - start , "seconds"

F1_score_LDA_optimal 0.620766640767
Time taken: 0.0594263432731 seconds

```

Figure 93: Code for optimal LDA classifier

```
import os
import pandas as pd
import matplotlib.pyplot as plt
os.getcwd()

file1=pd.read_csv('VR_nd_1.csv')
df=pd.DataFrame(file1)

import seaborn as sns
sns.set()
sns.pairplot(df, hue="class")
plt.show()
```

Figure 94: Code for scatter plot